ABSTRACT

LEAR, GRETCHEN CHRISTINA**.** Improving the Assessment of In Situ Timber Members with the Use of Nondestructive and Semi-Destructive Testing Techniques. (Under the direction of Bo Kasal.)

Common practice in evaluating existing buildings and their in situ timber members is in situ grading, where structural grades and the associated design values are assigned based on a visual inspection of the member and current grading rules and standards. This can be useful in that it provides a design value to architects and engineers that can be used in design and calculation, however, there are some drawbacks. Published design values are representative of entire species or species groups, not individual members, they are based on the testing of second generation growth, and they may be conservative to account for the natural variability of wood. Additionally, deterioration can be difficult to locate and even harder to quantify through visual inspection.

As a result of this practice, member strengths are typically underestimated which can cause unnecessary remedial work or member removal. To improve the assessment of in situ timber members, nondestructive and semi-destructive testing should be used to arrive at more appropriate strength values for individual members, as well as to locate and quantify the presence of deterioration.

Five nondestructive and semi-destructive testing techniques were researched including stress wave, radiography, resistance drilling, core-drilling and tension micro-sampling, of which all but stress waves were tested. A two part experiment was perform to assess the ability of these techniques to either gain a better estimate of in situ timber strength or detect and quantify deterioration.

Findings showed that core-drilling could substantially improve the estimate of in situ member strength over the practice of assigning design values based on current standards and grading rules. Research on stress wave and experimentation of tensile micro-specimen sampling showed that further research and improvement to the techniques should to be done before these methods are be used to reliably estimate member strength.

X-ray investigation and resistance drilling both proved their ability to locate deterioration, and resistance drilling gave reasonably accurate quantification of void presence. Although not tested during experimentation, research showed that stress wave investigation may be useful for the detection of deterioration.

IMPROVING THE ASSESSMENT OF IN SITU TIMBER MEMBERS WITH THE USE OF NONDESTRUCTIVE AND SEMI-DESTRUCTIVE TESTING TECHNIQUES

by
GRETCHEN LEAR

A thesis submitted to the Graduate Faculty of
North Carolina State University
in partial fulfillment of the
requirements for the Degree of
Master of Science

CIVIL ENGINEERING

Raleigh

2005

APPROVED BY:

_____ _____

_____
Chair of Advisory Committee

BIOGRAPHY

Gretchen Lear received her undergraduate degree from North Carolina State University, graduating summa cum laude in December of 2003. During the summers from 2003 to 2005 she participated in the investigation of historic timber structures in the Czech Republic, a program jointly funded by the National Science Foundation and the Czech Grant Agency, and organized by North Carolina State University and the Czech Academy of Sciences. Lear is a National Science Foundation Graduate Fellow and will be receiving her Master of Science degree in May of 2006.

TABLE OF CONTENTS

LIST OF TABLES

Page

LIST OF FIGURES

Page

CHAPTER 2

CHAPTER 3

CHAPTER 4

LIST OF SYMBOLS AND ABBREVIATIONS

ALSC- American Lumber Standard Committee, Inc.
NDS- National Design Specification for Wood Construction
ASTM-American Society for Testing and Materials
λ – wavelength (length)
f – frequency (1 / time)
V – stress wave velocity (length / time)
L- length/distance between two points (length)
T- time (time)
δ- logarithmic decrement (amplitude change / cycle)
A_o – initial amplitude measurement (displacement)
A_j- amplitude j cycles apart (displacement)
j- number of cycles between measured amplitudes
α- attenuation factor (amplitude change / unit length)
x- length of stress wave propagation (length)
A_x- amplitude at the propagation length x (displacement)
E_d - dynamic modulus of elasticity (force / area)
ρ - mass density of the member (mass / unit volume)
υ – Poison's ratio
h - Plank's constant
c - velocity of light (length / time)
E – radiation energy (work)
I_X - emergent intensity of radiation beam (rate of energy emission)
I_O - initial intensity of radiation beam (rate of energy emission)
t - thickness of the material (length)
μ - linear absorption coefficient (1 / length)
Ug - geometric unsharpness (length)
S - size of the focal spot within an X-ray tube (length)
a - distance from the source to object (length)
b - distance from the object to imaging material (length)
RM – Resistance Measure (length^2)
h- height of specimen (length)
LVDT- Linear Variable Differential Transducer
f_c -compressive strength of the core (force / area)
F_{max} -failure load (force)
l – length of core sample (length)
d_c - diameter of the core (length)
r^2 – correlation coefficient
Es- Static Modulus of Elasticity (force / area)
Ed- Dynamic Modulus of Elasticity (force / area)
$F_{bending}$ – Bending Strength (force / area)
$F_{compression}$ – Compressive Strength (force / area)
$F_{tension}$ – Tensile Strength (force / area)
WCLB – West Coast Lumber Inspection Bureau
KH1- Beam one from Kutna Hora

KH2- Beam two from Kutna Hora
N - Beam from Namést
P1 – Beam one from Praha
P2 – Beam two from Praha
$x_{0.05}$ - ASTM lower 5th percentile strength calculated using the t-distribution (force / area)
$\bar{x}_{ASTM}$ - average ASTM compression specimen response (force / area)
$t_{\alpha, n-1}$ - critical value associated with a given probability level, α, and degrees of freedom v.
SD_{ASTM} - standard deviation of ASTM compression specimens (force / area)
$\bar{x}_{core}$ - average response of cores (force / area)
SD_{core} - standard deviation of core response (force / area)
f_t - tensile strength (force / area)
b – base dimension of the tensile specimen (length)
h - height dimension of the tensile specimen (length)
$\bar{x}_{tension}$ - average micro-tension specimen response (force / area)
$SD_{tension}$ = standard deviation of micro-tension specimens (force / area)

CHAPTER 1

INTRODUCTION

The need for structural assessment can arise from multiple motivations including performance reports to address structural adequacy, historic preservation and building change of use to name a few. The time and cost of inspections is justified with the assurance of safety gained, the protection of capital investments and minimization of costs involved with maintaining the structure.

For historic structures, quality assessments of members allows for the maximum retention of original material. Preservation of original structural fabric and the associated construction conserves the cultural significance of the building including architectural qualities and building techniques as well as the historic and socially important aspects associated with the structure. Gaining understanding of building material durability, capacity, behavior and use, as well as building techniques and craftsmanship from existing structures provides knowledge that can be applied to present-day construction.

Quality assessment begins with the assessment of the members and components that make up the structure as a whole. Common practice in evaluating and assessing timber members in existing structures is in situ grading, the assignment of structural grades through the application of grading rules. Grading rules are published by a variety of organizations and written for different species and regions, such as [1] and [2]. Grading organizations that write grading rules and the grading rules themselves are certified and monitored by the American Lumber Standard Committee, Inc. (ALSC).

A visual inspection of the member under consideration is performed and naturally occurring characteristics and deterioration are inventoried. Natural characteristics

include features such as knots, slope of grain and seasoning checks while deterioration includes damage from insect infestation or fungal decay. After the visual inspection, a structural grade is assigned based on the size, number and location of growth characteristics according to the member's size and structural use.

After establishing the member grade with appropriate grading rules, design values for visually graded timber published in the *National Design Specification* (NDS) *for Wood Construction* [3] are referenced to establish mechanical property design values. NDS design values are categorized by species, size and grade. Most of the visually graded dimension lumber design values are based on the testing of full size specimens in accordance with ASTM D 1990 [4], while visually graded timbers, decking, and some species and grades of dimension lumber are based on the provisions of ASTM D 245 [5] [3].

This study will concentrate on improving the strength estimate of in-situ timbers (127 mm by 127 mm [5 in by 5 in] or larger) [3] whose design values are established in accordance with ASTM D 245 and as such the remainder of discussion will focus on this standard and its methods. ASTM D 245 prescribes for the adjustment of clear wood property values, provided by test methods in ASTM D 2555 [6], by strength ratios and adjustment factors. Strength ratios and adjustment factors are based upon natural characteristics present within the material, environmental conditions and the intended structural use. This practice of reducing clear wood values is based on extensive research covering tests of small clear specimens and of full-sized members as well as detailed studies of strength and variability of clear wood and the effect of various factors and defects on those properties [5].

There are several drawbacks associated with this type of assessment and assignment of design values to in situ timbers. The published NDS design values are based on the testing of new timbers and may not represent mechanical properties typically found in older timbers. At this point, new timber that is harvested for construction is second generation growth. It is fast grown to produce wood quickly, and the result is reduced density and mechanical properties. In older existing structures it would be common to find first generation growth. These timbers were harvested from forests that were slow grown, and most likely have higher density and mechanical property values. The application of current NDS design values does not consider this factor and can under estimate the member's mechanical properties.

In addition, allowable stress values published in NDS and based on ASTM D 245 practices are based on the clear wood values that are representative of an entire species or species group and not individual members. In doing so, the values must account for the natural variability within the species and conservative property values are published to account for weak members. Excluding modulus of elasticity and compression perpendicular-to-grain values, the resulting values from ASTM D 245 are based on a 5% exclusion limit; meaning that 95% of members in a species group and stress grade are expected to have strengths that are above that established by ASTM D 245 and published in the NDS [5]. Assessment deals with individual members (or small groups) and not whole species groups, so the application of design values based on the species as a whole may be inappropriate.

As opposed to underestimating individual member properties, current inspection techniques could overestimate member capacities if areas of deterioration are not located

and the extent quantified. Detection and quantification of biotic deterioration is difficult or even impossible through visual inspection. Biotic deterioration refers to the damage caused by the attack of living agents such as bacteria, fungi, or insects. Loss in weight, stiffness and strength can occur before decay can be visually detected. Mechanical properties can be reduced by ten percent before visual indicators are present, and when a weight loss of only five to ten percent is detected, the loss in mechanical properties can be as large as 80 percent [7].

The assessment of in situ timber members can be improved in two ways, first by gaining more accurate estimates of individual member strengths and second by locating and quantifying deterioration. This study investigates the ability of nondestructive and semi-destructive testing techniques to do this. Several techniques were researched and applied to members to predict individual member strengths or locate and quantify deterioration. This study includes a description of the nondestructive and semi-destructive testing methods investigated, details of testing, results and discussion of the findings.

CHAPTER 2

REVIEW OF NONDESTRUCTIVE AND SEMI-DESTRUCTIVE TESTING TECHNIQUES

Five nondestructive and semi-destructive testing techniques were researched for their ability to improve the assessment of in situ timbers. Background information on their technology and application, with respect to strength assessment and/or deterioration detection and quantification, is discussed for each.

2.1 STRESS WAVES

Stress wave investigation has long been used for nondestructive investigation of wood members. Time of flight or the corresponding calculated velocity is the most common stress wave parameters used during timber investigations, however, attenuation and frequency spectrum analysis can be used as well. Discussion will be limited to these applications.

2.1.1 Equipment

2.1.1.1 Background and Technology

The use of stress waves in nondestructive testing is based on the propagation of sound waves through material and is widely used for detecting interior voids and deterioration in structural members, as well as mechanical property measurement. Sonic stress waves, commonly referred to simply as stress waves, are those with frequencies within the audible range. Ultrasonic stress waves are inaudible, having frequencies above 20,000 Hz.

Waves are transmitted by elastic materials, and propagate through a material by means of the oscillatory motion of the material particles. Wave forms are defined by the particle motion relative to the wave propagation through the material. The most commonly used wave form is the longitudinal, or compression, wave in which particles oscillate in the same direction as the wave propagation. Transverse waves cause particle oscillation perpendicular to the direction the stress wave is moving. As longitudinal waves are the most commonly applied stress wave for in situ evaluation, discussion will be limited to this wave form.

Characteristics of sound waves are frequency, the number of oscillations per given time increment, and the wavelength, which is the distance taken for the completion of one cycle. Wavelength is inversely proportional to the frequency; therefore low frequencies correspond to longer wavelengths and high frequencies with short wavelengths. Wavelength λ is related to the frequency, f ,and velocity of the wave, V, as follows:

$$\lambda = \frac{V}{f} \qquad \textbf{Equation 2.1}$$

Speed and attenuation of sound waves are the primary parameters used for nondestructive evaluation. Wave speed is simply determined through the relationship

$$V = \frac{L}{T} \qquad \textbf{Equation 2.2}$$

where V is velocity, L is the distance between two points along the path of the sound wave, and T is the time taken to traverse the distance L. Velocity of sound in the material can then be used to predict mechanical properties through empirical relationships or indicate voids and/or deterioration and will be discussed further in coming sections.

Attenuation, which is the amplitude loss of the stress wave, results from two sources; scattering at material interfaces and absorption. Attenuation, or damping, of the stress wave as it propagates has been shown to have correlation to material strength [8]. Kaiserlik presented data from experiments [9] where the average rate of attenuation was used in a model with other parameters to predict tensile strength. The model improved the estimation of tensile strength over traditional empirical relationships from a correlation coefficient of $r^2 = 0.697$ to $r^2 = 0.819$.

The rate of attenuation can be express by logarithmic decrement, the loss of amplitude per sinusoidal cycle, and is given by Equation 2.3 where δ is the rate of decay, A_o and A_j are the amplitudes of two waves j cycles apart.

$$\delta = \frac{1}{j} \ln \frac{A_o}{A_j} \qquad \textbf{Equation 2.3}$$

Attenuation can also be characterized with a similar but slightly different parameter, attenuation factor. The attenuation factor is the loss in amplitude per unit length of propagation for an advancing stress wave. Equation 2.4 defines the attenuation factor, α, where x is the length of propagation, A_o is the initial amplitude, and A_x is the amplitude at point x.

$$\alpha = \frac{1}{x} \ln \frac{A_0}{A_x} \qquad \textbf{Equation 2.4}$$

2.1.1.2 Sounding

Sounding is one of the oldest methods used to inspect in situ timber members and provides a quick inspection procedure to identify serious decay within members. With sounding, the timber member is struck by a blunt object, typically a hammer. From the resulting sound tone, a trained inspector can make inferences to the member's condition.

This method has the advantage of being able to rapidly screen timber members, however, it is highly subjective and diagnosis can vary between inspectors. Sound quality can be affected by factors other than decay which can complicate the interpretation. In addition, sound interpretations cannot quantify the extent of decay, and sounding only indicates serious decay, not initial or moderate, even when experienced persons perform the tests. In order to address these drawbacks of the sounding methods, more technical experiments using stress waves can be conducted.

2.1.1.3 Sonic Stress Waves

Velocity Measurement

Sonic stress waves can be imparted into a member with a simple mechanical impact from a hammer or blunt object in the transverse or longitudinal direction. Two accelerometers, mounted in the impact device and/or placed on the member, are used to detect passing stress waves and record time measurements.

Transverse wave investigation requires access to two opposing faces of the member, illustrated in Figure 2.1. The impact device contains an internal accelerometer. At the point of impact when the stress wave is induced, the accelerometer starts the timer. A second accelerometer is situated on the opposite face of the member and stops the timer when the wave front is detected. The thickness of the member is equal to the pathlength the stress wave travels and is used as the length parameter to calculated wave velocity, refer back to Equation 2.2

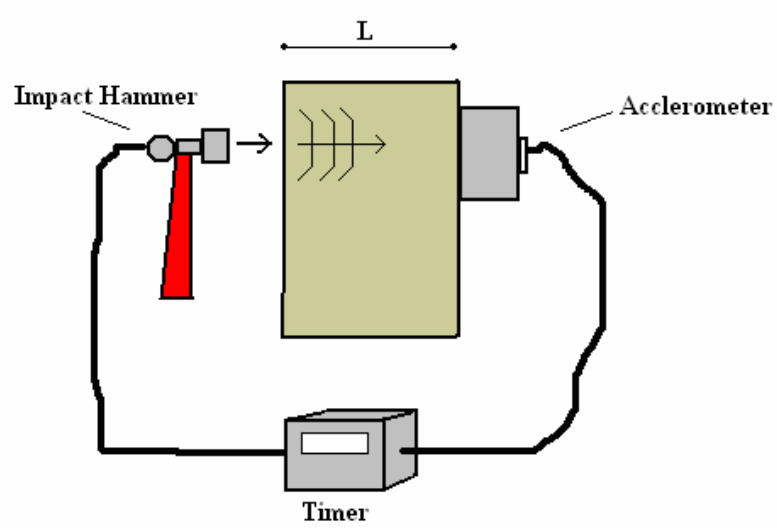

Figure 2.1: Configuration for stress wave testing using impact hammer in transverse direction

Longitudinal stress waves can be imparted in two ways, by a direct impact at the end face or impacting transducers embedded in the member, see Figure 2.2 and Figure 2.3. As the stress wave passes the first accelerometer a timer is started, then upon reaching the second accelerometer the timer is stopped. The average velocity can be calculated with the recorded time and measured distance between the accelerometers. When using embedded transducers, the angle between the transducer and member can affect the transit time if it is too large and should be considered when testing. More information on this technique can be found in [10].

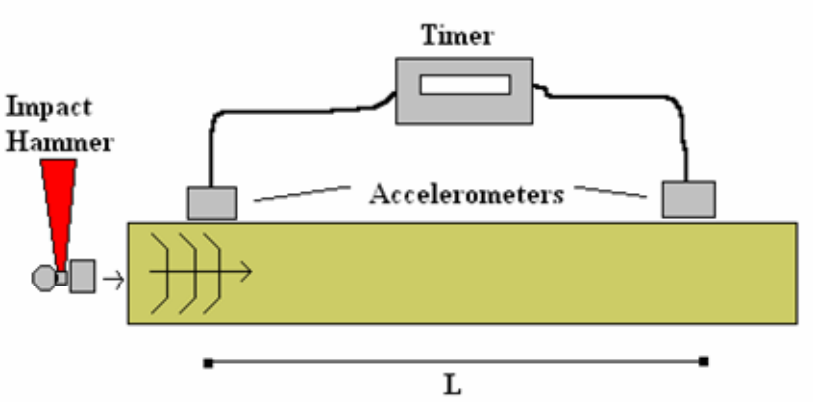

Figure 2.2: Configuration of stress wave testing using impact hammer in longitudinal direction, end face impact.

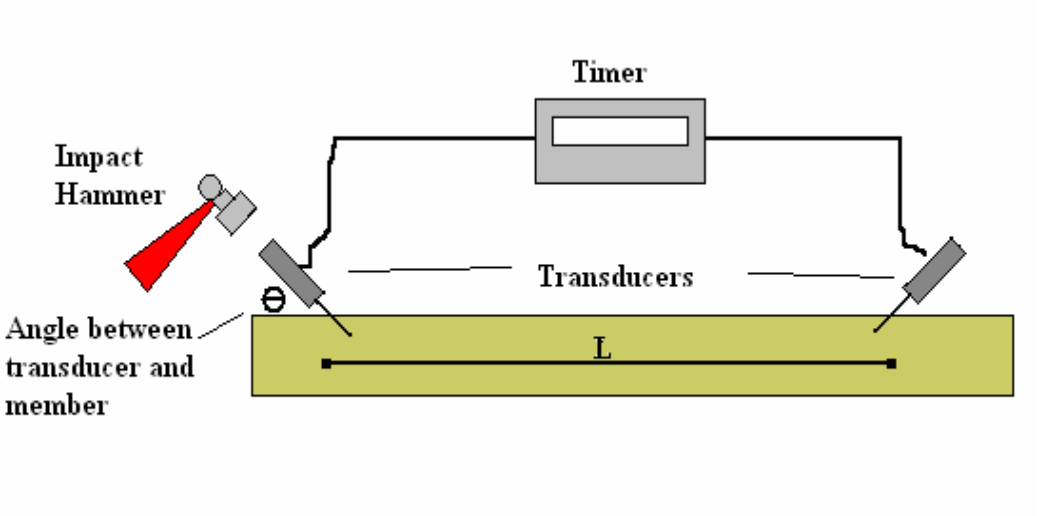

Figure 2.3: Configuration of stress wave testing using impact hammer in longitudinal direction, transducer impact.

Hammers are the typical devices used to impart mechanical stress waves in members. The material of the hammer head will change the frequency of the wave which it produces; softer materials will produce lower frequency stress waves, and conversely harder materials will induce higher frequencies. Additionally, the weight of the hammer will affect the frequency; heavy hammers will produce lower frequencies than light hammers because they experience a longer time of contact with the surface on impact [11].

Frequency Spectrum Analysis

Frequency spectrum analysis can be used to assess and quantify timber decay and has the advantage over traditional velocity measurement techniques in that only one member face is required for testing. As described in [12] and illustrated below in Figure 2.4, a specially designed probe containing an accelerometer and wired to an oscilloscope is attached to the member face. A hammer is used to induce the stress wave into the member. As the probe receives the stress wave signal, the oscilloscope transforms the time-domain signal into a frequency spectrum through Fast Fourier Transformation, Figure 2.5. Frequency is dependent on timber condition, therefore frequency ranges can be designated to levels of condition and provide an objective method for characterizing and differentiating degrees of deterioration. Multiple impact records can be compiled and plotted to produce three-dimensional plots of member cross-sections, illustrated in Figure 2.6 [12].

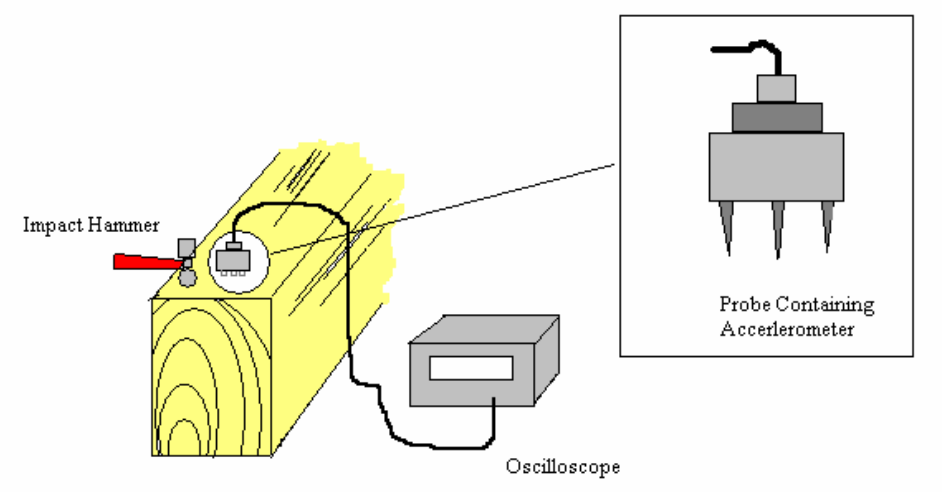

Figure 2.4: In situ stress wave set up for frequency spectrum data [12]

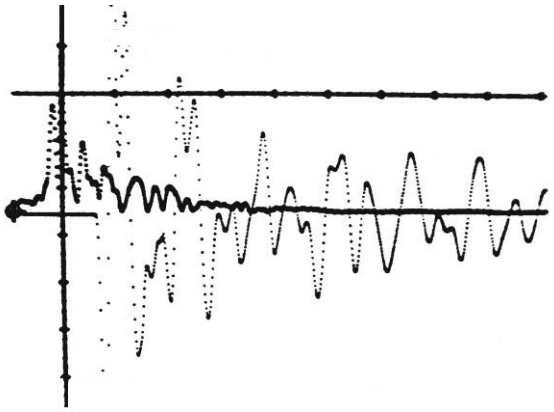

Figure 2.5: Sample time-domain wave form converted into the frequency spectrum [12].

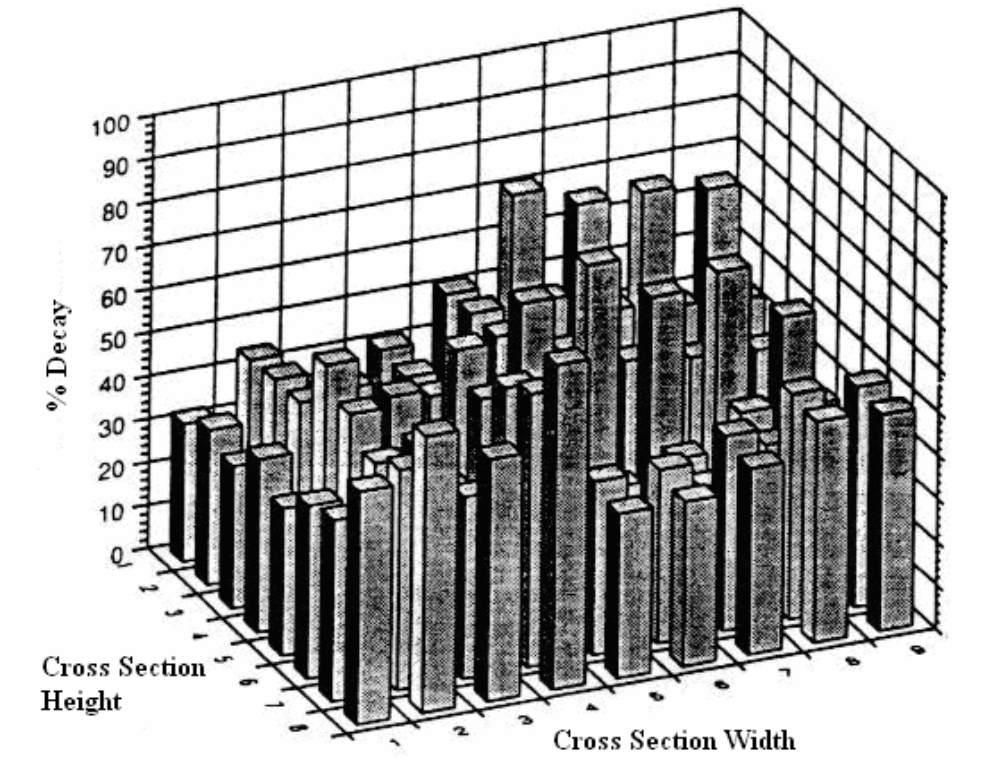

Figure 2.6: Frequency spectrum analysis: three-dimensional plot of the percentage of member cross section subjected to decay [12].

2.1.1.4 Ultrasound

The most common form of ultrasound utilizes a piezoelectric material, usually a quartz-crystal, which converts a supplied electrical current into oscillatory waves. During operation the transducer is supplied with an electrical current, converts it into a wave signal, and directs the wave into the material. A data acquisition system consisting of a signal detector, an analyzer, and a recorder collects and retains the wave information for further analysis [13].

Contact scanning requires transducers to be coupled to the material surface for direct transmission measurements. Air transmits sound waves poorly, so couplants are used to create complete contact between the transducers and material surface to limit signal retardation. The amount of energy that is transmitted into the material is

proportional to the coupling force applied to the transducer [14]. Common couplants include water, oils, greases, pastes and sometimes rubber when the transducers are held in place by hand. In some cases, the surface of the member may need preparation to ensure adequate coupling of the transducers. This can include planing, sanding or other methods of smoothing the surface.

Non-contact scanning uses transducers that do not require contact with the material surface to transmit ultrasonic waves into the material. Air can be used as the couplants in certain cases, which has the advantage of avoiding damage to the surface. Because of the difference between air and solid material impedance, the technology can be sensitive to surface roughness and experience significant energy reflection [15].

Ultrasonic testing frequencies are typically in the range of 20 kHz to 500 kHz, kept relatively low because of high wave attenuation in timber due to its inhomogeneous nature. Ultrasonic investigation is commonly used in timber grading with the transducers arranged at the ends of the lumber pieces to measure wave propagation directly along the fibers. For in-situ evaluation, that transducer configuration is not advantageous considering access to the member ends is most often limited. To address this limitation the transducers can be mounted on the same side of the member as shown in Figure 2.7. A signal is induced along the length of the member, transit time and pathlength is recorded, and velocity calculations are made. This configuration will neglect the condition of the member ends; however, it provides longitudinal ultrasonic stress waves and parameters that can be used to estimate global properties of the member.

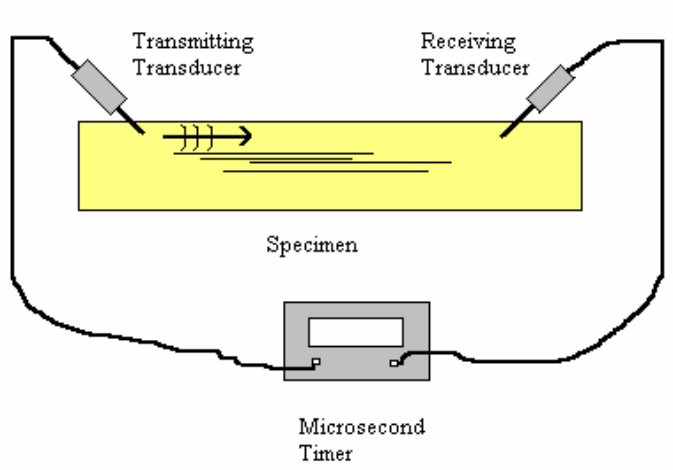

Figure 2.7: In situ ultrasonic testing in the longitudinal direction, end access is not required.

Transducers can also be arranged to impart a signal directly through the member as shown in Figure 2.8. Two transducers are oriented across from each other on opposite surfaces of a member, a signal is induced directly through the member, transit time and pathlength is recorded, and velocity calculations can be made. Access to opposite sides of an object is required for this type of configuration which can limit its use for in situ investigations.

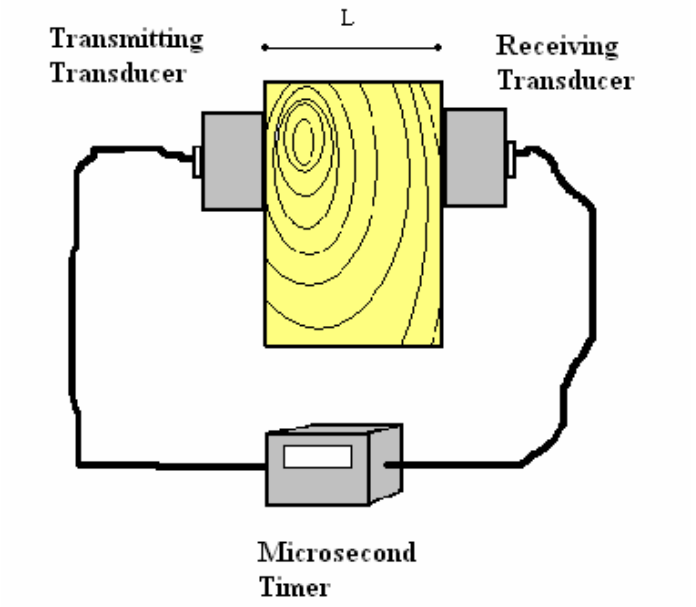

Figure 2.8: Ultrasonic transverse application

2.1.2 Application

2.1.2.1 Defect and Deterioration Detection

For void and defect detection, the wavelength plays a key role. In general, defects that are smaller than half the wavelength of the induced signal cannot be detected by the stress wave investigation. Therefore, ultrasonic stress waves (higher frequency, smaller wavelengths) have a greater ability to detect subtle interior voids and defects in materials than sonic stress waves. Ultrasonic stress waves have a higher susceptibility to wave attenuation and signal loss which can limit its use in detecting and quantifying deterioration and voids. Sonic stress waves have longer wavelengths and are not as sensitive to smaller defects and are useful in identifying larger, more significant voids and deterioration.

Velocity Measurement

Velocity of wave transmission can give an indication of material condition. As materials deteriorate, their stiffness is reduced. Wave velocity is proportionally linked to the square root of the material stiffness in which it is induced. Slower velocities or a longer transient time as compared to sound material suggests deterioration. With multiple scans, transient times can be mapped on the member, or two- and three-dimension plots can be constructed of the member surface to assess the condition. Longer transient times would be seen as high points on plots and would indicate deterioration or voids; see Figure 2.9 an example plot of stress wave times taken along the length of a member, not actual data. It is critical to calibrate the stress wave timing mechanisms to sound material

in order to establish a basis of comparison, and velocity measurements must be done in a consistent manner to minimize the variability in testing and results [16].

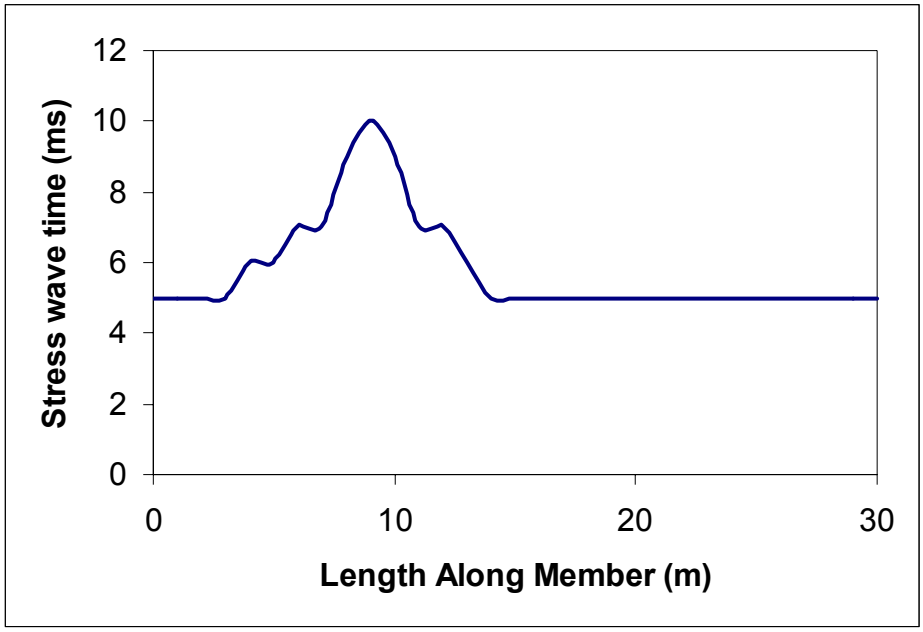

Figure 2.9: Example plot of stress wave testing.

Stress wave velocity in timber members is directionally dependent. Wood structure is mostly made up of long, tubular cells oriented along the tree trunk (longitudinally). For softwoods approximately 90 percent and for hardwoods 80-95 percent of the cells are oriented in the longitudinal direction. The remaining percentage is known as rays which are oriented in the horizontal axis [17].

In sound wood, longitudinal transmission velocities generally fall in the range of 3500-5000 m/s while in the transverse direction velocities are 1000-1500 m/s [10]. Stress waves induced in the longitudinal direction have a higher velocity because they travel along the vertically oriented cells and encounter little to no boundaries to impede their progression. Transverse waves encounter numerous boundaries and interfaces at the cell walls which reduce their velocity, illustrated in Figure 2.10.

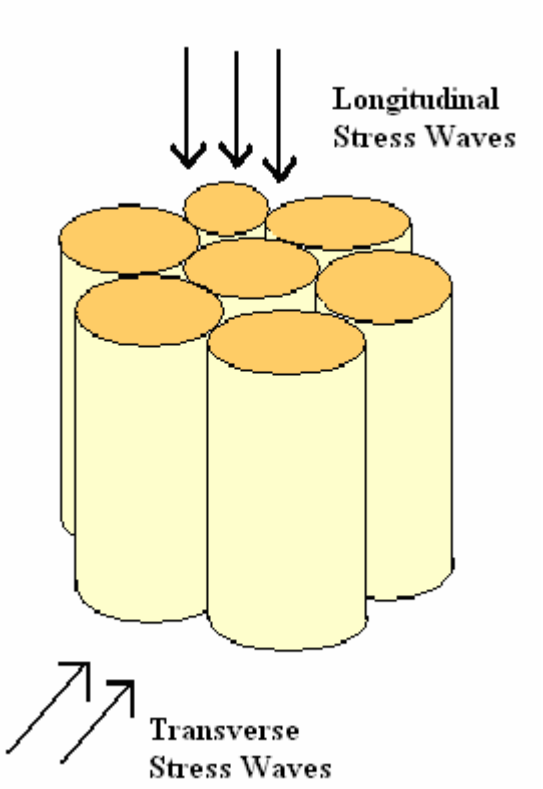

Figure 2.10: Illustration of wood structure and stress wave interaction.

Longitudinal stress waves travel the span the member and give the average velocity along the length. This velocity measurement is a global parameter which can be used to estimate properties of the member as a whole. Transverse waves travel over a localized portion of a member; their velocities are local parameters and are used to evaluate only local properties and conditions at the testing site.

Speed of stress wave transmission in degraded timber members is reduced as compared to sound members. A 30% reduction in the transmission time implies approximately 50 % loss in strength, while a 50% reduction in the transmission time indicates a severely decayed member and extreme loss in strength [10]. In order to compare transmission speed, sound timber speed must first be established for a base line

to compare degraded member sections. Tables of stress wave velocities (for both the longitudinal and transverse direction) for sound timber of different species have been complied based on experimentation that can be referenced as a source of comparison; however member specific measurements are superior as variability exists within species.

Transverse paths over the cross section of members are most advantageous for decay detection as longitudinal waves can bypass areas of decay. Multiple transverse stress wave readings can be set up in a grid system, spanning the horizontal and vertical directions of the member to map out areas with longer transit times and suspected deterioration. Areas of concern can then be analyzed with a finer grid to map out the boundary of the deteriorated regions. An example mapping from [18] is shown below in Figure 2.11.

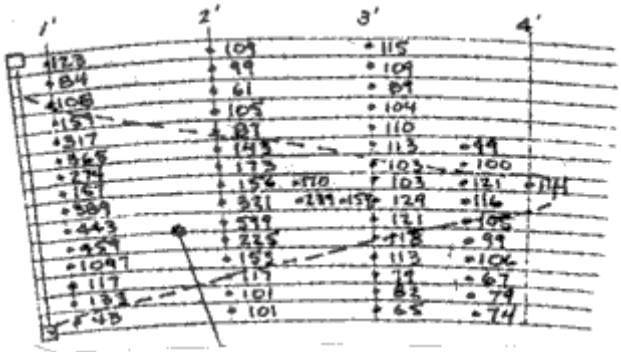

Figure 2.11: Example mapping of deteriorated regions using stress wave transmission times [18].

Attenuation

Deterioration can be identified by the degree of stress wave attenuation. As stress waves travel through a sound member, the wave amplitude reduces with time in a steady manner and the sinusoidal waves are equally spaced. In a degraded member the

amplitude of the waves will decrease at a more rapid pace as energy is lost at a higher rate to reflection and absorption [19]. A representation of wave behavior in a sound and degraded member is shown below in Figure 2.12.

Directional propagation considerations, with respect to grain orientation, should be made for timber applications. The rate of attenuation increases when the number of material boundaries encountered is high. Transverse stress waves will meet boundaries at every cell wall and will experience more attenuation than waves traveling parallel to the grain and along the long tubular cells which are only partially interrupted by medullary rays [20].

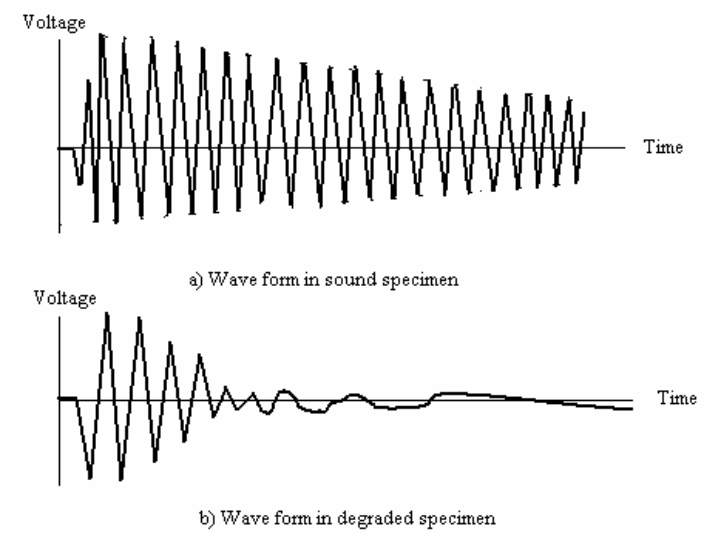

Figure 2.12: Example stress wave behavior a) sound member b) degraded member

Frequency Spectrum Analysis

Stress wave frequency spectrum analysis can provide extensive information on the deterioration level of a member. As explained in [12], the natural frequency of the wood is determined by the properties of the wood structure, and is inversely proportional

to the square root of the mass and directly proportional to the square root of the stiffness. Because decaying wood losses stiffness and mass, the natural frequency drops below that of sound wood. Different frequencies are produced based on the amount of deterioration within the member; even incipient decay can be detected which can be difficult with velocity measurements. Amplitude of the stress waves can also be a direct indicator of the portion of the wood subjected to different levels of deterioration. As a result of multiple scans, contour maps of the member's cross section can be produced to quantify and plot the extent and location of deterioration.

Plots of the frequency spectrum can be used to detect and quantify the amount and distribution of timber deterioration. The area under the frequency spectrum curve, and within a frequency range associated with a deterioration level, has a positive correlation with the amount of wood subjected to that deterioration level. The combination of the frequency plots and the three-dimensional plots of the cross sections allows the distribution of varying decay levels and sound wood to be quantified and provides a basis for quantitative evaluation of the residual strength of the wood member [12].

Ultrasonic Tomography

Cross-sectional images of timber members can be produced with the data collected during ultrasonic investigation. Two dimensional images are produced by compiling reflection data collected by illuminating the sample with multiple scans from different directions around the member. All characteristic parameters, time of flight, amplitude, frequency, etc., can be used in the data collection to produce the images. One of three algorithms (transform technique, iterative technique, direct inversion) is then applied to the collected data to produce the tomographic images. The ultrasonic

tomographs can reveal structural elements in lumber such as knots, grain deviation, cracks, compression wood, and fungal attacks, and voids [21]. See references [15] [21] [22] and [23] for further information on equipment, application and examples.

2.1.2.2 Mechanical Properties

No direct relationship between stress wave parameters and material strength exists in current theory, one of the fundamental challenges facing the technique. Estimation of mechanical properties is done through empirical relationships related to stress wave velocities, dynamic modulus of elasticity or stress wave attenuation established through experimental research. This is a practice which is generally accepted as long as strong correlations can be shown [24] [25]. Prediction of mechanical properties using stress wave parameters is largely based on the principle that correlations exist between mechanical properties and the modulus of elasticity. Stress wave analysis can effectively measure modulus of elasticity; however it requires significant extrapolation of measurements to predict ultimate strength [24].

Velocity Measurement

Sound travels at different speeds through different materials and is affected by two main properties of the material, the modulus of elasticity and density. Poisson's ratio also has a minor effect on the wave velocity. After establishing stress wave velocity in a member with the relationship presented in Equation 2.2, the relationship below can be used to calculate the dynamic modulus.

$$E_d = V^2 \rho * \left[\frac{(1+\upsilon)(1-2\upsilon)}{(1-\upsilon)} \right] \qquad \textbf{Equation 2.5}$$

This equation, where E_d is the dynamic modulus, V is the wave velocity, ρ is the mass density in, and υ is Poisson's ratio, is the representation of wave propagation in a three-dimensional medium. The simplified one-dimensional wave form equation for a homogeneous and isotropic material is commonly used for dynamic modulus of elasticity estimations without the consideration of Poisson's ratio, Equation 2.6. Although wood is neither homogeneous nor isotropic, several researchers have found that one-dimensional wave theory is appropriate for describing wave behavior in timber [26].

$$E_d = V^2 \rho$$

Equation 2.6

Density of the member may be difficult to determine and may require sampling for laboratory testing. A small sample will only give local information on member density so multiple samples along the length of the member will be required for estimating the global, overall density of the member.

After estimates of E_d have been made, empirical relationships are used to estimate timber mechanical properties. These experimentally established empirical relationships have varying correlation values, some of which can be strong and others weak. The complex nature of wave propagation in timber influences the ability to predict strength properties and the presence of naturally occurring defects influences the ability to predict the performance of timber members [8].

As an alternative to using empirical relationships between stress wave parameters and mechanical properties, sampling can be used to calibrate stress wave measurements with strength properties. Stress wave measurements can be made and followed by sample extraction at the same location. The samples can then be tested destructively to

correlate the stress wave parameter to strength. This relationship can then be applied to remaining members under investigation. The correlation between the sample strength and stress wave parameters will vary and is highly dependent on the number of samples taken to establish the correlation. Strong correlations have been shown when adequate sampling to establish the relationship to stress wave parameters is done [27].

2.1.3 Limitations

Several factors can effect the transmission of stress waves in timber, control stress wave application parameters and make interpretation of results difficult. Frequency selection may be subject to the material condition and defect size. Wood has a higher rate of attenuation then most structural material but deterioration will cause increased attenuation effects. Attenuation can be so severe that signals can be completely lost or used only on small member sections. Attenuation will worsen with high frequencies, but high frequency transmissions are also more sensitive to internal defects. The result is that higher, more sensitive transmissions are limited to spans sometimes too short for any practical use. Low frequency transmissions will not experience as much attenuation and can span greater distances; however they are less sensitive to small defects within the member.

Characteristics of the member such as its geometry, ring orientation and preservative treatments, the physical properties of transducers, the mechanical loading on the member, and its moisture content and temperature [20] can all affect stress wave velocity and attenuation and should be carefully considered. Equipment and measurement conditions should also be taken into account, including the coupling agents and their bond ability, the sensitivity and frequency response of transducers, the difficulty in

controlling impact durations and energy from impact hammers, and the frequency selection for parameters investigated. More information on the specific effect of these factors and other influences beyond the scope of this paper can be found in a multitude of references including [9] [11] [12] [20] and [28].

Access to in situ members may also limit the use of some stress wave testing techniques. This would include both the access to appropriate member faces as well as issues related to location, such as areas that would require scaffolding or those that could make proper equipment use difficult. Environmental conditions, such as heat and moisture, and the surface condition of the member can make application of stress wave equipment problematic and can affect transmission data making repeatable experiments difficult.

Error can arise in ultrasonic testing due to inadequate coupling of transducers. Air is a poor transmitter of sound waves, so the transducers must have adequate surface contact with the testing member to limit the retardation of the transmission. Common couplants include materials which can adversely affect the surface of the member in question. One must consider the effects of such couplants on the member associated with the surface finishes, chemical reactions that might incur, and any damage that might be the result of removal or clean up. In addition, some surface preparation is commonly called for that can alter the appearance of the member including sanding or leveling of the transducer site to promote ultrasonic transmission.

2.1.3.1 Deterioration and Decay Detection

Longitudinal waves can give realistic average values of the beam stiffness but can be significantly affected by defects such as ring shakes, localized decay and moisture

gradients. The waves can bypass these areas, only giving record of the fastest transit times [29]. Stress wave times are also unaffected by damage caused by termites as shown in [30], which can lead to inaccurate estimates of degradation damage and mechanical properties.

Transverse transmissions are better for deterioration detection and can provide information on its distribution, however there are some drawbacks. As pointed out in [29], internal seasoning checks can be mistaken for deterioration, moisture content gradients can alter propagation times but be difficult to measure on heavy timbers, and knots close to transducers and oriented with their longitudinal axis in the direction of wave propagation can increase the wave velocity giving misleading data and material representation.

Speed of transmission comparison can be hindered if base line transmission speeds for sound material is not available. If transit speeds of sound material can not be established on site, tables of sound transit times for different species can be consulted. However, not all species have been thoroughly tested to establish speed of transmission of sound members, especially in hardwoods, and variability within species still exist which influence the velocity comparison [31]. Additionally, accurate species identification must be established in order to use these tables reliably and moisture content (of the member of interest comparative to samples used for tabulated speed values) will have to be considered. Moisture content will cause an increase in propagation time with increased moisture content up to approximately 30% [10]. Up to 30% moisture content, velocity reduces rapidly with increasing moisture. Above approximately 30% moisture content there is a sharp change in the effect of moisture on

velocity and velocity decreases slowly with additional moisture [32]. The effects of preservative treatments, grain orientation and wave propagation direction may also be a factor in assessing velocity comparisons for deterioration detection.

2.1.3.2 Mechanical Property Prediction

Predictions can be subject to many sources of error including accurate measurements of the member density. Accurate density measurements cannot be measured in a nondestructive manor and therefore must be found by other means and used in combination with stress wave velocity to predict the dynamic modulus. Other methods include tabulated values associated with various species, pilodyn testing, hardness tests, or core sampling. Of these, core sampling and lab evaluation are the most accurate measurements of density. Density established with core samples can be useful, however it will provide only local densities values. Since density of the member may change along the length, multiple samples will be required to establish a mean value for the member as a whole.

Assumptions of the path length of stress wave transmissions can be inaccurate, affecting the dynamic modulus predictions. Pathlength, L in Equation 2.2, is assumed to be a straight line between two locations, but it can be extended due to internal features such as knots, grain deviations or material separations.

Empirical relationships to estimate mechanical properties can have a varying degree of correlation, some quite weak. Independent studies have also published conflicting results on correlation values. Additionally, [24] states that investigators and vendors at times overstate the correlation between measured quantities and the strength of the tested structural component and that strong correlations are questionable because of

the indirect link between the parameters and the strength. Property estimate correlations are further reduced due to compounded correlations. Typically a dynamic modulus is calculated from stress wave velocity measurements, which has its own correlation value. After estimating the dynamic modulus, empirical relationships, with varying correlation coefficients, are used to predict strength values. The total correlation between the stress wave parameter and the predicted strength value would then be the product of the two correlation coefficients, a reduction in total correlation since correlation coefficients are less than one (excluding perfect relationships).

2.2 RADIOGRAPHY

Radiography uses penetrating radiation to inspect and gain insight of the internal structure of members. A radiation source is used to emit a beam of radiation directed towards an object of interest. Objects under investigation will have varying absorption of radiation based on the material density and thicknesses. Opposite the source of radiation and behind the object of interest is a radiation sensitive film or recording medium that produces images, see Figure 2.13. This noninvasive procedure allows for extensive investigation into issues such as structure composition, hidden internal materials and flaws, and state of preservation, which at times cannot be gained by other means.

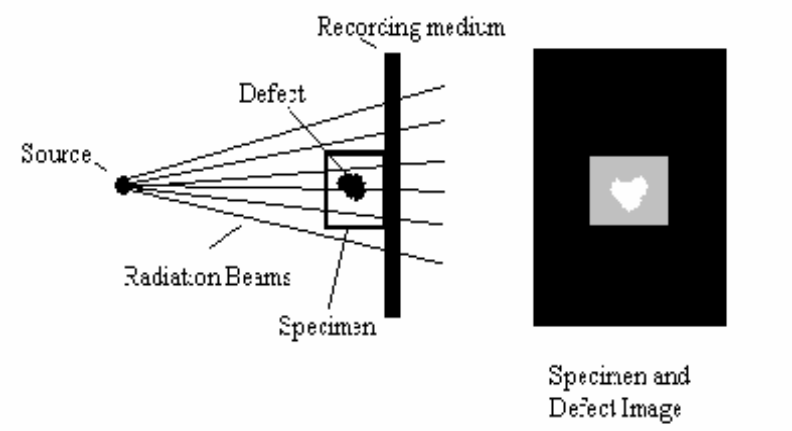

Figure 2.13: General arrangement for radiographic imaging

Digital imaging systems and digital radioscopy have seen advancement because of their traditional use in security, bomb and drug detection, and forensics as well as industrial non-destructive testing for quality assurance. The advancement seen from these commercial uses have lead to the development of highly portable and user friendly systems that can be run either on battery or with common AC/DC adaptors depending on the system. Laptop computers are generally used with these systems and allow for nearly instant image viewing and manipulation. Such advancements in design and technology have led the technology to be readily applied to in situ structural investigations.

2.2.1 Equipment

2.2.1.1 Background & Technology

Penetrating radiation used in radiography is generated from several sources, most commonly electrons, neutrons, gamma rays and X-rays. Electrons used in radiography are produced either by radioactive decay or high-energy X-ray impact on a heavy metal. Because of the strong absorption of electrons by all materials, the penetration power is

limited and restricts the usefulness of this radiation source to thin, low density material [33].

Neutrons are produced by linear accelerators or nuclear reactors and are prone to absorption by organic material. Neutrons are rarely used for in situ investigation for multiple reasons including the limited access to linear accelerators or nuclear reactor sources, the expense of equipment and operation, issues related to the difficulty of on site equipment set up, limitation to small areas of investigation due to the narrowness of the radiation beam produced, poor reaction of neutrons with film, and the possibility of objects becoming radioactive after investigation [33].

These drawbacks limit the use of electron and neutrons as radiation sources for in situ investigation and the remainder of the discussion will focus on gamma and X-ray radiation sources.

Gamma rays and X-rays are the most commonly used sources of radiation used for radiography. They are short wavelength electromagnetic radiations which are physically the same but differ in the way they are produced. Both travel in straight lines at the speed of light, can be diffracted but not deflected, and are unaffected by electrical or magnetic fields. The rays penetrate matter, the degree of which is dependent on material type, density and thickness as well as the radiation energy [22] [33].

Gamma Rays

Gamma rays are emitted during the radioactive decay of unstable isotopes, each having a characteristic energy and intensity for the radiation it emits. The high energy levels of the gamma rays create substantial penetration capabilities. Isotope energy remains constant, however, the intensity decays with time as indicated by the half life.

The wavelengths of the radiation produced by the gamma sources are distinct and limited as opposed to X-rays which have a broad wavelength spectrum.

Although gamma and X-rays are physically the same, the production differences have a distinct effect on gamma rays use for in situ evaluation. Gamma rays have the advantage of a portable nature since radioactive isotopes do not require the external energy or cooling sources that X-ray generators do. The elimination of external power, as well as the reduction and compactness of the equipment, make the method more mobile and less expensive.

The advantages of a radiation source with no external power are limited. The radioactive isotopes continually generate radiation and require special containers lined with lead for storage to protect against the harmful effects of the radiation on living tissue. In addition, when use of the source is needed it must be removed from the storage container by means of a remote controlled mechanical device. The source also has a limited life span as it loses its intensity over time, depending on the half-life of the isotope in use, and the high energy radiation of gamma rays cannot be controlled, resulting in poorer quality imaging with lower contrast than X-rays [33].

X-rays

X-rays are produced when high-speed electrons impact matter. Energy is lost upon impact and a small fraction is converted into short wavelength radiation. The remaining impact energy is mostly converted to heat. The X-ray spectrum is comprised of two underlying spectrums, the line spectra and the continuous or 'white' spectra. The line spectrum is specific to the material under investigation and has specific wavelengths. The continuous spectrum is the one used in radiography and is produced by the rapid

deceleration of the electrons on impact and has a broad range of wavelengths [15]. Wavelength and energy are used to characterize X-rays and are related through the equation below where E is the radiation energy, h is Plank's constant, c is the velocity of light and λ is the radiation wavelength. From inspection, higher energy will have shorter wavelengths, allowing for more penetration capability.

$$E = \frac{hc}{\lambda} = \frac{1.24}{\lambda}$$ **Equation 2.7**

X-ray Generation

X-ray tubes are a key component in the generation of X-rays beams for traditional X-radiography. A cathode and an anode are contained within a glass bulb under vacuum. The cathode contains a wire filament which will emit a continuous stream of electrons when heated to incandescence. The anode contains a target at which the electrons are directed. It is at this target that X-rays are produced upon impact. This target is generally made of tungsten for two reasons, first, it is a good source of high-energy X-rays and second, it has a high melting point. Most of the energy used for X-ray production (99%) is converted to heat and most of this heat conversion takes place at the target so it is necessary to have target material which can withstand high temperatures.

The electrical tension between the anode and cathode causes the acceleration of the electrons to the target, and the electron stream is focused into a beam by a cylinder or focusing cup. After impact on the target, the X-rays exit through a window made of a light element, usually beryllium, that will not absorb much of the radiation as it passes. The target is oriented at an angle to the beam of electrons in order to project the x-rays out the window. The angle at which the target is oriented reduces the effective width of

the target and the X-ray beam width. This will have a large effect on the image production as a smaller effective target width produces sharper radiographs.

X-ray equipment is characterized by its potential (in volts) and current; factors which control the intensity and penetration capabilities of the radiation. Typical equipment has a range from 50 kV up to 320 kV, but for specialized uses up to 450 kV. For portable units a potential of 200 kV with an intensity of 3 mA is standard [22][33].

Radiation Attenuation

As X-rays and gamma rays pass through material attenuation occurs depending on the material composition, density and thickness as well as the energy of the radiation beam. This attenuation, or loss in intensity, is what makes radiographic inspection possible. The detection of the difference in radiation intensity is recorded to produce radiographic images for further inspection. The intensity of radiation upon exit of a material is given by the exponential expression

$$I_X = I_O \cdot e^{-\mu \cdot t} \qquad \textbf{Equation 2.8}$$

where I_X is the emergent intensity, I_O is the initial intensity, t is the thickness of the material and μ is the linear absorption coefficient per mm thickness, a material characteristic affected by the density.

Attenuation is also dependent on the radiation energies. Radiation beams with low energies are more readily absorbed and prone to scatter, resulting in less penetrative power. In contrast, higher energy beams will be more penetrative with less absorption and scatter occurring.

Imaging

Radiographic images are produced based on the intensity of radiation exposure on an imaging plane. Images can be permanently recorded using traditional film or paper mediums, or sensitive real-time imaging mediums integrated with digital systems and software.

Film radiographs are the traditional form of capturing images. These films have an emulsion that reacts and changes when exposed to radiation. Upon development, a negative image or "shadow image" is produced where denser areas, which allow less radiation exposure, appear lighter. This form of imaging has been limited for in situ evaluation when used with the traditional high-energy radiations for safety concerns as well as the high cost of the operation; however it does provide a permanent record of the investigation and film is relatively inexpensive to purchase and process.

Radioscopy, or real time imaging, was one of the first forms of radiographic imaging. Traditionally florescent screens were used with high-energy radiation sources to produce an image based on the ensuing radiation. The screen emitted light based on the radiation it was exposed to; brightness being proportional to the intensity of the ensuing radiation, producing a positive image. This method was more portable than film radiographs and offered the advantage of real-time images that could be utilized to improve the inspection. There was however safely concerns associated with the high-energy radiation source and such a technique was unable to record the images for future analysis.

With technological advances digital radioscopy has emerged without these drawbacks. The radiation source can be of a lower energy and detected radiation can be

recorded on reusable imaging screens and processed into digital images that can be stored for future use. Digital storage of images allows for powerful image enhancing tools to be utilized; giving more detail to images and allow for further information extraction.

Image Quality

High contrast and sharpness are desired and make inspection and interpretation of the radiographs easier. Geometric features relating to equipment and object positioning will affect the image sharpness. The image property known as *geometric unsharpness*, *Ug*, is given by an equation with variables *S*, the size of the focal spot within an X-ray tube, *a*, the distance from the source to the object, and *b*, the distance from the object to the imaging material.

$$Ug = S\ (b/a) \qquad \textbf{Equation 2.9}$$

Sharpness and image quality will decrease if the focal spot in the radiation equipment is large and with the increase in distance between the object and recording medium. Distance between the object and the recording medium should be kept at a minimum to improve image quality and to avoid image magnification and distortion. The distance *b* can be increased to produce a magnification of the object to inspect small features, but this should be done carefully to keep the unsharpness at an acceptable level [33].

The contrast of images is the amount of difference seen between densities and is an important quality issue since good contrasts distinguishes member features. Contrast of radiographic images is highly dependent on the recording material and energy levels of radiation. Lower energy radiation produces higher quality contrasts, but is limited in its

penetration ability and the range of densities it can produce on an image. Higher energy levels, while more penetrative, will have less contrast in images. Selection of radiation energy will most likely depend on the material investigated as well as the detail needed in the radiographs.

Image quality can be greatly affected by the selected view (the source, object, imaging plate relation). In general it is best to orient the radiation source and the image capturing material at right angles to the object surface to avoid gross distortions which make interpretation difficult. This however is not always plausible or desired based on the in situ member orientation and shape, the available access, or specific areas of interest on the object that do not lend themselves to this type of arrangement. This can cause increased difficulty in radiograph interpretations as a result of distorted size, orientation or overlapping images. It is helpful to place identifying markers on the imaging planes as a reference point to help identify the proper orientation of the image. This is true not only in cases where interpretation is suspected to be difficult, and it makes future interpretations of the images easier if the marker orientation is known or standardized. These markers should be of a material that will easily appear on the radiograph and should be placed on the outer edge of the imaging planes to avoid interfering with the area of interest.

Orientation of the radiation beam must also be carefully considered when using radiography for deterioration or crack detection. It must also be noted that for crack detection, the radiation beam must be parallel to the crack or the crack must be sufficiently large to be detected.

Image Enhancement

Digital imaging systems offer the ability for image enhancement. Laptop computers can process the images onsite many times and perform numerous manipulations to improve image clarity. Manipulations would include contrast adjustments, brightness, color processing, figure orientation and magnifications. A feature useful for image interpretation reverses the gray scale so that darker areas will correspond with areas of higher density, producing a more intuitive represented image of the member. Software can also produce grid overlays and measure image features on screen. Onsite imaging and enhancement also gives inspectors the advantage of viewing their work to make further images and adjustments or corrections as necessary for their investigation needs.

2.2.2 Application

Radiography has been used since the 1960's for defect and deterioration detection investigations of in situ structures. Original use of high energy x-ray sources limited radiographic investigation, but the development of digital radioscopy systems has increased its use due to reduced safety concerns and cost, the ability to produce images nearly in real time with reusable imaging plates, and the capability to perform initial image assessment and manipulation on site [34]. Application on notable structures includes Thomas Jefferson's Academicals Village at the University of Virginia, Monticello, and the Narbonne house in Salem Massachusetts. Radiographic images were used to investigate the timber condition as well as verify the existence and condition of metal fasteners and hardware and answer questions of internal or hidden construction

techniques [34][35]. For this research application, the interest lies in x-ray use to locate deterioration in timber members and discussion will be limited to that topic.

Attenuation is a function of the radiation energy, member thickness and, important for material condition inspection, density. Timber condition can be assessed by examining the density variations of radiographic images. Decay will appear as areas with less density resulting from the breakdown of the material.

Stages of deterioration can be identified through the examination of the radiographs. Sound wood will present a clearly defined wood structure including annular rings or grain, and optical density will be uniform. Partial decay will show loss in the wood structure, annular rings will appear but will be vague, and the optical density will vary over the material showing areas of density deviation. Decayed areas will have lost the wood structure, appearing only as an amorphous mass. Horizontal separation lines will appear resulting from the material breakdown, and decay pockets will be identifiable. Advanced decay will have the same features, but they will be more severe and extended through the member [36].

High resolution images of wood members can be produced which will show density variations between early wood and late wood. This distinction in density variation allows for grain to be visible in the images, as shown in Figure 2.14. Variations or loss in grain distinction can be used to assess timber construction as well as identify areas where deterioration or infestation has set in. Figure 2.15 is an example of a deteriorated member; the lighter portions of the image correspond to loss in density due to decay and the grain pattern in lost in this area as well.

Disruption in grain structure can be used to locate internal features such as knots and grain deviations. Insect damage has been identified and located using radiography on timber members. Mechanical damages, such as fractures, drill holes, cuts, or naturally occurring cavities can also be identified.

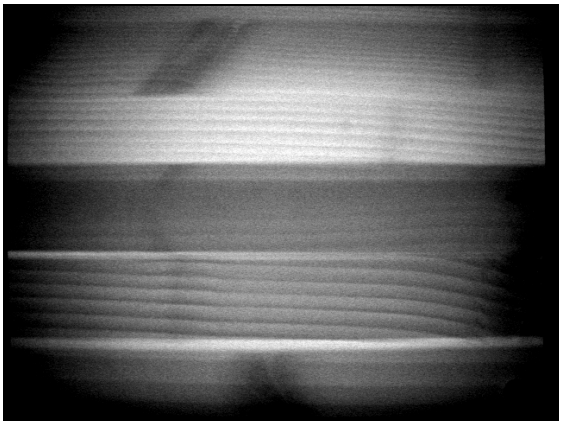

Figure 2.14: Example of sound wood with wood grain visible in x-ray image, laminated timber beam.

Figure 2.15: Example of deterioration visible in x-ray image.

2.2.3 Limitations

While radiography offers the ability to view internal characteristics of members, there are limits and disadvantages to the techniques. Radiographic investigation can commonly identify deterioration and defects in timber material; however defect depth can

be hard to establish, and the extent of deterioration cannot be quantified. Radiographic images produce a two dimension representation of the inspected timber member by compressing data through the thickness into one plane. Therefore the density data and images produced represent the average density of the member through the thickness. This fundamental imaging process does not allow for information to be gathered on the depth of internal features and can make detection of cracks or defects that are oriented perpendicular to the radiation path difficult. This also makes estimates on the amount of material lost to degradation and decay difficult based on single images of the member. Sound wood structure can also be superimposed over deteriorated areas and make interpretation and quantification difficult.

More images, taken from different angles and on different faces, would help in gaining perspective on the extent of internal damage. This would raise the time and cost associated with the investigations. Research into the ability to quantify deterioration through image manipulation and radiographic data is, however, being investigated currently.

Detection of internal flaws using radiography can be limited by size and orientation of defects. Locating internal cracks requires that the crack be of adequate size, at least 2% of the member thickness according to [22], and must be oriented parallel to the radiation beam to be detected.

Although reduced with the development of low energy portable x-ray systems, safety can be a concern which can limit its use. Radiation is not detectable to human senses but it is very harmful to living tissue. With these characteristics, it is important to monitor radiation exposure when using radiography. This is especially true when using

high energy sources needed for inspecting high density or thick members. Safety risks can be minimized by monitoring exposure and using good protective practices with radiation. Exposure is most commonly monitored using pocket dosimeters or film badges worn by personnel at investigation sites. The level of exposure can be controlled by simple means. Restrictions should be placed on the source intensity and the emission direction and all persons in the area should be kept informed as to when exposures are done as well as kept out of the immediate area of radiation investigation [22].

Limitation on the intensity or energy level of the radiation source can also limit investigation of materials. Thick members may be difficult to examine with the low energy radiation sources that are used for in situ investigations. If the member is too thick not enough x-rays will be transmitted to produce quality images, or the time required to scan with adequate results will be excessively long [37].

Member arrangement can also make positioning of the source and imaging plates very difficult and require equipment solely for access purposes, as well as more thought and time put into the set up and interpretation of the images. Problems placing image capturing materials opposite radiation sources can arise in many situations. Most equipment currently used for radiographic investigation requires access to opposing sides of a member, which for in situ testing may not be available. View choice may also be obstructed by other structural material making desired view of the member inaccessible.

In addition to these functional issues, radiography is also a more expensive form of nondestructive testing than many other alternative methods. Portable units make members more accessible for inspection, and allow for processing the images onsite with little to no costs, but the initial costs of the equipment is expensive. Limitation on source

energy will also increase time needed and costs incurred with inspection of thick or very dense members.

2.3 RESISTANCE DRILLING

The most common damage to timber members comes from deterioration which can inflict internal damage without surface indicators until the damage is considerable and severe [38]. Resistance drilling gives a semi-destructive method that inflicts minimal damage to the member surface while giving information on the internal condition of timber members. Resistance drilling has been used in many applications including tree growth and health investigations, bridge and building investigations, and in the termite and pest control industry.

2.3.1 Equipment

Resistance drilling offers a non-destructive means of analyzing the quality of the interior material in wood members. Resistance drills use small diameter (1.5-3.0 mm [0.6-0.12 in]) needle-like drills to bore into timber members and measures the resistance the drill bit encounters as a function of the penetrated depth. Resistance drills have electric motors and are battery operated, offering portability for field investigations. Drill bits are flexible, tungsten steel-tipped needles that will vary in length depending on manufacturer. Drill weight will also vary with manufacturer but will typically be close to three kilograms [6.6 pounds]; equipment shown in Figure 2.16 and Figure 2.17.

Figure 2.16: Resistance Drill

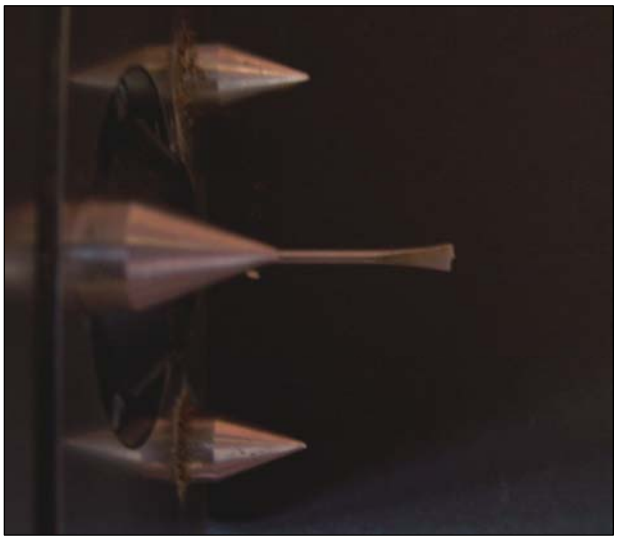

Figure 2.17: Resistance drill needle

The drill bit is advanced and rotated at a constant speed throughout the drilling. The torque required to maintain the constant cutting speed corresponds to resistance and is recorded and graphed with respect to the penetration depth [38]. Graphing of resistance data can be done with paper strips, wax paper, or recorded and stored electronically on computer. Peaks in drilling plots correspond to higher resistance or density, while dips and low points are associated with lower resistance and density;

example graph presented in Figure 2.18. For this figure, the area above the red line indicates reduced resistance.

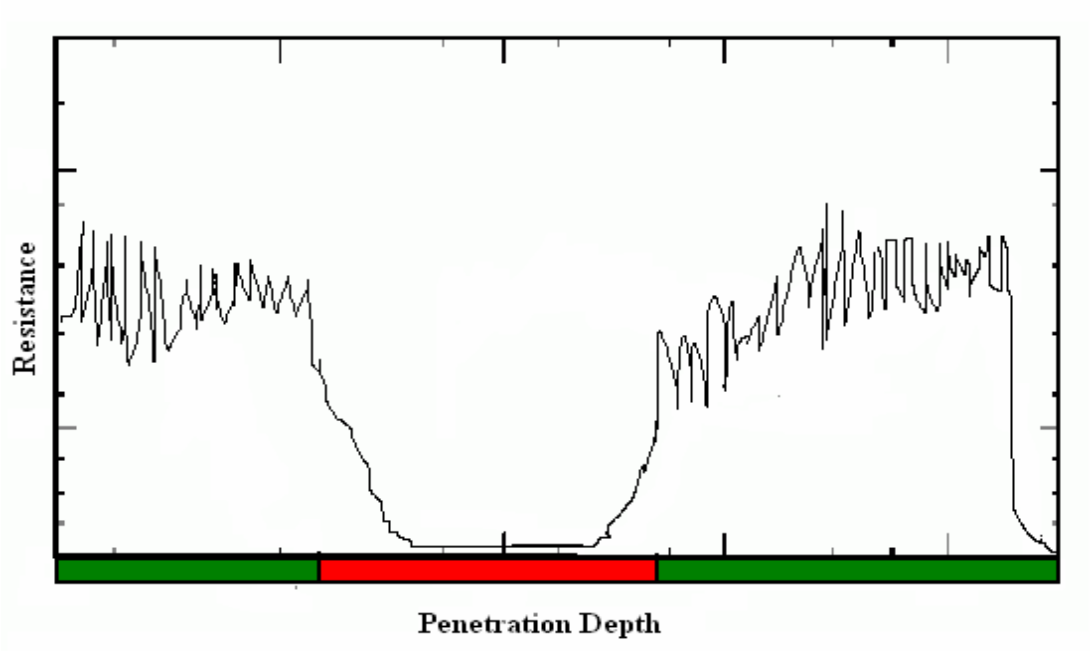

Figure 2.18: Sample resistance drilling log

2.3.2 Application

Resistance drilling is used to locate and quantify deterioration in wood members. Resistance observed while drilling is proportional to density variations, or relative densities, of the timber member. Less drilling resistance requires less torque production by the motor. Areas requiring less torque are associated with reduced density such as points with interior voids, deterioration, splits or cracks [35].

Logs of multiple drillings from different directions, over the cross-section, and along the length of the member can be compiled and organized to map the condition of member. These plots can define the cross-sectional condition at a point along the member and/or the plots can be used to map the extent and penetration of deterioration along the member length.

Different levels and sources of deterioration will exhibit different drilling resistance patterns. Peaks and valleys will differentiate between areas of high and low densities. Total decay will offer no resistance and the drilling profile will appear as a zero flat line where voids are present. Deteriorated material will show some resistance, however, below that of sound wood. Sound wood will require more torque production from the drill motor and show high resistance. Sound wood will still exhibit peaks and valleys associated with early and late wood resulting from their density variations.

Insect damage has distinct drilling patterns. As insects, such as termites, target different parts of wood, they leave some areas intact and others void. Drill plots will show repeating spikes in resistance as the drill passes through the sound wood left behind and the voids resulting from the insect infestation [39].

While resistance drilling offers a sound method for detecting and measuring interior damage in timber members, it offers no quantification of mechanical properties. Studies have shown that the correlation of the drill resistance to the density of the timber member is variable, citing weak correlation coefficients between r^2=0.21-0.69 from [35] and correlation coefficients as high as r^2=0.85 for wood at ten percent moisture content from [39]. Even with strong correlation between drilling resistance and density values, the relationship between density and mechanical properties is not well defined.

Feio *et al* [40] performed comparative tests between destructive tests and resistance drilling. Feio *et al* [40] used a parameter termed a Resistance Measure (RM) which allowed for the resistance drilling results to be compared to the density and strength values obtained destructively.

$$RM = \frac{\int_0^h Area}{h}$$

Equation 2.10

The RM parameter is the ratio between the integral of the area of the drill diagram and the height of the test specimen *h*. Feio *et al* [40] showed that the correlation between the RM value and measured density to be r^2= 0.71 for new timber and r^2= 0.68 for old timber. RM had a correlation to modulus of elasticity of r^2= 0.60 for new timber, and r^2=0.64 for old timber. Correlation of RM to longitudinal compressive strength was shown to be r^2= 0.59 and r^2= 0.64 for new and old timber respectively [40].

The use of the RM value to estimate mechanical properties is questionable. The area of a resistance drilling plot can be affected by multiple parameters including drill bit sharpness and general equipment use such as drill orientation. On a single member, changes in the orientation of the drill with respect to growth rings will change the calculated RM value with each drilling. Drill orientation into the pith results in drilling perpendicularly through many tightly spaced growth rings, drilling oriented outside the pith encounters less growth rings which are spaced out, see Figure 2.19. The RM value could be highly variable for a single member, producing variable estimates of the mechanical properties [41].

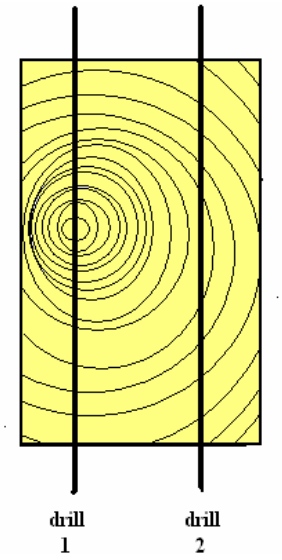

Figure 2.19: Drill orientation effect on annular rings encountered

Resistance drilling can, however, be used to estimate mechanical properties of members based on the quantification of deterioration and basing calculations on the remaining sound material and information on clear strength that can be estimated with other non- and semi-destructive testing.

2.3.3 Limitations

As with most investigative techniques, limitations exist that can prevent the use of resistance drilling. Accessibility is a common factor and includes issues such as limited space to fit drill equipment, achieving the required alignment to drill desired areas with limited space, complete obstruction from other structural members or elements, and issues of location such as height or orientation that makes the option of drilling unavailable. Equipment itself might limit accessibility based on the length of drill bit with regards to the member dimensions and drilling the full desired dimension. Drilling

equipment can also become heavy and cumbersome to the operator after multiple drillings and extended use.

Cross-sectional mapping can be very useful for locating and identifying extent of internal damage, but it can require multiple, time consuming drillings. Multiple drillings, if any are allowed at all, may be limited by member surface décor, significance, or property owner objections, eliminating mapping ability.

The small diameter drill needle has a low stiffness making it at times too flexible. The drilling needle can bend and follow growth rings as it penetrates the member. This can cause deviation in the drilling path and inaccuracy in drilling profiles, especially if the path deviation goes undetected.

2.4 CORE-DRILLING

Core samples are most commonly circular specimens tested in compression to establish the compressive strength of the material. Core samples provide a local property value that can then be used to make inferences on the member's overall strength.

Equipment includes manual or electrically driven drills for core extraction, as well as load cells and fixtures for testing the cores. Core samples will vary in size depending on equipment, but the premise behind this semi-destructive testing technique is that the extraction of cores will leave holes that are smaller than most knots found in timber members and will not compromise the strength [35][42]. Voids left by drilling should be plugged to prevent moisture and insect penetration, reducing the likelihood of introducing decay at the coring location, to restore some of the minimal compressive strength lost and help to preserve the appearance of the member [35][42].

Core samples can provide multiple indicators of the member's general condition and wood anatomy, as well as be destructively tested to extract mechanical property information used to make inferences about the whole member.

2.4.1 Equipment

Incremental borers were originally used for measuring the growth and investigating the health of trees. Borers can be manual or electrical, but both contain a hollow bit made of steel to produce small radial cores. Manual corers are auger-like tools operated with a brace-and-bit motion. To prevent breakage of drill bits, starter holes can be made with a punch mounted hammer or an electric drill. Drilling can also be made easier by applying soap or wax to the drill bit.

Hollow drill bits can be specially fabricated to fit on standard power drills [43]. This can greatly reduce the time required for core sampling. Speed should be monitored so that drill bits and cores are not damaged, especially in dense woods or if metal fasteners could be present.

Drill bits, used manually or power driven, should be kept sharp and clean to maintain quality core sampling. Dull or dirty bits can cause core samples to appear damaged or decayed as well as cause cores to jam within the bit [43][44]. After taking samples, the cores should be stored and transported in safe containers. Containers should be appropriate for the samples and provide adequate protection and air tightness if required. Containers should also be labeled with member, date, location, and other pertinent information [44].

A core drill was developed to extract quality timber core samples for compressive strength, parallel-to-fiber testing [45]. Core samples are taken from clear sections of the

member and are drilled to produce a specimen with annular rings oriented perpendicular to the longitudinal axis of the specimen. Proper drilling and annular ring orientation is important in order to obtain samples that can be tested along the fibers.

Friction forces, which can become large during drilling and make quality core extraction difficult, were minimized with the design of a drill bit which has an increasing diameter along the length from tip to shank. To prevent lateral motion of the drill during extraction, the drill is attached to the member with a special fixture, and a mechanical feed is used to maintain a constant drilling speed; shown below in Figure 2.20, Figure 2.21, Figure 2.22, and Figure 2.23 [42][35].

Figure 2.20: Mechanical core drill for extracting samples for destructive testing.

Figure 2.21: Mechanical core drill bit.

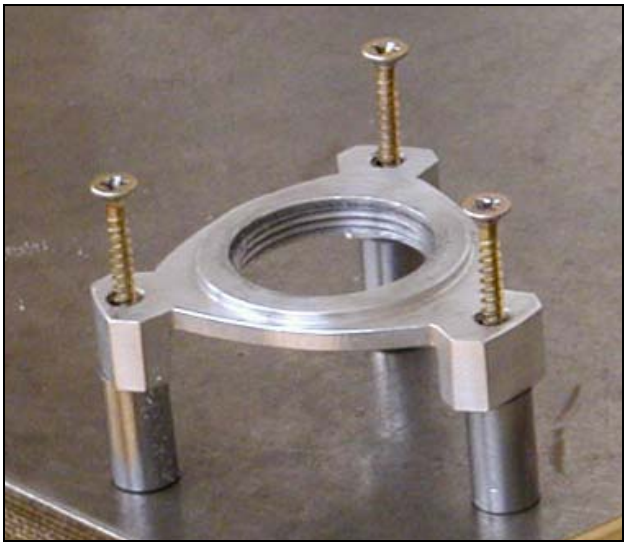

Figure 2.22: Threaded fixture to attach core drill to timber member.

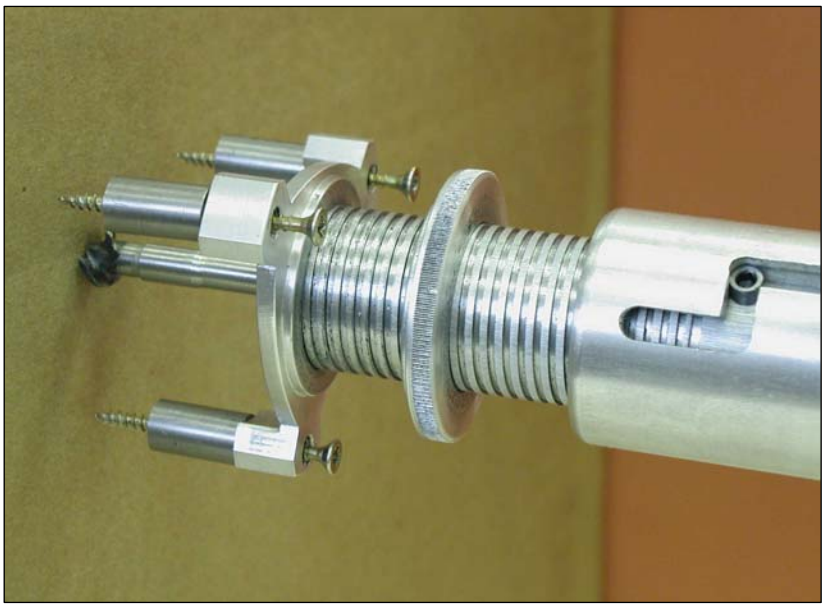

Figure 2.23: Mechanical feed to maintain constant cutting speed while drilling.

Resulting core specimens have a diameter of 4.8 mm [0.19 in] and the hole left in the member is 10 mm [0.39 in] in diameter, corresponding to the largest diameter of the drill bit. The length of the cores must be at least 20 mm [0.79 in] in order to minimize the bias of annular rings due to the variation in density between early and late wood. (20 mm [0.79 in] corresponds to the European standards length requirement for compression testing [42])

Fixtures for the compression testing of the cores along the fibers were also designed and fabricated in order to apply the compressive load parallel to the timber fibers as well as distribute the loading along the length of the core, see Figure 2.25 and Figure 2.25. The specimen is placed into the cylindrical space between the compressive jaws with the fibers oriented parallel to the loading; loading applied by a load cell. A gap is left between the two compressive jaws in order to allow the specimen to deform. Two

miniature linear variable differential transducers (LVDT) are used to monitor the displacement between the test fixtures and measure the deformation of the core.

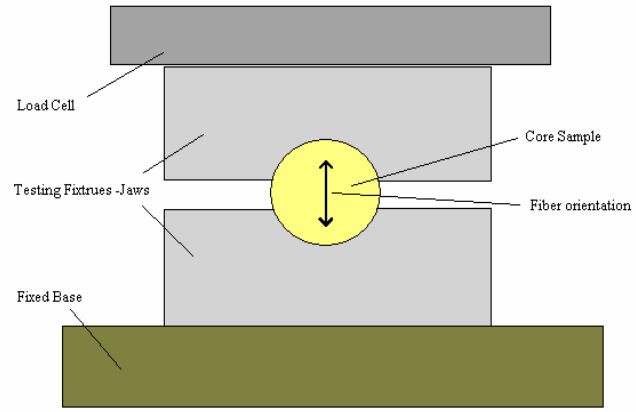

Figure 2.24: Schematic of fixture used for compressive testing of core samples

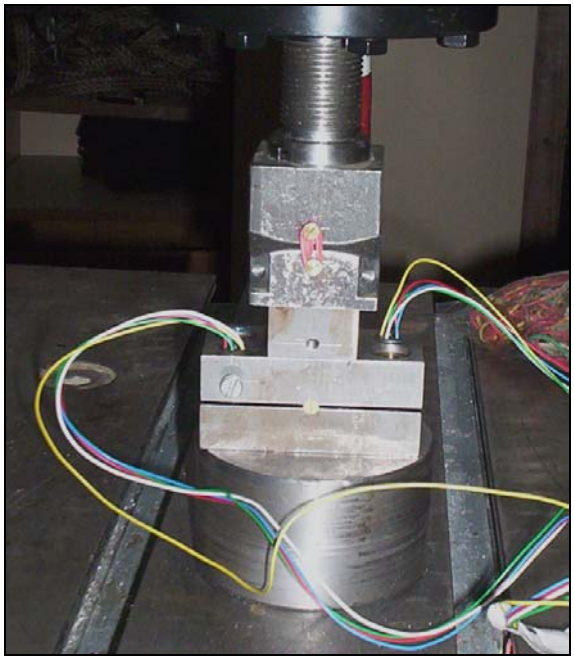

Figure 2.25: Testing fixture used for compression testing of core samples

2.4.2 Application

Small diameter cores are generally extracted from members and tested in compression, but a variety of properties can be established including density, moisture content, modulus of elasticity and other strength properties. Cores are routinely used for species identification through microscopic investigation, dendrochronology, microscopic inspections for signs of early decay, as well as visual examination and measurements of preservative treatment penetration and retention in the member [10]. For this application, core samples are use to establish mechanical properties and discussion will be limited to the compressive testing of cores.

Cores samples are extracted from clear sections of a member and destructively tested to gain information on the mechanical properties of the member. Core samples of materials such as concrete, mortar or masonry which are considered isotropic and homogeneous can be tested along the longitudinal axis of a core sample for compressive testing. This can not be done with timber cores since wood is an anisotropic material whose properties are directionally dependent. Strength along the wood fibers is most critical because it directly controls parameters such as bending, tensile, and compressive capacities. To achieve testing that induces load along the wood fibers, the cores must be oriented so the load is applied perpendicular to the longitudinal axis of the core, see Figure 2.26 [45].

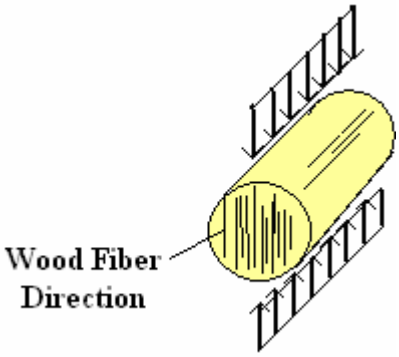

Figure 2.26: Load orientation for compression testing of core samples

Proper alignment of the core sample in the testing fixtures is crucial for accurate compressive strength estimates and modulus calculations. Timber has its greatest strength along the fibers; misalignment of the core sample in the fixtures creating an angle between the fibers and loading will cause reduced estimates of the mechanical properties. Even slight misalignments will affect the data gained from the testing and result in conservative property approximations [42].

During testing, the compressive force and the deformation of the core are monitored and recorded to produce a load-deformation curve; sample plot shown in Figure 2.27. The modulus of elasticity cannot be directly calculated from the load-deformation plot because of a multiaxial stress field created due to surface restraints, Poisson's ratio and the geometry of the specimen [42]. The slope of the load-deformation plot maps directly to the modulus of elasticity, a relationship presented in [42].

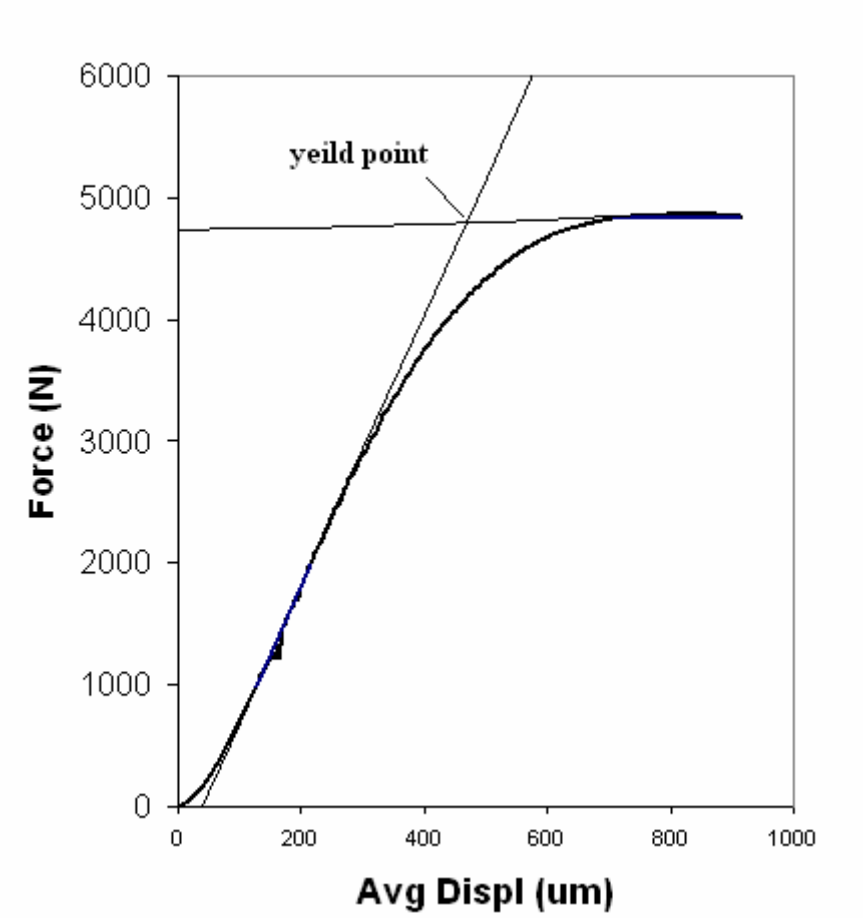

Figure 2.27: Example load-deformation plot for core compression test parallel to fiber

Calculation of specimen apparent compressive strength utilizes the following equation.

$$f_c = \frac{F_{\max}}{l \times d_c}$$ **Equation 2.11**

This equation reflects fundamental mechanical principles, stress being equal to force divided by area. f_c is the apparent compressive strength of the core, F_{max} is the failure load, and l and d_c are the length and diameter of the core respectively. f_c is considered the apparent compressive strength because the pressure distribution over the core sample

cannot be made uniform during testing as well as end effects that cannot be eliminated [42].

The failure load, F_{max}, is taken as the yield point of the load-deformation curve. Due to surface restraints, Poisson's effect and the geometry of the core, a distinct yield point does not exist. The yield point is therefore defined as the intersection of the lines extended from the two quasi-linear portions of the plot [42], illustrated in Figure 2.27.

Kasal *et al* [42] performed standard compressive and tensile testing in accordance to the American Society of Test Materials (ASTM) specifications [46] on specimens and compared the results to data found with core sampling and testing of the same member. Kasal *et al* [42] showed a strong relationships between the core and ASTM specimen compressive strength and modulus with correlation coefficients of $r^2 = 0.89$ and $r^2 = 0.76$ respectively.

Theoretically, the correlation between cores and ASTM samples should be one, however, error in correlation can be attributed to the destructive nature of the testing as well as the variation in the material along the member. The destructive nature of the testing did not allow for the samples to be used for both ASTM and core testing. Samples were taken from the same vicinity of the member, however, variation between samples still existed due to the natural variability of timber [42]. Deviation in loading angle with respect to the grain during core testing would also incur error in correlation. As stated before, wood fiber alignment can be difficult and strength estimates are sensitive to any deviations, causing reduction in predicted strength values.

Correlation between core compressive strength and the tensile strength of ASTM samples was not particularly strong. Kasal *et al* [42] cut core samples in the vicinity of

the necked portions of the ASTM tension samples after testing and found a correlation coefficient of only $r^2 = 0.67$. The low correlation can be related to the ASTM sample itself. The strength of the ASTM small clear sample, with a specified cross section of 4.8 x 9.5 mm [0.19 x 0.37 in], will be affected by the amount of early and late wood present in the sample. The sample cross section may not be large enough to contain an adequate amount of annular rings to remove the bias of the early and late wood effect, especially for species with wide annular rings [42]. Kasal also noted the precarious nature of relating the compressive strength to tensile strength due to the difference in loading methods and failure modes which can lead to error in correlation.

Random sampling of the member must also be considered to gain an accurate representation of the member strength. This can be done through dividing the member into sections, assigning numbers to each segment, and then using a random number generator table to select areas for sampling.

2.4.3 Limitations

Limitations of the core drilling techniques for establishing material properties include the local characteristic of the data gained and accessibility issues. As with any technique that utilizes small specimens, the core samples taken from a member give information about the specific location from which it was taken. Timber can have significant variability between and within species as well as along a single member. In order to make global estimations of a member's mechanical properties based on the core drilling technique, multiple samples must to be taken along the length of the structural element. Multiple samples also allow for the effects of individual irregularities in cores to be averaged out during the testing.

Large numbers of samples may also be required to establish a certain degree of reliability. Increases in drilling and sample extraction will increase time requirements on site and during testing which can increase the expense of the investigation. In addition, increased drilling, if drilling is allowed at all, may not be permitted in historically significant buildings or structures of importance for reasons of aesthetics or disruption to member fabric. Limited sampling can reduce the reliability of property estimations and reduce the usefulness of the technique.

Access to in situ members can deter the use of the core drilling procedure. Fixtures are used to secure the drill to the member and prevent lateral movement and regulate speed during drilling. Member location could make the attachment of the securing equipment difficult, as well as create a complex or awkward position for drilling. Members in small enclosed areas may also eliminate the use of the drill if space will not allow for drilling perpendicular to the surface. The drill attachment also requires a flat surface on the member and a large enough area for attachment. The dressing, or cut, of the member may not provide a flat, plane surface with enough area to drill in a position which is perpendicular to the fibers; such as near the edge of members where space to attach the drill is limited or when drilling at an angle to the surface is required.

Cores should be drilled in the radial direction in order to produce samples which will be useful for testing the compressive strength along the fibers. This will require surface inspection of the member and its grain to locate the appropriate position for drilling. This could be difficult if the grain is not pronounced, well defined, or a surface treatment such as paint obscures the grain pattern.

Core testing is intended to give data on the clear wood compressive strength of the member; therefore a clear sample must be taken and used with this technique. Core samples must also be taken away from defects or discontinuities in the member. This can be difficult if clear areas do not correspond to the needed fiber direction, clear areas are inaccessible with equipment, the surface is deteriorated, or clear areas are obscured by member finishes.

2.5 TENSION MICRO-SPECIMENS

Bending strength evaluation is an important aspect of in situ evaluation of timber members as it is one of the predominant modes of loading, but estimations of the bending properties in situ can present a challenge. With information on the member's tensile properties, bending strength estimates can be made; tensile strength has been related to bending strength and is considered to be approximately equal [35][5]. Tensile properties have a poor correlation with compression properties therefore tensile strength can not be estimated using information attained with the core drilling technique [5]. Specimens can however be extracted to evaluate the tensile properties of in situ members with the following technique.

2.5.1 Equipment

Tension micro-specimens are made with two cuts of a thin-kerf saw oriented at 45° to the surface of the member, creating a triangular specimen. The depth of the cut, and therefore the triangle side width can be adjusted from 3 to 8 mm [0.12 to 0.31 in] to produce a sample that can range in areas from 4.5 mm^2 to 32 mm^2 [0.007 in^2 to 0.05 in^2]. During sampling, however, cutting depths are adjusted to produce specimens with areas

of approximately 8mm^2 [0.012 in^2] so that results are directly comparable to ASTM tension specimens [35], [46]. A guiding track is mounted on the member for the cut of the specimens and must be aligned to extract samples along the fibers of the member. The guide steers the saw in a straight, consistent path for the two cuts needed to produce a uniform sample and must be mounted on the member in a manner such that the path of the saw will not intersect areas with visible defects such as knots, checks or deterioration. Equipment and sample specimens are shown below.

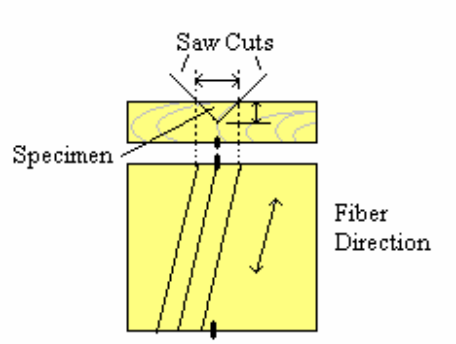

Figure 2.28: Schematic of specimen sampling
Cross-sectional and plan view

Figure 2.29: Tension micro-specimen equipment, kerf saw and guiding track

Figure 2.30: Tension micro-specimens (mounted in grips for testing)

After extraction, the samples are mounted with epoxy on wooden blocks to provide a location for gripping during tensile testing, see Figure 2.30. The mounting reduces the possible influence on findings due to the local end affects of gripping the

samples [35] [45]. Specimens should be planed or sanded to reduce the cross section at the mid point of the samples to ensure failure at that location. Specially designed grips are used in the tension testing of the samples as well as a displacement transducer to measure the displacement during loading, see Figure 2.31 and Figure 2.32.

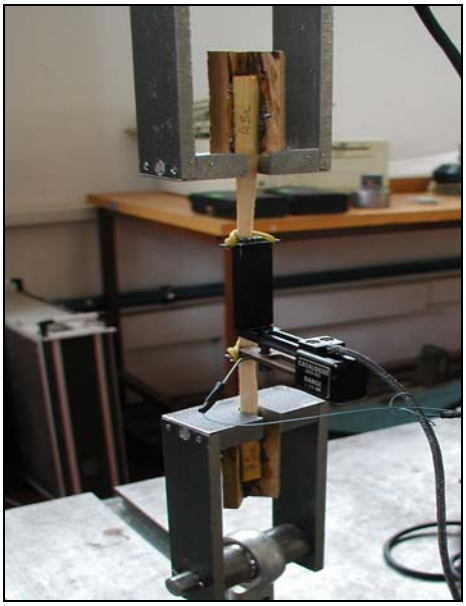

Figure 2.31: Tension micro-specimen in grips and with displacement transducer attached for testing

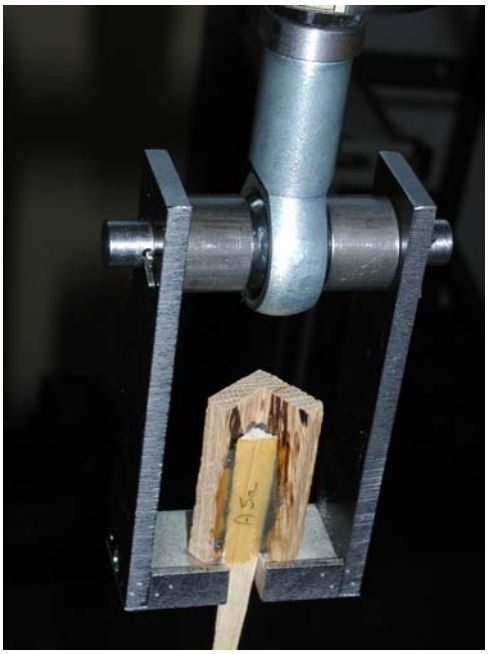

Figure 2.32: Grip used during testing of tension micro-specimens

2.5.2 Application

After sample extraction and preparation through sizing, sanding and mounting for experimentation, as discussed above and shown in Figure 2.30, the samples are tested under tensile loading to find the ultimate tensile strength along the grain as well as the modulus of elasticity. A schematic of testing set up is shown below in Figure 2.33.

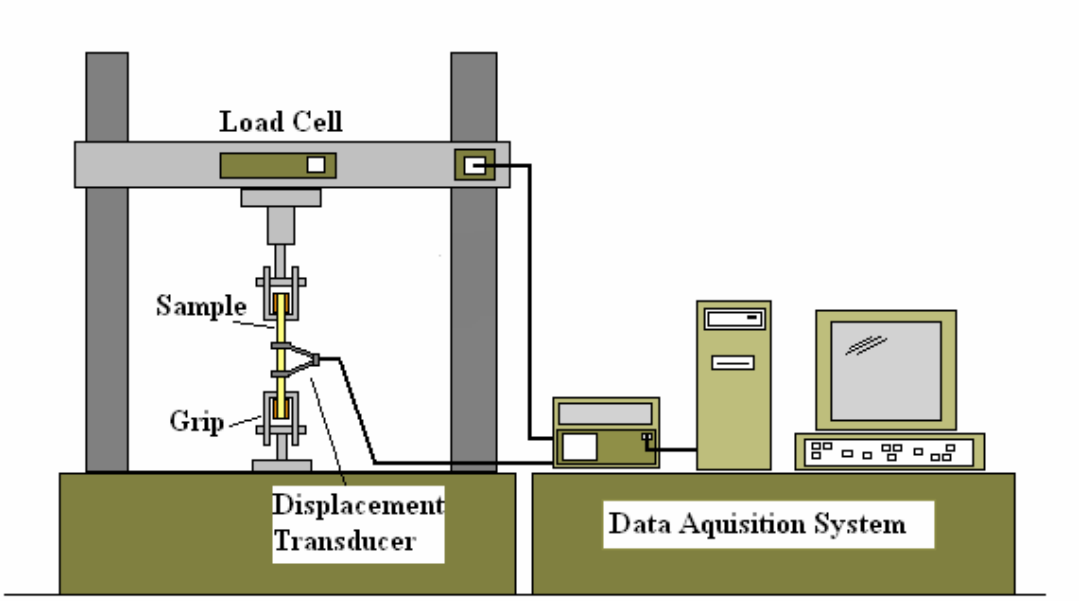

Figure 2.33: Tension micro-specimen testing set up

The maximum tensile load for each specimen is the load at failure, and the allowable tensile stress is calculated by

$$f_t = \frac{F_{\max}}{\frac{1}{2}bh} \qquad \textbf{Equation 2.12}$$

where f_t is the tensile strength, F_{max} is the failure load, and b and h are the base and height of the tensile specimen respectively, see below in Figure 2.34.

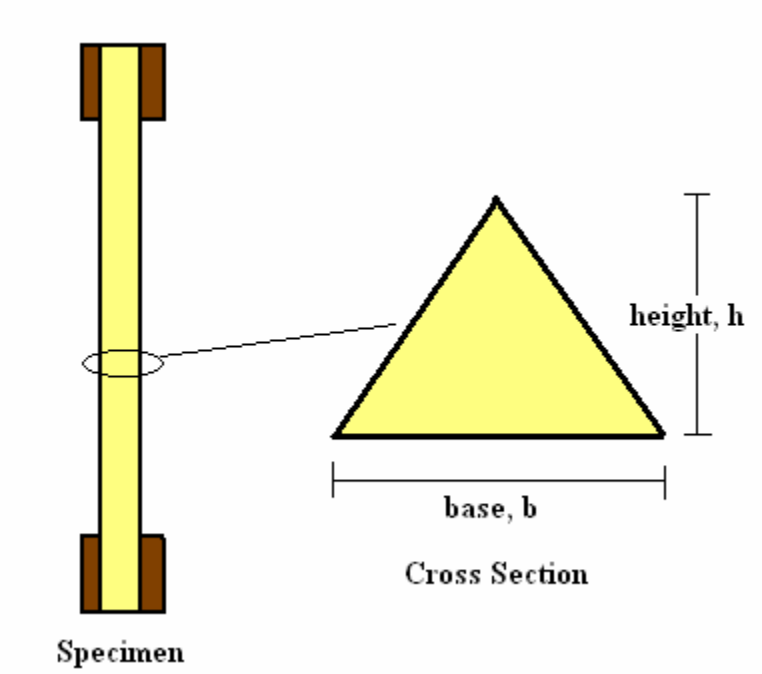

Figure 2.34: Tensile micro-specimen cross section dimension

From recorded data, the stress-strain curve is plotted and the modulus of elasticity along the timber fibers is determined as the slope of the linear trend line that fits the data, see Figure 2.35. The experimental and equipment design is such that the cross sectional area of the tension micro-specimens are comparable to the cross sectional area of the standard ASTM tension specimens for small clear wood, therefore no correlation is needed for comparison to the standard tests [35] [45].

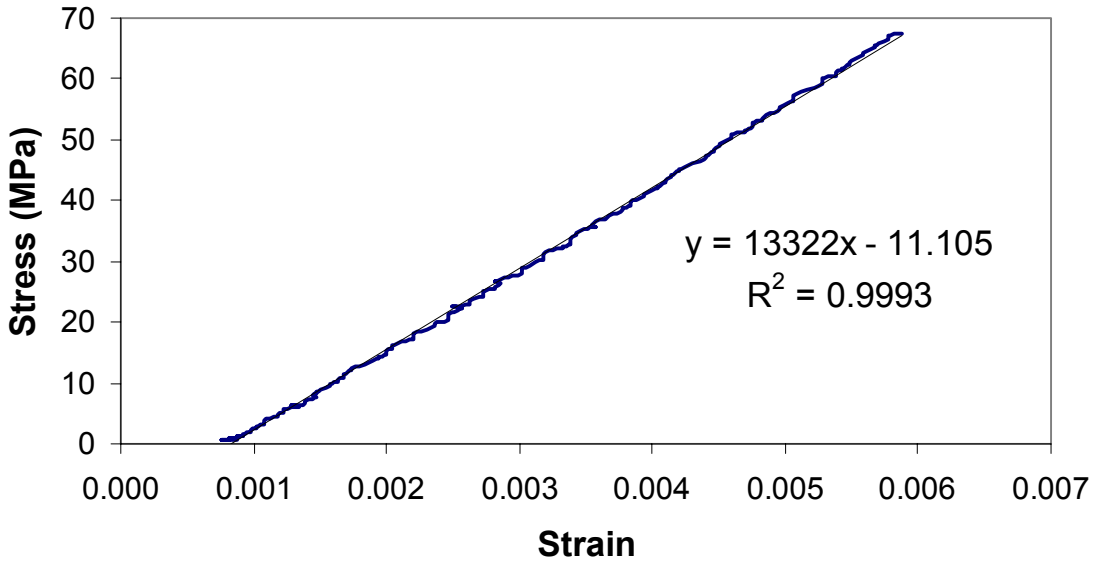

Figure 2.35: Sample stress-strain plot of a tension micro-specimen test

2.5.3 Limitations

Tension micro-specimens are very sensitive to grain deviation. Sampling is intended to be directly along the grain of the member to achieve accurate values for tensile strength along the grain. Maintaining sampling along the grain is difficult and caution must be taken to extract quality samples. The mounting of the track guide to ensure a cut along the timber fibers is essential in extracting a quality tension sample. Specimen behavior is sensitive to grain direction and any deviation from the fiber direction will cause a reduction in the apparent strength predictions. In contrast, the modulus of elasticity is not affected by the deviation from the grain in the specimens. Testing of samples remains within the elastic limit and therefore relatively accurate measurements of the modulus of elasticity are obtained.

Cutting technique and imprecise equipment can affect the sample quality and reduce the reliability of the testing technique. More precise and accurate tension sampling equipment would improve the technique by producing more uniform, quality

samples. At present, however, sample quality is a major drawback of the technique and can cause variability in test data, and an inaccurate representation of member properties.

The size of the tensile specimen may also lead to some of the variability. The small cross-section of the specimen may not provide for the inclusion of enough growth rings to eliminate the bias of the early and late wood densities, a factor which could affect the resulting stress calculated from specimen to specimen. This source of variability could be reduced if the size of the specimen were increased, however this would increase the destructive nature of the method and perhaps limit its use in situ. This is, however, an issue with ASTM tension specimens as well since the ASTM specimens have a comparable cross section to the tension micro-specimens.

As with all techniques that use small size specimens, the data obtained through tension micro-specimen sampling and testing is limited due to its local characteristic. Wood's natural variation within and along a member can cause deviations in material properties of samples depending on the location of extraction. To overcome the variability, relatively large numbers of samples may need to be taken in order to obtain reliable values that are representative of the member tensile strength.

Selection of the sampling sites must be carefully planned to ensure a randomized sampling [35]. Restrictions on the number and location of samples that can be taken from members due to historical significance, decorative finishes or other preservation concerns can limit the use of the technique and diminish the reliability and accurate representation of the member properties.

2.6 ADDITIONAL CONSIDERATION- MOISTURE MEASUREMENT

Elevated moisture content of members can affect the results of nondestructive and semi-destructive testing, particularly stress wave behavior. Moisture content also has a surprisingly strong influence on mechanical properties and should be considered when inspecting in situ members. Moisture infiltration in structural systems is a common source of damage to structural materials and moisture measurements can help to identify water infiltration paths as well as locate areas that may need further investigation to assess damage and material condition associated with elevated moisture exposure.

These factors should be considered during in situ assessments and moisture measurements can be used to aid in nondestructive and semi-destructive investigations.

2.6.1 Equipment

Oven drying of wood specimens is the traditional method of measuring moisture contents; however this method is not suitable for in situ investigations and therefore hand held moisture meters are commonly used. Substantial data exists for wood to calibrate moisture meters, allowing moisture content to be quantified from meter readings based on wood species and temperature [47]. Quantified moisture readings represent the water weight in the member as a percentage of the oven dry weight of the member.

Moisture meters can be described and grouped by the principles on which they operate; resistance, capacitance, voltage, microwave, or thermal methods. Resistance methods utilize the electrical resistance of the material, capacitance methods measure radio-frequency power loss, and voltage methods measure moisture in terms of a DC voltage across a known resistor. Microwave methods also utilize radio-frequency power loss but at higher frequencies, and thermal methods are based on temperature change

associated with moisture content changes [47]. In situ member assessments are generally intended to evaluate current structural conditions and are not intended as long term monitoring exhibitions; therefore hand held moisture meters are most often employed and discussion will be limited to these devices.

Hand held moisture meters utilize the electric properties of materials to measure moisture content and are most commonly of the resistance and capacitance type. Resistance-based moisture meters are employed in probe-type or pin meters while capacitance methods are applied with surface or pin-less meters.

2.6.1.1 Pin Meters

Pin meters, those which operate on resistance principles, are commonly employed for in situ timber investigations. Pins are driven into the member and the resistance to electrical current is measured between them. Electrical resistance of material will vary depending on the moisture content. As moisture content increases, the resistance of the material reduces and the conductance increases. Water is a good conductor and wood is a poor conductor of electrical current, therefore the effect of the moisture content on the resistance properties makes pin meters well suited for timber investigation.

Pin length will vary depending on manufacturer and can be as long as two inches, allowing for the investigation of thick members. Pins should be inserted into the member so that they and the current flow are parallel to the grain. If oriented perpendicular to the grain the current will encounter more resistance as it crosses grain boundaries, which will be reflected in the moisture readings [48].

Meters with insulated pins measure moisture content at the depth of the pin penetration since the electric current only flows and the resistance is only measured in

between the un-insulated tips of the pins. This allows for collecting moisture content readings at multiple depths to evaluate moisture gradients. In contrast, un-insulated pin meters do not allow for moisture content readings at specified depths. Electric current will follow the path of least resistance, i.e. the wettest layer penetrated by the pins; therefore the reading will represent the wettest portion of wood [48] [49].

Pin meters are limited at low moisture contents. Below six or seven percent moisture content, the effect of moisture on the member's resistance properties is comparable to that of wood alone and accurate measurements of moisture are not attainable. The fiber saturation point is the upper limit range on readings from pin-meters; although conductivity of wood increases as the moisture increases, past the fiber saturation point the increase is much smaller and erratic, eliminating the ability to take reliable readings [50]. Increased temperatures will increase conductance and published correction factors should be applied to readings on specimens with temperature over 90°F or below 70°F [49].

Moisture readings of wood materials can be affected by species, grain distribution, temperature, chemical treatments, as well as the skill of the operator. These sources produce variability in readings. Standard deviation for resistance meters is from 0.5 to 1.5 percentage points, meaning that resistance meter readings at their best will be off by one percentage point about five percent of the time [49].

2.6.1.2 Pin-less Meters

Pin-less meters, operating on dielectric principles, operate at the surface of the timber member. A frequency signal is sent into the timber by transmitting electrodes and

received by surface contact electrodes. Attenuation of the frequency signal indicates the degree of moisture contents [47].

Unlike pin meters, the pin-less meters can estimate moisture content levels down to zero percent, with less precision however [49]. At elevated moisture contents, the pin-less meter can give some estimates on moisture content; however the fiber saturation point is still the upper reliable limit.

Since pin-less meters do not penetrate the member they are more susceptible to influence by the material near the surface. Material more than approximately 0.32 mm [0.125 in] below the surface is not properly weighted in the moisture reading [49]. Temperature affects dielectric properties, in a more complex manner than it does on conductance based readings. Adjustments should be made accordingly with reference to published charts, examples of which can be found in [49].

Pin-less meters are also influenced by factors other than moisture content, species, grain distribution, temperature, etc., which causes some variance in reading. Standard deviation for dielectric meters is from 1to 3 percent, in other words, the readings would be expected to have an error of one percent approximately 15 percent of the time [49].

2.6.2 Application

Moisture content readings can identify areas in members which have elevated moisture contents, creating environmental conditions that support biotic deterioration. Recognizing areas prone to biotic attack allows for further investigation to identify and quantify any existing damage.

Biotic deterioration refers to the damage caused by the attack of living agents such as bacteria, fungi, or insects. Each of these has multiple species that can cause

damage, sometimes severe, or total destruction of a timber member. Each requires life sustaining conditions; oxygen, tolerable temperatures, a food source, in this case wood, and moisture.

Elevated moisture contents, beyond the fiber saturation point and allowing for free or unbounded water, foster the growth of decay fungi that destroy timber fibers and weaken the member. Typically, moisture contents of members below 20% will not harbor fungal growth. Elevated moisture within a member will also increase the chance of insect attack and is, according to [10], the most significant contributing cause of insect attack. Infestation can also attract insect hunting birds, such as woodpeckers, whose damage to the timber can be greater than the insects'.

Decay from these living organisms can substantially reduce material properties. Mechanical properties can be reduced by ten percent before visual indicators are present. A weight loss of only five to ten percent, the loss in mechanical properties can be as large as 80 percent. Below in Table 2.1 is the probable strength loss associated with early decay of softwood [7], (only a demonstration of the possible effect of decay on mechanical properties). In order to determine the remaining strength of in situ members, additional research would be required; however it is clear that decay can greatly inhibit a member's load resistance ability.

Table 2.1: Percent loss of mechanical properties due to early decay (5-10% weight loss) [7].

Strength Property	Average strength loss due to decay in percent
Static Bending	70
Impact Bending	80
Modulus of Elasticity	70
Compression Parallel to Grain	45
Tension Parallel to Grain	60
Compression Perpendicular to Grain	60
Shear	20

Moisture content strongly influences mechanical properties of timber members as well as cause dimensional changes. In general, elasticity and strength parameters decrease with increased moisture content up to the fiber saturation point, as illustrated by Figure 2.36. The effect of moisture content on mechanical properties is also linked to the quality and size of the timber as shown in [52] and [53]. Adjustments are made to mechanical properties to account for moisture content differences, and it is commonly assumed that the strength variation below fiber saturation point can be described by a negative exponential function [54]. Extensive discussion on this topic and the effects of moisture on the mechanical properties of timber beyond this scope can be found in [54].

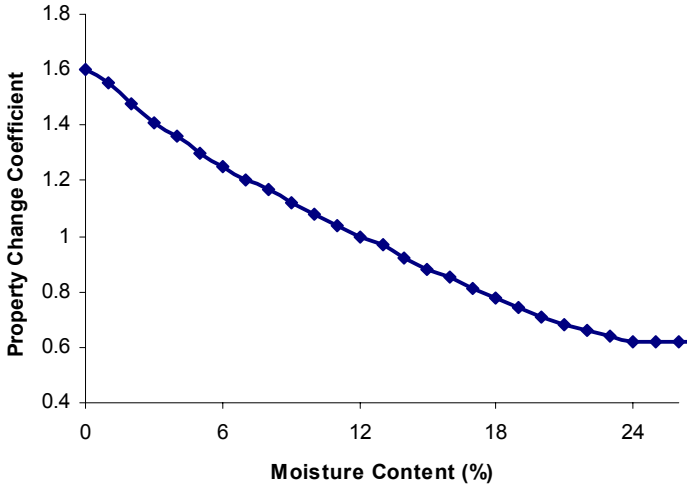

Figure 2.36: The effect of moisture content on mechanical properties [55].

2.6.3 Limitations

Meters can be affected by parameters other than the moisture content including timber species, grain distribution, temperature, chemical or preservative treatments, as well as the skill of the operator [49]. Limitation based on meter type also exists. Pin meters have the drawback of leaving holes in the specimen as well as the inability to measure low moisture contents. They are also more sensitive to temperature factors than the pin-less meters and require correction changes. Pin-less meters do not alter the material surface but good contact to the surface, which can be difficult with rough or warped members, is required for accurate readings. Pin-less meters are also more sensitive to density differences and generally require correction or settings specific to the member. Additionally, the lack of penetration into the member makes pin-less meter's readings biased to surface material conditions.

CHAPTER 3

EXPERIMENTATION

Of the nondestructive and semi-destructive techniques researched, four were selected for experimentation. Core-drilling and tension micro-specimen sampling were selected for the strength assessment portion, while x-ray investigation and resistance drilling were used for deterioration detection and quantification.

Stress waves were not used for deterioration assessment due to experimental limitations and equipment availability in addition to the extensive research already performed using stress waves for locating deterioration, see [56] and [57]. Stress wave investigation was eliminated from the strength assessment portion due to the variable and conflicting correlations between stress wave parameters and mechanical properties reported by researchers, see Table 3.1 and Table 3.2 as well as reference [26] and [40]. The correlation coefficients between static and dynamic modulus of elasticity presented in Table 3.1 can be rather strong, however, the correlation is effected by wood specie, environmental conditions, and in wood that is not clear or has preservative treatments applied. Table 3.2 demonstrates the weak and variable correlation reported by researchers between the static modulus of elasticity and varying mechanical properties.

Table 3.1: Correlations between dynamic and static modulus of elasticity

Dynamic Modulus of Elasticity Correlation to Static Modulus of Elasticity			
	Material	**Static Loading**	**r^2**
Bell *et al* (1954) [26]	clear wood	compression	0.96
	clear wood	bending	0.96
Galligan & Courteau (1965) [26] [58]	lumber	bending	0.92
Porter & Galligan (1973) [26]	lumber	bending	0.92
Gerhards (1982) [26]	knotty lumber	bending	0.76
	clear lumber	bending	0.90
FPL-RN-0274 [59]	preservative treated piles	bending	0.58
Feio *et al* [40]	old lumber		0.65
	new lumber		0.70

Table 3.2: Correlations between static modulus of elasticity and mechanical properties

Static Modulus of Elasticity Correlation to Mechanical Properties			
Bending	**Property**	**Static Loading**	**r^2**
Hoyle (1961) [26]	Es to $F_{bending\ (flatwise)}$	flatwise	0.52-0.62
Hofstrand and Howe (1963) [26]	Es to $F_{bending\ (flatwise)}$	flatwise	0.56
Pellerin (1963) [26]	Es to $F_{bending\ (flatwise)}$	flatwise	0.58
Hoyle (1964) [26]	Es to $F_{bending\ (flatwise)}$	flatwise	0.58
Kramer (1964) [26]	Es to $F_{bending\ (flatwise)}$	flatwise	0.77
Johnson (1965) [26]	Es to $F_{bending\ (flatwise)}$	flatwise	0.72-0.74
Hoerfer (1962) [26]	Es to Fbending (edgewise)	flatwise & on edge	0.42
Hoyle (1964) [26]	Es to Fbending (edgewise)	flatwise & on edge	0.32
Sunley & Hudson (1964) [26]	Es to Fbending (edgewise)	flatwise & on edge	0.46
Corder (1965) [26]	Es to Fbending (edgewise)	flatwise & on edge	0.41
Johnson (1965) [26]	Es to Fbending (edgewise)	flatwise & on edge	0.64-0.76
Littleford (1965) [26]	Es to Fbending (edgewise)	flatwise & on edge	0.44-0.64
Miller (1965) [26]	Es to Fbending (edgewise)	flatwise & on edge	0.48-0.71
Hoyle (1968) [26]	Es to Fbending (edgewise)	flatwise & on edge	0.45
Compression	**Property**		**r^2**
Hofstrand & Howe (1963) [26]	Es to Fcompression		0.71
Pellerin (1963) [26]	Es to Fcompression		0.61
Hoyle (1968) [26]	Es to Fcompression		0.45
Feio *et al* [40]	Es to Fcompression		0.62-0.67
Tension	**Property**		**r^2**
Hoyle (1968) [26]	Es to Ftension		0.56-0.75

3.1 STRENGTH EVALUATION

Five beams, from three different locations, were taken out of service and used for the strength evaluation experiments. All beams were of the species *Piceas abius*, common name Norway Spruce, and taken from structures in cities of the Czech Republic; two beams from Prague, two from Kutna Hora, and one from Namést. The beams were photographed and measured before they were cut into small sections to take samples.

Each beam was cut, divided and labeled into small sections. The beams were first planed to remove a thin layer of outer wood and to square the pieces. The square beam was then cut along the length to produce two narrow boards with a width of 50 mm [2 in]. The material between the cuts which produced the two narrow boards was saved for tensile test sampling. The two narrow boards were next cut again along the length three or four times, depending on the beam depth, to produce 50 mm x 50 mm [2 in x 2 in] square cross section pieces. These long square pieces were then cut along their lengths at 200 mm [8 in] intervals to produce a final piece for sampling, a 50 x 50 x 200 mm [2 x 2 x 8 in] prism. From each of these rectangular sections, up to two core samples were taken.

Labeling of the rectangular specimens and their corresponding core samples was done to reflect the board from which they came, their vertical position on the board and their location along the length of the board. Cuts illustrated in Figure 3.1.

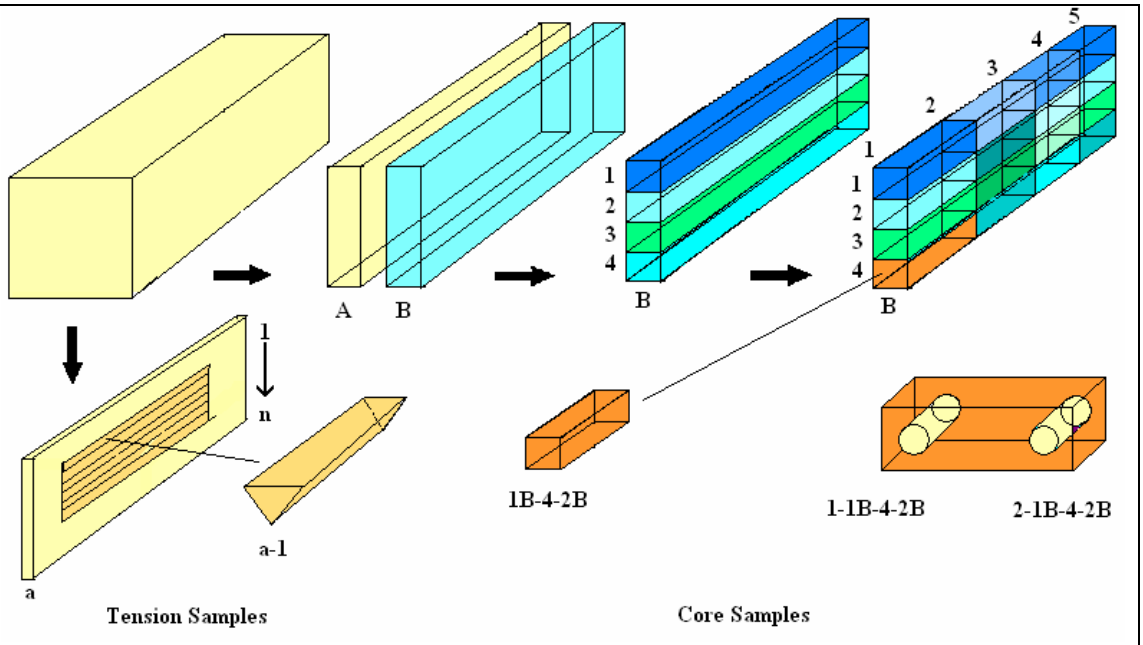

Figure 3.1: Schematic of beam sectioning and labeling system.

3.1.1 Visual Grading

Prior to cutting and sectioning, photographs were taken of all the beams and were used for the visual grading portion of experiment. Photos included the full member and the multiple faces of the beams, at least three faces for each beam. The dimensions of the beam, measured before sectioning, were used to establish the scale of the photos. With a working scale, visual inspection and measurement of growth characteristics for each face of the beams was performed and recorded.

After taking an inventory of the growth characteristics for each beam, the criteria presented by the West Coast Lumber Inspection Bureau (WCLB) in *Standard Grading Rules No. 17* [1] was used to assign an appropriate grade to each beam. Although Norway Spruce is not a domestic west coast specie, it has been covered by the WCLB grading rules since 2002. Design values for the corresponding timber grade were then found in the NDS Supplement [3] and assigned to the beams.

Design values for Norway Spruce timbers are currently not available in the NDS Supplement; however design values for Norway Spruce dimension lumber were included for the first time in the 2006 edition. In order to arrive at design values for Norway Spruce timbers, the dimension lumber values were compared with the domestic species whose timber values are available. A close relationship to the dimension lumber values of Spruce-Pine-Fir was found. Making the assumption that the timber design values would also have a close relationship to one another, and for illustration purposes, the design values for Spruce-Pine-Fir timbers were use as a substitute for the Norway Spruce timber values.

3.1.2 Core-Drilling

3.1.2.1 Equipment

As described in the section *Core-drilling*, a drill was specially designed to extract small core samples which are tested destructively to estimate the compressive strength of in situ timber members. Core samples had a diameter of 4.8 mm [0.2 in] and a minimum length of 20 mm [0.8 in]. Samples were tested in compression in specially designed fixtures and were oriented so that load was applied along the grain. Deformation during loading was monitored and recorded by two miniature LVDTs. A load-deformation plot was constructed from the data to identify the specimen yield point. The slope of the load-deformation also correlated directly to the modulus of elasticity in compression. See section *Core-drilling* for a detailed description of equipment and data analysis.

3.1.2.2 Experiment

Each of the five beams was cut as described above to produce the 50 x 50 x 200 mm [2 x 2 x 8 in] rectangular pieces. Up to two cores could be extracted from each of the rectangular prisms. Variation in sample size resulted from beam dimension in addition to some or part of the rectangular pieces being unusable due to deterioration in the member. Cores that were discovered to be damaged or have deterioration after drilling were also discarded. The core sample numbers are listed below in Table 3.3.

Table 3.3: Core sample count for individual beams

Beam	Number of Core Samples
Kutna Hora 1 (KH1)	59
Kutna Hora 2 (KH2)	34
Namést (N)	47
Praha 1 (P1)	36
Praha 2 (P2)	40

After extraction and labeling, all core samples were placed into an environmental chamber and equilibrated at 22°C and 65 % relative humidity. Each cylindrical core sample was then tested in compression along the grain using the equipment described earlier. Load and deformation were recorded during testing and used to construct a load-deformation plot, see example in Figure 3.2. Note that the deformation is an average between the two LVDTs.

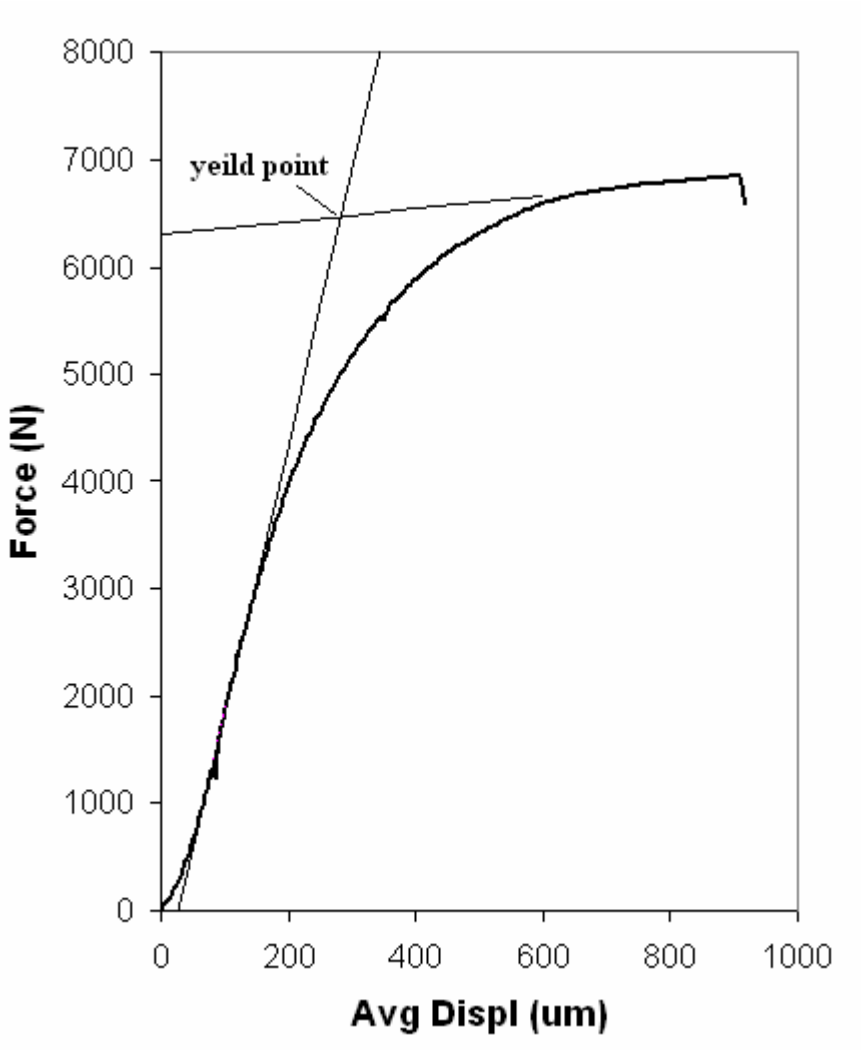

Figure 3.2: Sample load-deformation plot

The failure load was taken as the yield point in the load-deformation plot. After establishing the failure load, apparent compressive strength of the core specimen was calculated with Equation 2.11.

A uniform stress field does not exist during the testing of the cores, as explained in the section *Core Drilling* in Chapter 2, and because of this the modulus of elasticity could not be calculated directly from the load-deformation plot. The modulus of elasticity was instead established through the relationship between the slope of the load-

deformation curve and the modulus of elasticity in compression along the fibers; a relationship established using ASTM compression testing standards [46], presented in [42], and shown below in Figure 3.3.

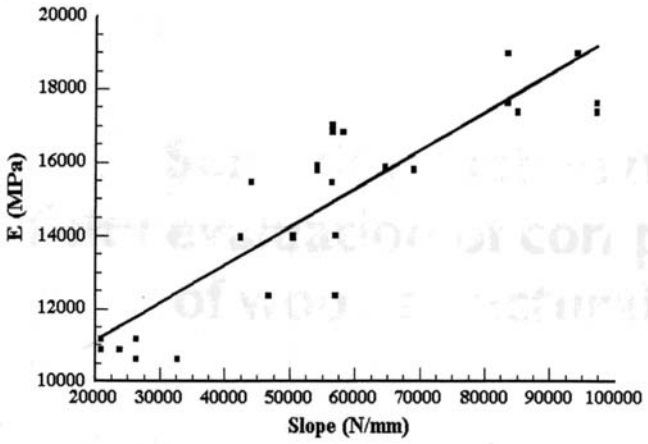

Figure 3.3: Relationship of core sample load-deformation slope to modulus of elasticity along the fiber [42].

3.1.2.3 Statistical Analysis

After obtaining the apparent compressive strength and modulus of elasticity from the core sample testing, a statistical analysis was performed to estimate design values for each beam that would be compared with values obtained through visual grading. The number of core samples needed to obtain a reliable estimate of design values was also a question that was addressed.

For each beam, the cores were given a number from one to n; n equal to the number of core samples for that particular beam. These numbers where then used to randomly select core samples using a random number generator. A small number of outliers with very low strength values were eliminated from the data group due to

experimental error during testing. Following the methods presented in [60] for the calculation of strength based on core drilling, a t-distribution was applied to the data.

Strength estimates obtained represented the lower 5th percentile ASTM specimen strength corresponding to the core data. Core testing and ASTM compression testing cannot use the same samples due to the destructive nature of the testing, and due to the natural variability of wood, specimens taken at different locations will have variation in their mechanical properties. Differences in geometry and testing methods also affect the relationship between core samples and ASTM compression samples. Because of these factors, there is no direct correlation between ASTM compressive specimens and core samples and core data must be converted to corresponding ASTM values. This conversion relationship is found in [42] and shown in Figure 3.4. The lower 5th percentile strength calculation corresponds to the accepted practice in wood design and ASTM D 245 [5] in establishing conservative design values to account for the natural variability of timber.

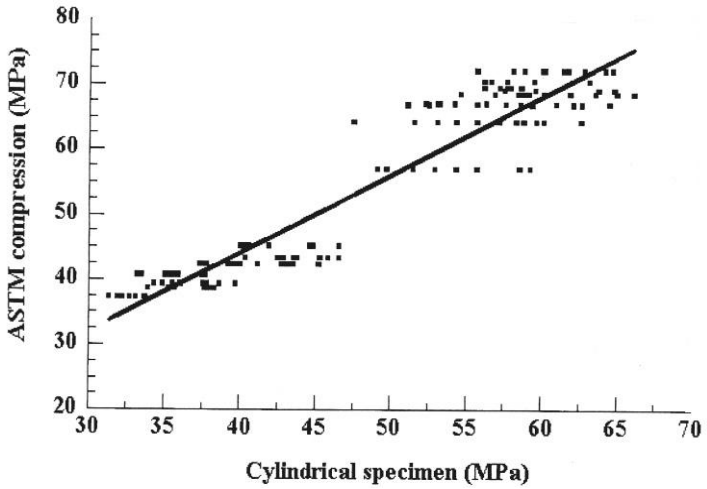

Figure 3.4: Relationship of core sample compressive strength to ASTM specimen compressive strength, relationship presented in [42].

Six samples sizes were selected to examine the effect of sample size, n, on the reliability of the estimated clear wood strength values; n = 2, 3, 4, 5, 8 and 10. For each sample size the same procedure and application of the t-distribution was followed to calculate the design value.

The standard equation for calculating confidence intervals for a t-distribution was applied:

$$x_{0.05} = \bar{x}_{ASTM} - t_{\alpha,n-1} SD_{ASTM} \qquad \textbf{Equation 3.1}$$

Where

$x_{0.05}$ = ASTM lower 5th percentile strength calculated using the t-distribution

$\bar{x}_{ASTM}$ = average ASTM compression specimen response obtained directly from data presented in [42].

$t_{\alpha, n-1}$ = critical value associated with a given probability level, $\alpha = 0.05$ and degrees of freedom v. The value v is given by the sample size minus one, n-1.

SD_{ASTM} = standard deviation of ASTM compression specimens

The critical t-distribution values can be readily found in t-distribution tables for the corresponding probability levels and degrees of freedom. Standard deviation of the ASTM compression specimens was obtained through linear transformation of cylindrical specimen test values to the ASTM values and their relationship presented in [42]:

$$SD_{ASTM} = \frac{SD_{core}}{\bar{x}_{core}} \bar{x}_{ASTM} \qquad \textbf{Equation 3.2}$$

where

$\bar{x}_{core}$ = average response of cores

SD_{core} = standard deviation of core response

Ten iterations for each sample size were performed and the average and standard deviation calculated to obtain a representation of the sample size estimation properties. The lower 5th percentile value using the total number of cores from the individual beams was also calculated for comparison purposes.

The strength values estimated up to this point represented the clear wood strength value and are not the final design values. To arrive at design values, the clear wood strength values estimated from a random sample of four specimens (sample size selection discussed in Results and Discussion section) were adjusted for the naturally occurring growth characteristics according to ASTM D 245. Naturally occurring growth characteristics were observed and recorded through the inspection of photographic images of the full size members.

3.1.3 Tension Micro-Specimens

3.1.3.1 Equipment

As described in the section *Tension Micro-Specimens,* a thin-kerf saw and guiding system were use to extract triangular specimens from timber member surfaces. Specimens were mounted on wood block grips and tested in tension along the fibers to failure; the load at failure was taken as the maximum tensile load. An extensometer mounted over the mid-span monitored the deformation under loading, allowing for a load-deformation plot, a stress-strain plot, and the calculation of the tensile modulus. See

the section *Tension Micro-Specimens* for a detailed description of equipment and data analysis.

3.1.3.2 Experiment

Narrow pieces of the beams, with full member depth and length, were left after cutting the 50 mm [2 in] wide boards for the core sampling. These pieces were used for tension sampling. Due to the condition and size of the individual beams, the number of tension samples that could be taken varied as shown in Table 3.4. Because of the reduced size and the presence of deterioration, no sound material was available to take tension samples after core sample specimens were cut from the Namést beam.

Table 3.4: Tension micro-specimen count for individual beams

Beam	Number of Micro-Tension Specimens
Kutna Hora 1	23
Kutna Hora 2	26
Namést	0
Praha 1	10
Praha 2	14

After the micro-tension specimens were cut, they were mounted with epoxy to wooden block grips for testing and labeled according to beam and location. They were then sanded in the mid-span to reduce the cross-section and promote failure in that region. Before testing, the specimens were placed into an environmental chamber and equilibrated at 22°C and 65 % relative humidity. Micro-tension specimens were tested to failure under tensile loading along the grain. After failure, the location, dimensions and type of failure were recorded for each specimen. Load-deformation and stress-strain

plots were constructed for each specimen using the data obtained from the extensometer, see Figure 3.5.

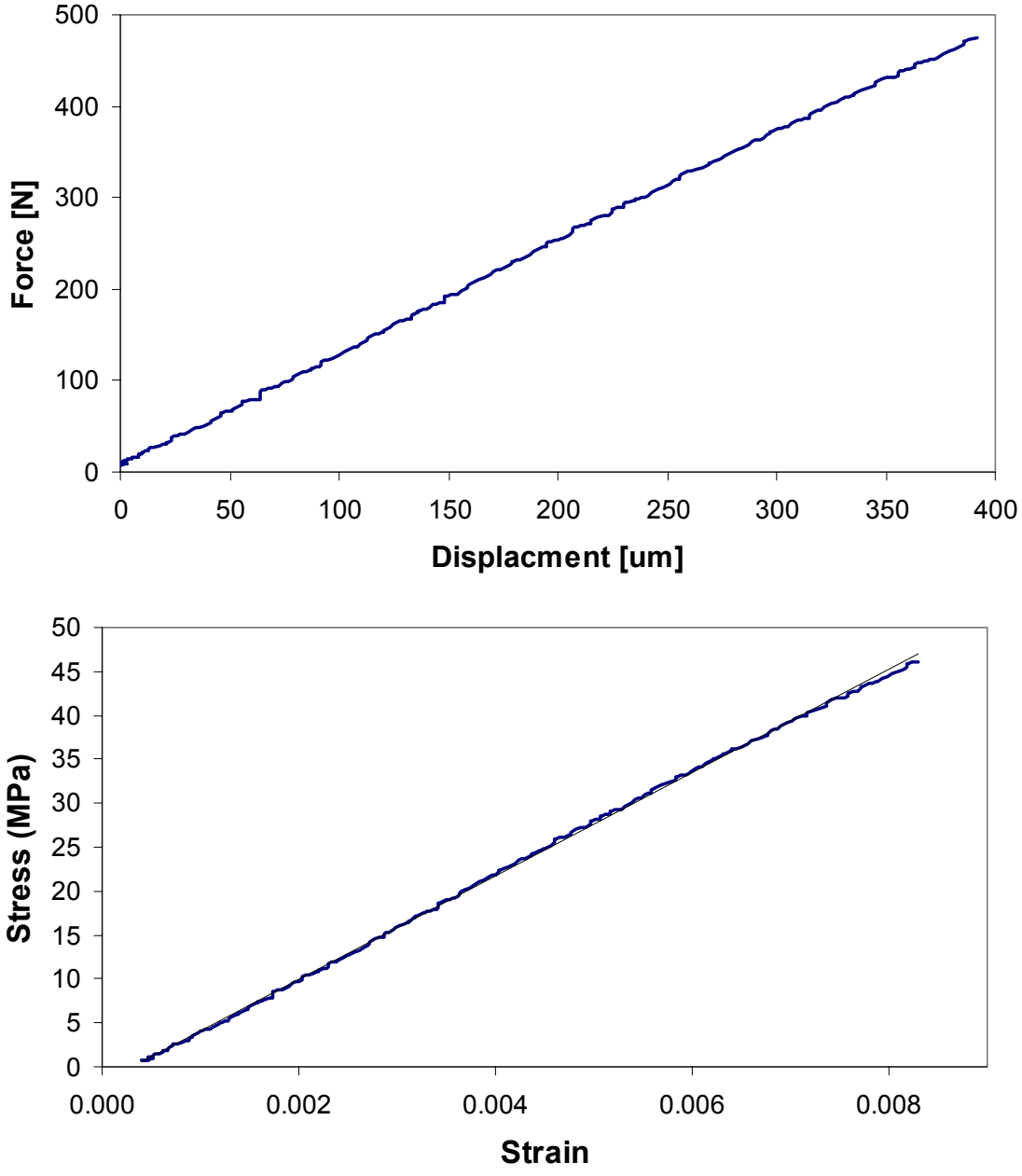

Figure 3.5: Tension micro-specimen load-deformation and stress-strain diagrams

The maximum tensile load for each specimen was the load at failure, and the allowable tensile stress was calculated by Equation 2.12 and the modulus of elasticity was taken as the slope of the linear trend line fit to the stress-strain diagram.

3.1.3.3 Statistical Analysis

After obtaining the tensile strength and modulus of elasticity from the micro-tensile specimen testing, a statistical analysis was performed to estimate design values for each beam that would be compared with values obtained through visual grading. The number of micro-tensile specimens needed to obtain a reliable estimate of design values was also a question that was addressed.

For each beam, the tension specimens were given a number from one to n; n equal to the number of tension specimens for that particular beam. These numbers where then used to randomly select tension specimens using a random number generator. Following methods presented in [60] for the calculation of strength based on micro-tension sampling, a t-distribution was applied to the data to find the lower 5^{th} percentile specimen strength. The lower 5^{th} percentile strength calculation corresponds to the accepted practice in wood design and ASTM D 245 in establishing conservative design values to account for the natural variability of timber.

Four sample sizes were selected to examine the effect of sample size, n, on the reliability of the estimated clear wood strength values; n = 2, 3, 4, 5. For each sample size the same procedure and application of the t-distribution was followed to calculate the design value. The standard equation for calculating confidence intervals for a t-distribution was applied:

$$x_{0.05} = \bar{x}_{tension} - t_{\alpha,n-1} SD_{tension}$$ **Equation 3.3**

where

$x_{0.05}$ = ASTM lower 5th percentile strength calculated using the t-distribution

$\bar{x}_{tension}$ = average micro-tension specimen response

$t_{\alpha, n-1}$ = critical value associated with a given probability level, α = 0.05 and degrees of freedom *v*. The value *v* is given by the sample size minus one, n-1.

$SD_{tension}$ = standard deviation of micro-tension specimens

The critical t-distribution values can be readily found in t-distribution tables for the corresponding probability levels and degrees of freedom. Note that no conversion to corresponding ASTM values is needed due to comparable specimen area. Ten iterations for each sample size were performed and the average and standard deviation calculated to obtain a representation of the sample size estimation properties. The lower 5th percentile value using the total number of micro-tension specimens from the individual beams was also calculated for comparison purposes.

Due to factors that will be discussed in the results and discussion portion of this paper, application of adjustment factors to adjust clear wood strength values to obtain design values was not possible.

3.2 DETERIORATION DETECTION AND QUANTIFICATION

The top section of a circular utility pole taken out of service was used for the deterioration detection and quantification testing. The pole was taken out of service because it had experienced a phenomenon known as stove piping, a hollowing of the top

portion of the pole. Below the deterioration in the top portion, sound wood existed. Two techniques, x-ray investigation and resistance drilling, were applied along the length of the member to test their ability to detect and quantify deterioration.

The pole section had a total length of 1143 mm [45 in] with an average diameter of 323 mm [12.7 in]. Five levels were designated along the length of the beam as areas for testing; two near the bottom, one mid-level, and two near the top, see Table 3.5 and Figure 3.6.

Table 3.5: Testing levels and location on pole section

	Diameter (mm) [in]	Distance from Bottom (mm) [in]
level 1	315 [12.4]	1016 [40]
level 2	318 [12.5]	813 [32]
level 3	328 [12.9]	305 [12]
level 4	330 [13.0]	140 [5.5]
level 5	323 [12.7]	610 [24]

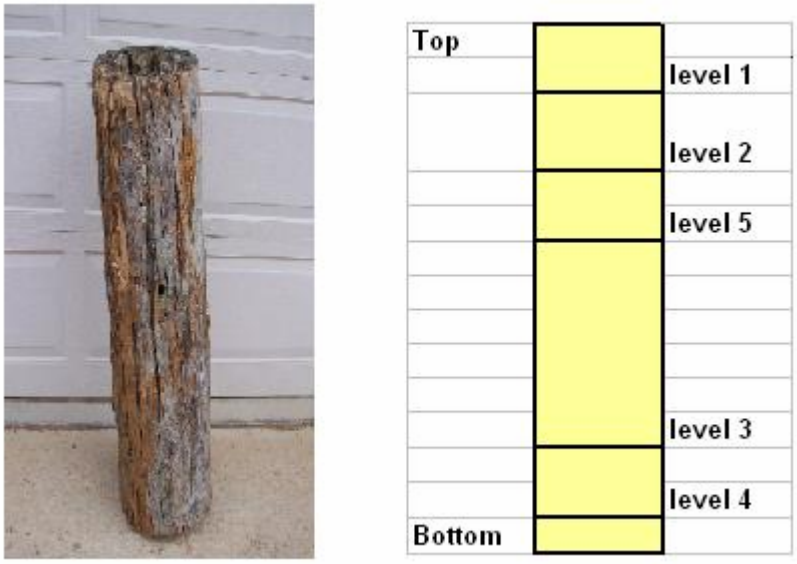

Figure 3.6: Pole photo, and level schematic

3.2.1 Radiography

3.2.1.1 Equipment

Equipment included an x-ray source, imaging plates, scanner and development software. The portable x-ray source used for investigation was the XR-200 produced by Golden Engineering in association with Science Application International Corporation, SAIC. The XR-200 was a battery operated pulsed x-ray source with a maximum energy of 150 kV.

The imaging plates, scanner, and development software were all part of the Logos Imaging digital imaging system. Imaging plates were 203 mm x 432 mm [8 in x 17 in] flexible phosphor imaging plates which, after exposure, were mounted on special tubes for insertion into the scanner where the images were developed and processed. Images were digital and are saved for post-processing. More information on radiography found in Chapter 2.

3.2.1.2 Experiment

At each of the five beam levels, x-ray images were taken. For ease of experimentation and to secure the pole in a fixed position, the pole was mounted on saw-horses and fixed in place with wedged wood boards clamped to the sawhorses. The x-ray source was set up on a tripod 610 mm [24 in] away from the front edge of the utility pole and at a height to shoot through the middle of the pole. An imaging plate was mounted to the pole opposite the x-ray source to capture the image. The imaging plates were mounted so that the level under inspection was in the middle of the plates for levels one,

two and five. Levels three and four were captured in a single image because they were only 165 mm [6.5 in] apart. Set up for x-ray imaging of level one is shown in Figure 3.7.

a)

b)

c)

Figure 3.7: X-ray investigation set up. a) Side view b) View from Source through pole section c) Phosphorus plate mounted opposite x-ray source.

Twelve x-ray pulses were used to penetrate the pole section and capture the image without over exposure. Images were scanned and developed with the digital imaging system, and after development were enhanced by manipulating aspects such as the contrast level, brightness, sharpness as well as applying color.

3.2.2 Resistance Drilling

3.2.2.1 Equipment

The Resistograph used had a drilling needle with a tip diameter of 3 mm [0.12 in], a maximum drilling depth of 305 mm [12 in], and weighed between 2.7 and 3.2 kg [6 to 7 lbs]. Resistance was recorded as a function of the depth during drilling on a 1:1 scale. More information on resistance drilling and principles is presented in Chapter 2.

3.2.2.2 Experiment

Multiple drillings at levels one through four were taken of the pole section in order to construct plots of the level cross-sections. Two drillings were taken at 90° apart and three drillings at 60° apart and through the center of the pole in order to assess the cross section plot acquired if only two or three drilling were taken. To optimize drillings the first drilling was set as the 0°, then 60°, 90°, and 120° from the original drilling were measured off and drilled, see Figure 3.8.

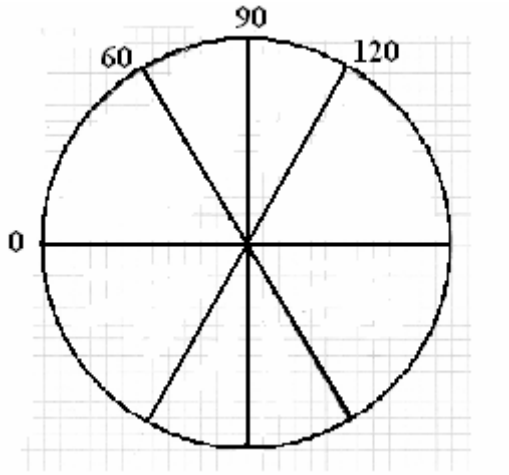

Figure 3.8: Schematic of drillings

Drilling of the fifth level consisted of only one drilling at the 0° orientation and was added after initial planning as a supplementary drilling to investigate the depth at which an internal void extended.

After all drillings were complete, the drilling plots for each level were compiled and plotted in their respective orientation to gain a graphical representation of the cross section and any voids detected.

CHAPTER 4

RESULTS AND DISCUSSION

4.1 STRENGTH ASSESSMENT

4.1.1 Visual Grading

After visually inspecting the beam photographs, appropriate structural grades were assigned based on the number and distribution of defects and growth characteristics. The beams were given grades as presented below in Table 4.1 NDS values associated with the given grades where then assigned to each beam in order to compare with the results of the core-drilling and tensile testing techniques, Table 4.2.

Table 4.1: Grades assessed to beams based on West Coast Lumber Inspection Bureau grading rules

Beam	Grade	Limiting Characteristics
KH1	Select Structural	Seasoning checks, slope of grain 1 in 40, largest knot = 15 mm [$^{3}/_{5}$ in]
KH2	Select Structural	Seasoning checks, slope of grain 1 in 15, largest knot = 36 mm [1 $^{2}/_{5}$ in]
P1	No. 1	Seasoning checks, no slope of grain, largest knot = 46 mm [1 $^{4}/_{5}$ in]
P2	No. 2	Seasoning checks, slope of grain 1 in 7, largest knot = 33 mm [1 $^{3}/_{5}$ in]
N	Select Structural	Seasoning checks, minimal slope of grain, largest knot = 25 mm [1 in]

Table 4.2: NDS design values assigned according to grade

	NDS Design Values (MPa) [ksi]				
	KH1	**KH2**	**P1**	**P2**	**N**
Grade	Select Structural	Select Structural	No. 1	No. 2	Select Structural
Compressive Strength	9.6 [1.4]	9.6 [1.4]	7.9 [1.15]	3.4 [0.5]	9.6 [1.4]
Bending Strength	8.6 [1.25]	8.6 [1.25]	6.0 [0.875]	3.4 [0.5]	8.6 [1.25]
Modulus of Elasticity	10300 [1,500]	10300 [1,500]	9650 [1,400]	6900 [1,000]	10300 [1,500]

4.1.2 Core-Drilling

4.1.2.1 Sample Size

Below is a summary of the compression testing with respect to sample size. For each sample size, the average strength from the ten iterations was used as a representative value obtained for that sample size. The representative sample size average was compared to the average strength calculated with all the samples taken from the beam. In Table 4.3 below, $x_{0.05}$ represents the lower 5^{th} percentile strength calculated with the student t-distribution, and the last column is the samples size's strength estimate as a percentage of the strength estimated using all the samples extracted from the beam.

Observation shows that at a sample size of three, at least 80 percent of the strength estimated with all the samples was achieved, and at four samples at least 90 percent. Samples sizes above four generally showed an increase in the strength percentage; however for this case the gain in strength estimation was not proportional to the effort required to gain and test the additional samples. A sample size of two produced

strength estimates that did not compare well with the strength estimates from all the cores, ranging in a percentage from 22 to 54.

Standard deviation at a sample size of two is large, and the calculations of the lower 5th percentile strength using the student t-distribution are highly affected. Sample sizes larger than two have significantly lower standard deviations which continue to reduce as the sampling size increases. The decrease in the standard deviation and the increased degrees of freedom, and the associated t-distribution critical value, are the sources of the improved strength estimates because the lower 5th percentile calculation is so sensitive to these variables.

The results show that a reliable estimate of a member's strength can be gained with as little as four samples. Increased sampling can provide improved estimates of strength; however for this case, and for similar cases it is expected that the gain would not be proportional to effort involved with sampling and testing of additional cores.

Table 4.3: Sample size core strength comparison to core strength established with all samples

Beam: Kutna Hora 1

Sample Size	Average $X_{0.05}$ (MPa)	Standard Deviation of 10 Iterations (MPa)	Percentage of all samples
n = 2	18.6	12.8	54
n = 3	29.3	4.4	85
n = 4	31.7	4.4	92
n = 5	32.2	3.1	93
n = 8	33.7	1.4	98
n = 10	33.6	1.3	98
n = 59 (all)	34.5	-	-

Beam: Kutna Hora 2

Sample Size	Average $X_{0.05}$ (MPa)	Standard Deviation of 10 Iterations (MPa)	Percentage of all samples
n = 2	8.0	28.9	24
n = 3	30.2	7.0	90
n = 4	31.3	5.5	93
n = 5	32.1	2.5	95

n = 8	32.7	1.9	97
n = 10	33.3	1.7	99
n = 34 (all)	33.7	-	-

Beam: Praha 1

Sample Size	Average $X_{0.05}$ (MPa)	Standard Deviation of 10 Iterations (MPa)	Percentage of all samples
n = 2	9.2	16.8	27
n = 3	27.9	5.0	82
n = 4	32.4	4.8	95
n = 5	30.3	2.4	89
n = 8	33.2	2.0	98
n = 10	32.9	2.3	97
n = 36 (all)	33.8	-	-

Beam: Praha 2

Sample Size	Average $X_{0.05}$ (MPa)	Standard Deviation of 10 Iterations (MPa)	Percentage of all samples
n = 2	15.5	22.7	22
n = 3	29.2	8.3	85
n = 4	33.4	5.2	97
n = 5	33.3	3.9	97
n = 8	32.2	2.5	94
n = 10	32.5	2.5	95
n = 40 (all)	34.2	-	-

Beam: Namest

Sample Size	Average $X_{0.05}$ (MPa)	Standard Deviation of 10 Iterations (MPa)	Percentage of all samples
n = 2	14.5	20.1	44
n = 3	30.0	8.8	92
n = 4	29.4	5.9	90
n = 5	29.8	6.0	91
n = 8	32.7	3.4	100
n = 10	32.4	2.2	99
n = 47 (all)	32.7	-	-

4.1.2.2 Design Values

Conversion of core sample clear wood strength values to ASTM lower 5th percentile strengths is done through the application of a Student t-distribution as described earlier. In order to apply this distribution and obtain reliable strength values, the data must be well behaving and follow normal distribution trends. Histograms for the core strength values of each beam were constructed to inspect the behavior of the data; shown below in

Figure 4.1 Figure 4.1 through Figure 4.5. The histograms showed that the core data was in fact well behaving and followed normal distribution trends including clustering of the data around the average and bell-shaped distribution characteristics. The t-distribution could therefore be applied for the calculation of ASTM lower 5th percentile strengths.

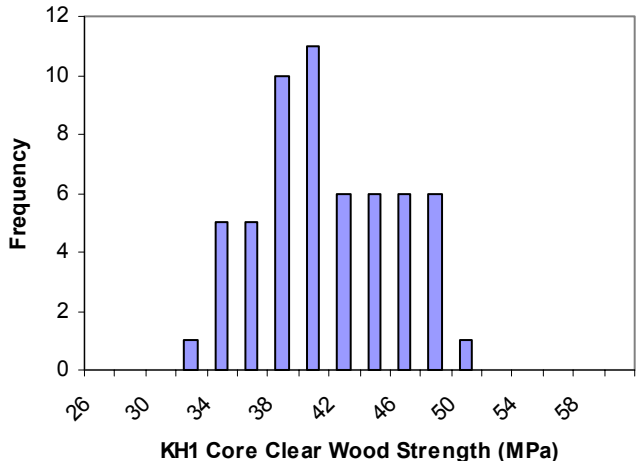

Figure 4.1: Beam Kutna Hora 1 Histogram

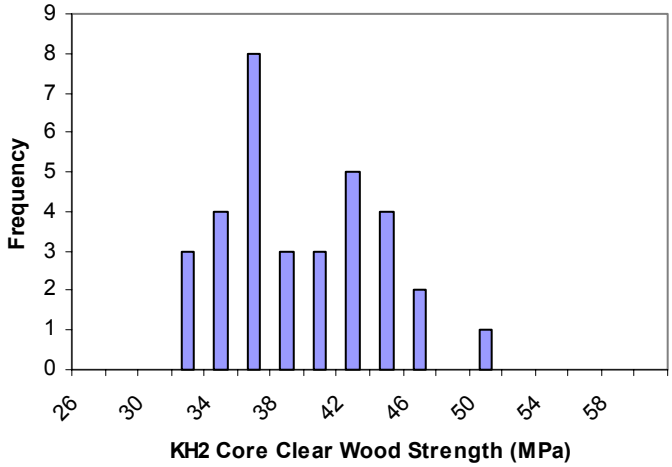

Figure 4.2: Beam Kutna Hora 2 Histogram

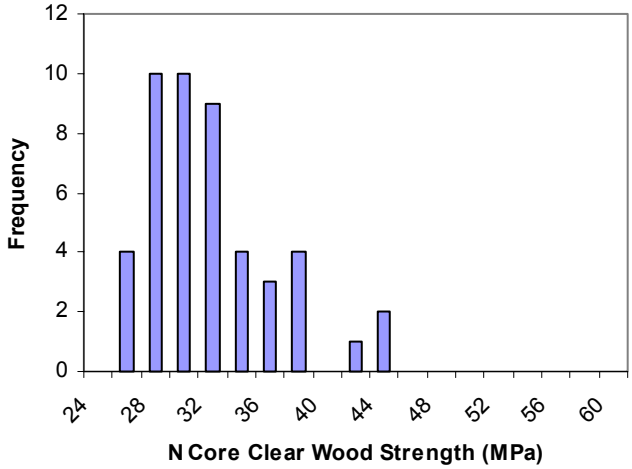

Figure 4.3: Beam Namést Histogram

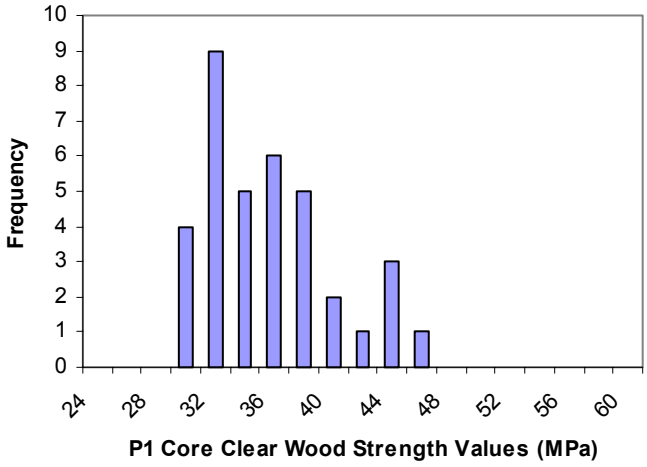

Figure 4.4: Beam Praha 1 Histogram

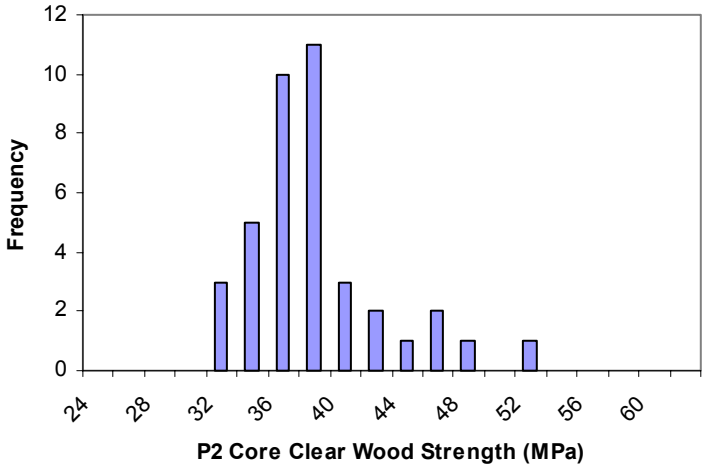

Figure 4.5: Beam Praha 2 Histogram

For each beam, the design values established through core-drilling data were based on a random selection of four samples; see discussion above for sample size selection reasoning. The lower 5th percentile clear wood value was calculated with the Student t-distribution and then adjusted in accordance to ASTM D 245 [5]. The same strength reducing characteristics that defined the visually applied structural grades where adjusted for with the appropriate ASTM strength ratios to arrive at the design values. A sample adjustment from a clear wood strength value to a design value is shown below in Table 4.4 and Table 4.5, and a summary of all the beams design values are presented in Table 4.6.

Bending strength estimates were also calculated based on the compressive strength data of the core testing. This is a viable procedure because the clear wood compressive strength of small, clear specimens is always less than the bending strength [42]. Use of the core sample compressive strengths therefore produces conservative estimates of the bending properties, nevertheless they will be specific to the individual member. The use of tensile strength estimates to predict bending strength would be more appropriate because tensile strength and bending strength are approximately equal [42] [5]. This was not possible however because tensile strength values were not available from the testing performed, as will be discussed in coming sections, and therefore compression data was used.

Table 4.4: ASTM D 245 adjustment table for beam KH2

Property	Limiting Factor	Strength Ratio, %	ASTM D 245 Table	Soft Wood Adjustment Factor
Bending	Knot 3 (36mm) [1 $^{2}/_{5}$ in]	0.81	2	
	Knot 3 (36mm) [1 $^{2}/_{5}$ in]	0.84	3	
	Knot 5 (34 mm) [1 $^{1}/_{3}$ in]	0.72	4	
	Slope of grain, 1 in 15	0.76	1	
	Controlling	**0.72**		**0.48**
Compression	Knot 3 (36mm) [1 $^{2}/_{5}$ in]	0.84	3	**0.53**
	Slope of grain, 1 in 15	1	1	
	Controlling	**0.84**		
MOE		**1**	5	**1.06**

Table 4.5: Clear wood to design value adjustment table for beam KH2

Property	Clear wood Strength Value		Adjustment Factor	Strength Ratio	Allowable Property	
	MPa	ksi			MPa	ksi
Bending	34	4.9	0.48	0.72	11.64	1.7
Compression parallel to grain	34	4.9	0.53	0.84	15.01	2.2
MOE	11,200	1600	1.06	1	11,864	1700

Table 4.6: Summary of beam design values bases on core-drilling

	Core-drilling Design Values (MPa) [ksi]				
	KH1	KH2	P1	P2	N
Compressive Strength	17.2 [2.5]	15.2 [2.2]	12.4 [1.8]	11.7 [1.7]	15.2 [2.2]
Bending Strength	15.5 [2.25]	11.7 [1.7]	10.3 [1.5]	7.9 [1.15]	12.7 [1.85]
Modulus of Elasticity	12400 [1800]	11700 [1700]	11700 [1700]	10300 [1500]	11000 [1600]

4.1.3 Tension Micro-Specimens

Lower 5th percentile clear wood tensile strengths were initially calculated as described in the Methods and Materials section of the paper. After initial calculations however, questions rose about the appropriateness of applying a t-distribution to the data

because calculated design values were extremely low and many were negative.

Inspecting the data showed high variability in the tensile strengths found in testing; the average strength response of the specimens was 55 MPa with a standard deviation of 25 MPa. A histogram, Figure 4.6, confirmed that the data was not well behaving and did not follow normal distribution trends, a criterion for applying the t-distribution. Because of this, a reliable ASTM lower 5th percentile strength could not be calculated for comparison with NDS design values using the t-distribution. The technique was therefore eliminated from further comparisons with current assessment methods for this research.

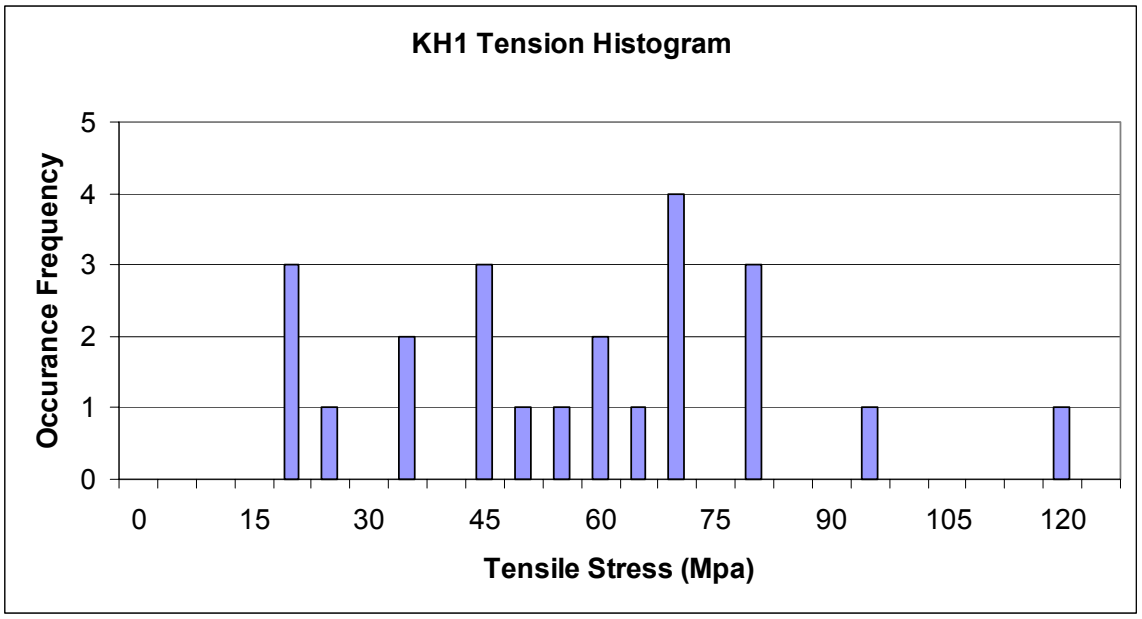

Figure 4.6: Tensile stress histogram showing variable nature of tensile results.

Some of the variability experienced in the testing resulted from the initial sampling of the beams. The samples that were taken had a wide range in quality, from high to low to damaged; damaged samples were discarded. Sources of variability in sample quality resulted from the inability to extract consistent samples due to the equipment used and grain pattern of the beams.

The equipment had a lot of play in its movements and did non hold set positions of angle, depth, or straight line cutting well. An improvement in the equipment to rectify these problems to make cuts more consistent could greatly improve the quality of samples extracted.

Sample quality in relation to grain direction was another problem. Fundamental to this technique is the ability to cut samples along the grain of the member. The grain of the beams had substantial deviation from a straight line along the length making sampling along the grain difficult to impossible. Tensile strength is sensitive to slope of grain within the sample and some of the variability in the data can be explained for this reason. Grain direction and the inability to obtain samples along the grain may limit the use of this technique for members with variable grain directions.

Sample preparation can also account for some of the variable data. During testing, several of the samples failed not in the narrow mid-span, but at the epoxy connection to the wooden blocks used to grip the samples during testing. This would indicate that the gluing of some specimens was not properly done to obtain a quality bond. Narrowing of the mid-span by sanding also introduced sample quality issues because maintaining a consistent cross-section was difficult.

The sample cross-section size may also contribute to the variability in strength values. Variability could be associated with the inability to include adequate growth rings to eliminate the bias of early wood and late wood; late wood is denser with higher tensile properties than early wood. The tensile micro-specimen is small to minimize the effect of extraction on the strength and appearance of the member. The small sample size limits the number of annular rings that can be captured, especially in wood with wide

annular rings, and samples that capture more late wood would exhibit larger tensile strengths. Increasing the size of the specimens to eliminate the bias between early and late wood could reduce the variability between samples, however the increase in size would limit the practically of the technique for use in situ and as a semi-destructive testing method.

4.1.4 Design Value Comparison

Below is Table 4.7 with the design values established with grading rules and published NDS values, and the design values obtained through core testing and applying ASTM standard D 245. The difference in the strength estimate from NDS values to core-drilling values is expressed as a percentage in the last column.

A comparison of the data showed that a significant increase in design values was obtained by utilizing the core drilling technique in this case. Strength design value estimates all increased by more than a third and modulus of elasticity estimates increased by a minimum of seven percent and up to a maximum of fifty percent.

Table 4.7: Comparison between NDS design values assigned with visual grading and the values obtained through core-drilling and ASTM D 245 adjustments.

KH1	**Grade =**	**Select Structural**	
	Design Value (MPa) [ksi]	NDS Value (MPa) [ksi]	Change (%)
Compressive Strength	17.2 [2.5]	9.6 [1.4]	+ 79
Bending Strength	15.5 [2.25]	8.6 [1.25]	+ 80
Modulus of Elasticity	12400 [1800]	10300 [1500]	+ 20
KH2	**Grade =**	**Select Structural**	
	Design Value (MPa) [ksi]	NDS Value (MPa) [ksi]	Change (%)
Compressive Strength	15.2 [2.2]	9.6 [1.4]	+ 57
Bending Strength	11.7 [1.7]	8.6 [1.25]	+ 36
Modulus of Elasticity	11700 [1700]	10300 [1500]	+ 13
N	**Grade =**	**Select Structural**	
	Design Value (MPa) [ksi]	NDS Value (MPa) [ksi]	Change (%)
Compressive Strength	15.2 [2.2]	9.6 [1.4]	+ 57
Bending Strength	12.7 [1.85]	8.6 [1.25]	+ 48
Modulus of Elasticity	11000 [1600]	10300 [1500]	+ 7
P1	**Grade =**	**No. 1**	
	Design Value (MPa) [ksi]	NDS Value (MPa) [ksi]	Change (%)
Compressive Strength	12.5 [1.8]	7.9 [1.15]	+ 57
Bending Strength	10.3 [1.5]	6.0 [0.875]	+ 71
Modulus of Elasticity	11700 [1700]	9600 [1400]	+ 21
P2	**Grade =**	**No. 2**	
	Design Value (MPa) [ksi]	NDS Value (MPa) [ksi]]	Change (%)
Compressive Strength	11.7 [1.7]	3.4 [0.5]	+ 240
Bending Strength	7.9 [1.15]	3.4 [0.5]	+ 130
Modulus of Elasticity	10300 [1500]	6900 [1000]	+ 50

4.2 DETERIORATION DETECTION AND QUANTIFICATION

4.2.1 Radiography

Below are the x-ray images taken at the five designated levels of the beam, starting at the top of the pole and working down. Recall that the utility pole was taken out of service due to the stove piping phenomenon. With stove piping, the top of the pole decays out from the middle creating a central void, the size of which decreases as the distance from the top increases.

Figure 4.7 shows level 1, five inches from the top. From the image you can see that there is an area of reduced density in the middle region appearing as light gray to white and the grain structure which is visible to the left and right has disappeared. This large area of reduced density indicates severe deterioration and a likely void. Although the left edge of the image is very light this does not indicate deterioration. Note that this area still shows the annular ring pattern and wood structure; this area is simply overexposed.

Figure 4.8 is the x-ray image of level two, thirteen inches from the top. This image continues to show an area of reduced density associated with deterioration just to the right of center. Note the area still appears lighter than the areas to the right and left, and there is no grain pattern visible. The area is however smaller and the width of the deteriorated area reduces as the depth increases. This image indicates that the suspected void is becoming smaller as the distance from the top of the pole increases.

Figure 4.9 shows level five, now twenty-one inches from the top of the pole. This image shows fairly uniform density over the cross section and the grain pattern is visible throughout as well. There are no areas that indicate the presence of deterioration. The

right side of the image has increased brightness; however this is again associated with overexposure. Figure 4.10 in the image for levels three and four. Like Figure 4.9, there are no areas of with a significant reduction of density and the grain pattern is visible throughout and indicates sound, solid material.

Figure 4.7: X-ray image of level 1

Figure 4.8: X-ray image of level 2

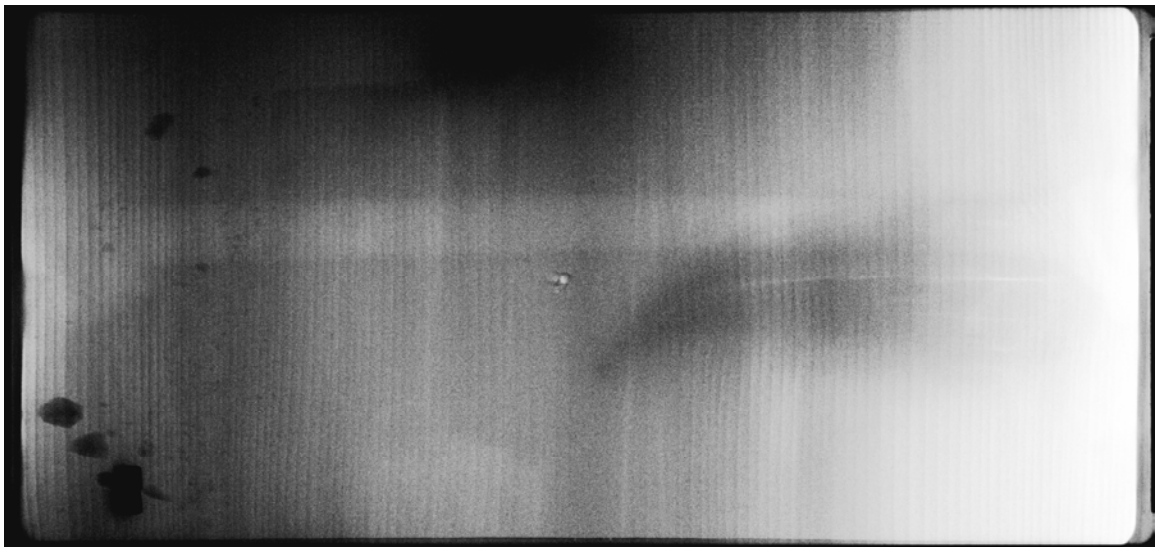

Figure 4.9: X-ray image of level 5

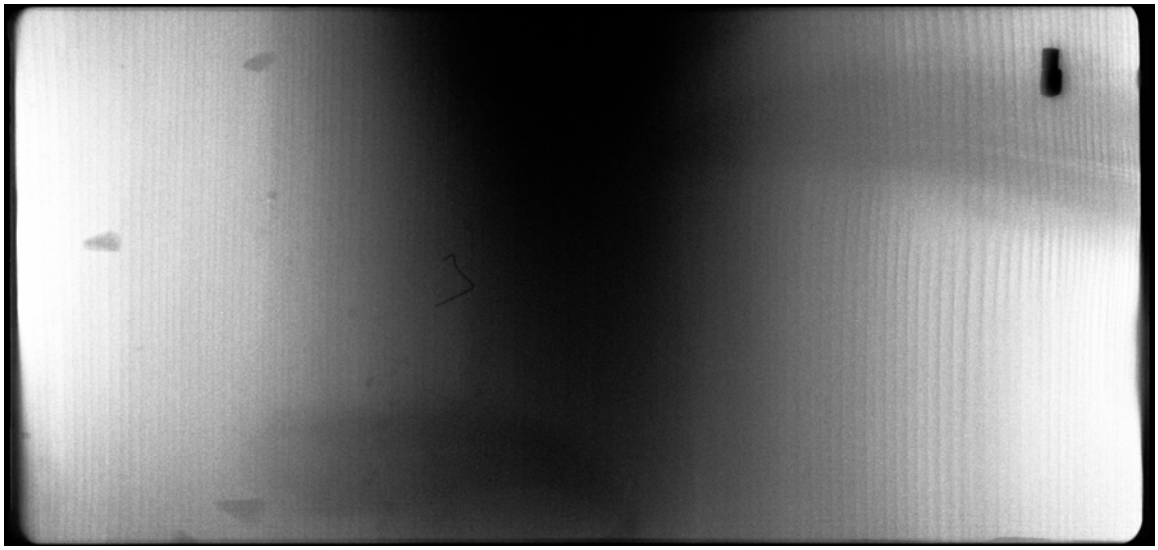

Figure 4.10: X-ray image of level 3 and level 4

The progression of these images reflects the deterioration pattern associated with the stove piping phenomenon. A large void is detectable at the top of the pole, and the size of the void reduces as the distance from the top increases. The images also indicate that the void ends at a distance between thirteen and twenty-one inches from the top with sound wood in the bottom section of the pole.

Such findings show that x-ray investigation can be used for the detection of deterioration in timber members with careful investigation of density variation and grain patterns. The amount of deterioration detected was not, however, able to be quantified. The projection of the depth of the member onto a two-dimensional plane does not allow for the measurement of the detected material loss. The dimension of deteriorated members which is perpendicular to the radiation path can be seen on images and give a general indication of deterioration size. It should be considered, however, that images represent the average density through the depth of the member and therefore areas of reduced density can be masked by areas of higher density.

4.2.2 Resistance Drilling

The drilling logs for each level were compiled and plotted to produce a graphical representation of the cross-section. Below in Figure 4.11 is one of the drilling logs taken of level one and is representative of all four drillings taken at that location. A long flat portion of the graph, from a penetration depth of 38 to 240 mm [1.5 to 9.5 in], indicated of complete loss in density and a large void. Outside the flat line portion, only a small amount of resistance was recorded, indicating deterioration of the material.

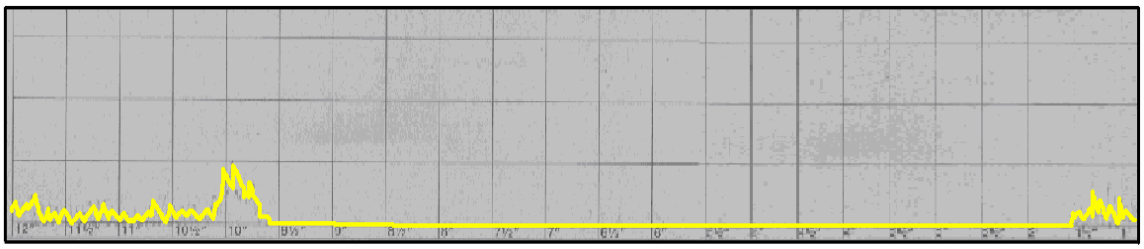

Figure 4.11: Drilling log of level one at 60°.

Figure 4.12 is the cross-sectional profile of level one produced by plotting the two drillings taken 90° apart, and Figure 4.13 is the profile produce with the three drillings at 60° apart. Only taking two drilling of the member captured a large portion of the internal void and gave a reasonable estimate of the void profile. The addition of one drilling provided an added reference point for graphing which improved the profile estimate. Figure 4.14 is a superimposition of the two drillings and graphically shows the improvement in profile gained with the additional drilling. For a numerical representation of the void profile gain, Table 4.8 shows the approximate areas of the void profiles obtained for two and three drillings at both level one and two.

The connection of reference points with straight lines to create the cross-sectional profile made a large assumption about the void profile between reference points. With only two drillings, the number of reference points was low at four, and the straight line

assumption spanned over a large distance. Three drillings provided two addition reference points for mapping interior voids and the distance between them was reduce, so the straight line assumption was over a smaller span. As the number of reference points increases, less assumption of void profile is made because of the additional information gained. Increasing the number of drillings over the cross-section would continue to improve the void profile estimation obtained, however this would be limited by the time and costs allotted for investigation. As little as three drillings provided an accurate profile of the internal void as can be confirmed with a comparison between the drilling plot of level one, Figure 4.14, and the photograph of level one's cross-section, Figure 4.15.

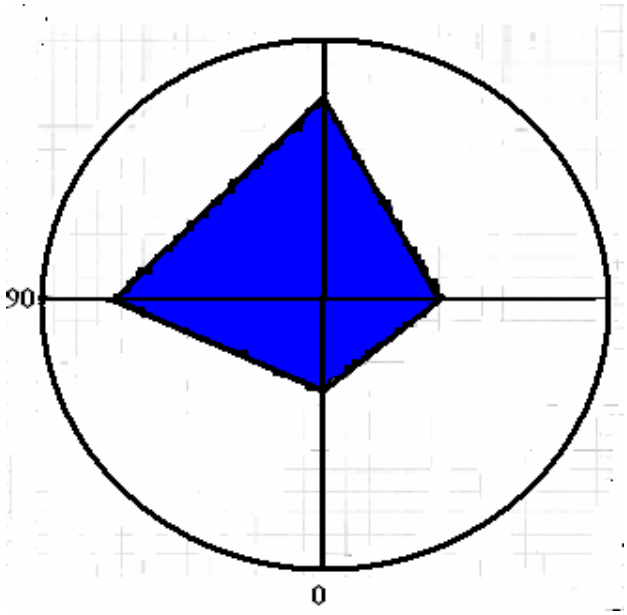

Figure 4.12: Void profile of level one produced with two drilling taken at 90° apart.

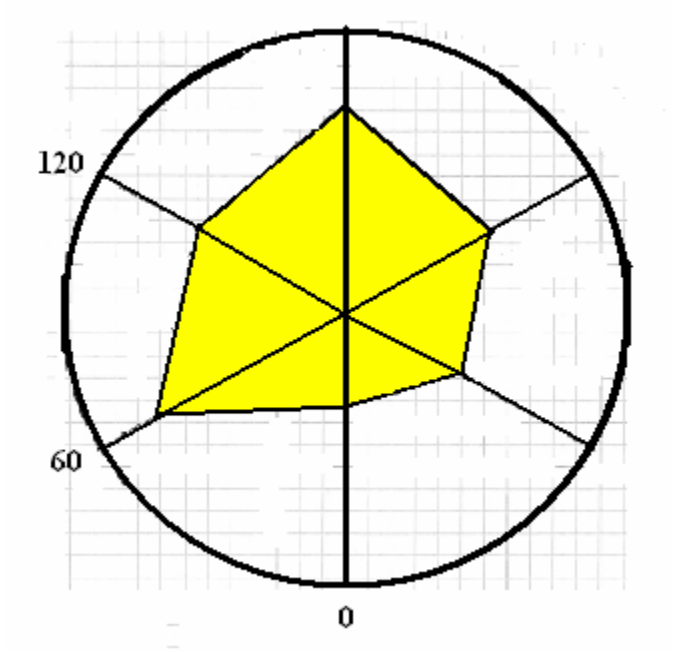

Figure 4.13: Void profile of level one produced with three drillings 60° apart

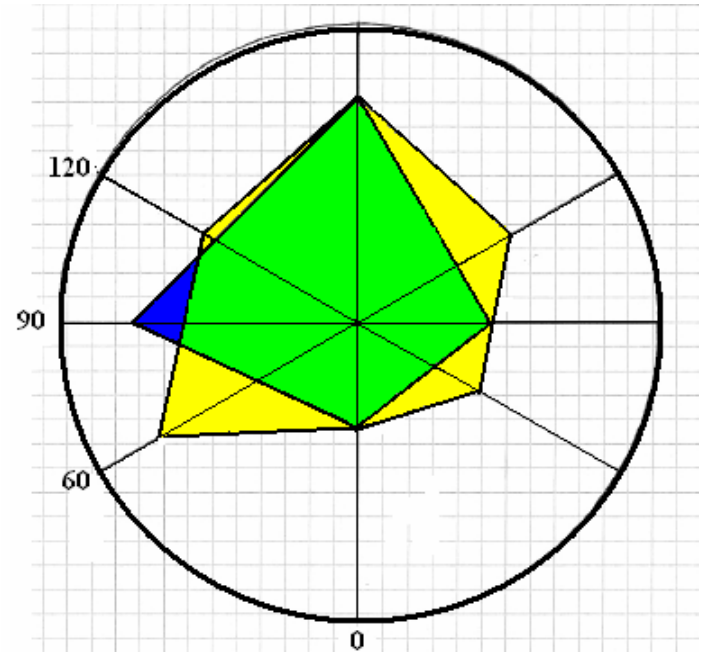

Figure 4.14: Superimposition of drilling profiles produced with two and three drilling of level one.

Figure 4.15: Photograph of level one cross-section

Table 4.8: Approximate area of void profiles produced with two and three drillings, both levels one and two.

Approximate Void Area (cm^2) [in^2]	
Level 1	
2 Drillings	157 [24.3]
3 Drillings	210 [32.5]
Level 2	
2 Drillings	66 [10.3]
3 Drillings	99 [15.3]

Below in Figure 4.16 is the void profile plot for level two; a superposition of the profiles constructed with two and three drillings respectively. Comparing the void profiles for levels one and two, a reduction in the area subjected to deterioration is observed. Table 4.8 numerically confirms this visual observation, showing that the void area has in fact reduced by more than 50%.

Resistance drilling plots shown in Figure 4.17 represent levels three through five, indicating no void presence at these levels. A photograph, Figure 4.18 , of the pole cross-section near level four confirms the presence of sound wood. These finding are consistent with the stove piping phenomenon, the void reduces as the distance from the top increases and sound wood is found below.

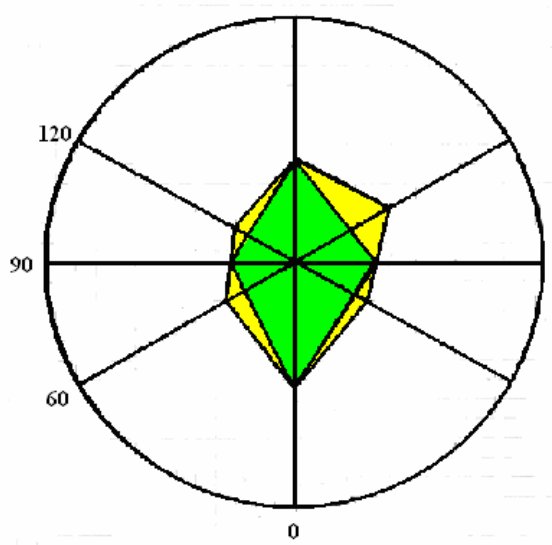

Figure 4.16: Superimposition of drilling profiles produced with two and three drilling of level two.

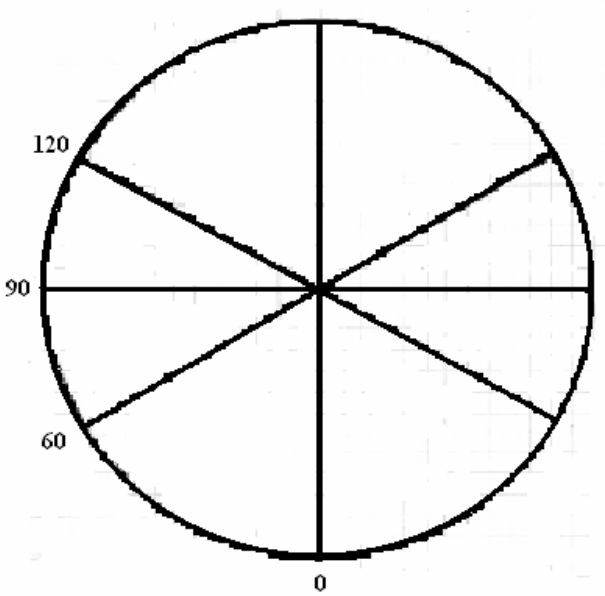

Figure 4.17: Void profile of levels 3, 4, and 5.

Figure 4.18: Photographs of pole cross-section near level 4.

Although resistance drilling logs plotted for the cross-section reflected the true cross-sections in the photographs, two notes should be made; first, an additional drill was required at level two, and second, needle bending was observed at level one.

The additional drilling at level two was needed because the initial drilling at the zero degree orientation did not correspond to the other drillings when the data was compiled for plotting the void profile. The zero degree drilling indicated no void at all; however the three other drillings indicated a substantial void in the center. Because the drillings were intended to penetrate straight through the center of the members, it was obvious that the zero degree drilling had deviated from the intended path. It was assumed that the needle followed a growth ring around the void and therefore the drill of level two at zero degrees was repeated. Misalignment of the drill, even if slightly angled, could

have contributed to the deviated path taken. Drilling of a round member where there is not a flat surface to bear the drill on increases the chance of misalignment during drilling.

Additionally, drilling needles can be overly flexible and can deviate from the intended path, as mentioned in the resistance drilling portion of Chapter 2. The assumption at level two was that the needle had simply followed a dense growth ring; however at level one where there was a significant void, deviation from the path was not due to growth rings.

When the needle was not surrounded by wood during drilling, as was the case when the large void was encountered, there was considerable circular vibration of the needle. The vibration increased as more of the needle length was unconfined from movement, and the needle saw considerable lateral displacements. When the needle encountered wood again it continued drilling at that point, away from the intended penetration path. Figure 4.19 shows the drilling at level one where the needle had obviously deviated from its intended path. This view demonstrates that although the path of the needle was intended to be straight, deviations can occur which can affect plots of void profiles. Therefore, void profiles should be considered estimates and not absolute indicators of void shape and size.

Figure 4.19: Deviation of resistance drill needle from intended straight path, level one.

4.2.3 Radiography-Resistance Drilling Comparison

A comparison of the x-ray images and the resistance drillings showed that the findings of the individual techniques support a common conclusion of the member's condition. Referring to Figure 4.7 and Figure 4.14, the x-ray image and drilling plot of the level one void profile both showed a significant void in the central region of the pole. The X-ray image and drilling plot of level two shown in Figure 4.8 and Figure 4.16 both revealed that the void detected at level one has reduced in size at this lower level. X-ray images of levels three through five, as well as the drilling logs for these levels, all reflected sound timber. Photographic images of the cross-sections at level one and level five confirmed the findings at these levels.

Both techniques were able to map out areas of decay and give indicators of deterioration extent, however, multiple applications of both the X-ray technique and the

resistance drilling were required for an understanding of the member as a whole. Individual applications of either technique offer only local information of the member's conditions at the point of application. X-ray investigation can reflect small spans of a member; consequently multiple images along the length could be required to make assessments of the member as a whole.

Resistance drilling offers more localized information of the member condition than X-ray images. The resistance drilling log represents only a three millimeter wide line section of the member under investigation. To assess a member as a whole, multiple drillings at individual cross sections and at different locations along the length of the member would be needed.

The application of these techniques could be limited by the time associated to use them; the use of each should therefore reflect the needs of a survey. X-ray investigation requires set of up of both the source and the images plates which can be time consuming as well as require special equipment for the placement. Additionally, depending on the X-ray system used, development of images for investigation adds additional time to the investigation. The time involved with the process of X-ray investigation can limit the number of images that can be captured for a project.

The same time restraint applies to resistance drilling investigations. Although it will depend on the size of the member investigated as well as the speed of the resistance drill used, the time for each individual drilling is usually between two and three minutes. The number of drillings that can be made can be limited by the time allotted for the member survey.

CHAPTER 5

SUMMARY AND CONCLUSIONS

Application of current grading rules and design values to in situ timber members in existing structures can underestimate their performance ability. Unnecessary removal or reinforcement of members can result in substantial additions to project cost and time. The inability to accurately locate and quantify deterioration can also lead to over confidence in members that have a reduced carrying capacity due to decay. This study confirmed that the use of nondestructive and semi destructive testing techniques can improve the assessment of individual timber members through better estimates of their mechanical properties and the identification and quantification of deterioration.

5.1 STRENGTH ASSESSMENT

The core drilling technique showed a significant improvement in mechanical property value estimates of individual members over the values assigned through traditional grading rules and NDS design values for all five beams tested. Additionally, testing showed that with a sample size of only four, reliable estimates of the member strength could be obtained. With the improvement over NDS design values and the feasibility of testing a small sample size, the core-drilling technique could greatly improve the assessment of in situ timber member strength.

Tensile data from testing was highly variable due to the inability to extract and prepare quality specimens for testing. The result of the testing was a variable data set that did not fit statistical distributions and could not be used for estimating reliable values of the member lower 5^{th} percentile strength. Design values were therefore not calculated

and compared with NDS values. Issues related to quality sample extraction and specimen size could limit this technique from in situ timber investigations.

5.2 DETERIORATION DETECTION AND QUANTIFICATION

The investigation into the capability of nondestructive and semi-destructive testing techniques involved two techniques, x-ray investigation and resistance drilling. X-ray images reflected the density variations of the member and therefore could be used to locate areas of low density associated with deterioration and voids. The sharpness of the images and the sensitivity to density variation also made grain pattern visible in images. Grain pattern could then be used for locating deterioration based on areas were grain pattern was lost due to cellular decomposition. Image enhancement greatly aided in the analysis of images and the ability to locate suspect areas. Although X-ray images were able to identify areas of deterioration, the quantification and state of deterioration in those locations could not be gained. X-ray images can only give indications on the amount of decay, an indicator that can be improved upon with images from different member faces.

Resistance drilling was able to locate and quantify deterioration. Drillings plotted areas of less density and the compilations of those plots gave profiles of the member's cross-section at the various drilling levels. Comparison to the photos of the cross-section showed that the void profiles constructed gave an accurate representation of the internal deterioration. The plots cannot, however, be used as an absolute measure of void size or shape due to the flexible nature of the drill and its tendencies to deviate from a straight drilling path in voids.

Both x-ray investigation and resistance drillings showed that they were capable of identifying areas of deterioration and give, to a varying degree, indication of its extent. X-ray investigation and resistance drilling have seen some use for the assessment of in situ timber members; however wider use of these techniques could greatly improve the practice of member assessment.

5.3 FUTURE RESEARCH

To continue to improve the assessment of in situ timber members, more research is required to both estimate individual member strengths as well as obtain accurate quantification of deterioration. After an extensive research of stress wave investigative techniques for timber members, a conclusion was made that the relationship between stress wave parameters and timber mechanical properties was not developed enough to accurately predict in situ member strength. Published research and their associated correlation values were inconsistent and at times conflicting depending on technique, species and stress wave parameters employed. Research opportunity lies in finding a method of applying stress wave techniques to in situ members and arriving at reliable estimates of the member's strength.

Improvement of the tensile technique applied in this investigation could be addressed. Correcting equipment details as well as addressing sample size for grain inclusion and the ability to extract samples along the grain could result in a viable technique for establishing tensile strength. Bending strength estimates could then be improved using tensile strength as an estimator instead of core compressive strength.

Accurate quantification of deterioration also needs to be addressed with future research. X-ray and resistance drilling techniques proved that they can accurately detect

areas of deterioration; however these techniques can be improved by adding the ability to quantify and identifying different stages of deterioration. Thoughts for X-ray investigation include the ability to assign different density levels to stages of decay as well as being able to accurately measure areas of reduced density, including those shadowed by sound material. Resistance drilling could be improved by addressing the issue of drilling path deviation associated with the flexible needle so that more accurate plots of member cross-sections can be constructed.

References:

1. Standard No. 17: Grading Rules for West Coast Lumber. West Coast Lumber Inspection Bureau, Portland. 1996.
2. Standard Grading Rules for Southern Pine Lumber. Southern Pine Inspection Bureau, Pensacola. 2002.
3. Supplement: National Design Specification. Design Values for Wood Construction. American Forest & Paper Association, Inc. 2005 Ed.
4. ASTM D1990-00(2002)e1. *Standard Practice for Establishing Allowable Properties for Visually Graded Dimension Lumber form In-Grade Tests of Full-Size Specimens*. ASTM International. For referenced ASTM standards, visit the ASTM website, www.astm.org, or contact ASTM Customer Service at service@astm.org. For Annual Book of ASTM Standards volume information, refer to the standard's Document Summary page on the ASTM website.
5. ASTM D245-00, Standard *Practice for Establishing Structural Grades and Related Allowable Properties for Visually Graded Lumber*. ASTM International. For referenced ASTM standards, visit the ASTM website, www.astm.org, or contact ASTM Customer Service at service@astm.org. For Annual Book of ASTM Standards volume information, refer to the standard's Document Summary page on the ASTM website.
6. ASTM D2555-05a. *Standard Practice for Establishing Clear Wood Strength Values*. ASTM International. For referenced ASTM standards, visit the ASTM website, www.astm.org, or contact ASTM Customer Service at service@astm.org. For Annual Book of ASTM Standards volume information, refer to the standard's Document Summary page on the ASTM website.
7. Stalnaker, J.J. and E. C. Harris. Structural Design in Wood. 2nd ed. Boston: Kluwer Academic Publishers, 2002.
8. Anthony, R. W. *et al*. Longitudinal Nondestructive Evaluation of New Utility Wood Poles. Vol. 1. TR-100864, Volume 1. Research Project 3078-01. Engineering Data Management, Inc. Fort Collins, CO. Electric Power Research Institute, Inc. 1992.
9. Kaiserlik, J. *Nondestructive Testing Methods to Predict the Effect of Degradation on Wood*.
10. Ross, Robert J., *et al*. Wood and Timber: Condition Assessment Manual. Madison, WI: Forest Products Society, 2004.
11. Beall, F.C. *Overview of the used of Ultrasonic Technologies in Research on Wood Properties*. Wood Science and Technology 36 (2002): 197-212.
12. Bozhang, Shi and Roy F. Pellerin. *Nondestructive Evaluation of the Degree of Deterioration in Wood: Stress Wave Frequency Spectrum Analysis*. In: Proc. 10th International Symposium on Nondestructive Testing of Wood. Lausanne-Switzerland: Presses Polytechniques et Universitaires Romandes, 1996: pp. 99-115.
13. Lempriere, Brian M. Ultrasound and Elastic Waves: Frequently Asked Questions. San Diego: Academic Press, 2002
14. Emerson, Robert *et al*. *Nondestructive Testing of Large Bridge Timbers*. In: Proc. 11th International Symposium on Nondestructive Testing of Wood. Madison, WI, 1999: pp175-184.
15. Bucar, Voichita. Nondestructive Characterization and Imaging of Wood. Berlin: Springer, 2003, pp 181-213.

16. Newman, Alexander. Structural Renovation of Buildings: Methods, Details, and Design Examples. New York: McGraw-Hill, 2001.
17. Dinwoodie, J.M. Timber: Its Nature and Behavior. 2nd ed. New York: E&FN Spon, 2000.
18. Zombori, Balazs. *"In situ" Nondestructive Testing of Built in Wooden Members*. NDT.net 6.3 (March 2001). 14 Feb. 2005 http://www.ndt.net/article/v06n03/skatter/skatter.htm.
19. Ross, Robert J. *et al*. *The Relationship between Stress Wave Transmission Characteristics and the Compressive Strength of Biologically Degraded Wood*. Forest Products Journal 47.5 (1997): 89-93.
20. Bucar, V. and I. Bohnke. *Factors Affecting Ultrasonic Measurements in Solid Wood*. Ultrasonics 32.5 (1994): 385-388.
21. Bucur, Voichita. *Techniques for High Resolution Imaging of Wood Structure: A Review*. Measurement Science and Technology 14 (2003): R91-R98.
22. Raj, Baldev and T. Jayakumar and M. Thavasimuthu. Practical Non-Destructive Testing. 2nd ed. New Deli: Narosa Publishing House, 2002, pp77-99.
23. ASTM E494-95(2001). Standard Practice from Measuring Ultrasonic Velocity in Materials. ASTM International. For referenced ASTM standards, visit the ASTM website, www.astm.org, or contact ASTM Customer Service at service@astm.org. For Annual Book of ASTM Standards volume information, refer to the standard's Document Summary page on the ASTM website.
24. Peterson, M.L, J. Downs III and R.M. Gutkowski. *Nondestructive Inspection of Timber Bridge Structures*. In: Proc. Nondestructive Evaluation of Civil Structures and Materials. Boulder, CO: University of Colorado, 1996: pp. 55-67.
25. Anthony, Ronald W. and Jozsef Bodig. *Application of Stress Wave-Based Nondestructive Evaluation to Wood.* In: Proc. Nondestructive Evaluation of Civil Structures and Materials. Boulder, CO: University of Colorado, 1990: pp. 257-276.
26. Ross, Robert J., and Roy F. Pellerin. Nondestructive Testing for Assessing Wood Members in Structures: A Review. Gen. Tech. Rep. FPL-GTR-70. Madison, WI: US Department of Agriculture, Forest Service, Forest Products Laboratory. 1991. pp. 27-48
27. Alexander, A Michel. *Accuracy of Predicting In Situ Compressive Strength of Deteriorated Concrete Seawall by NDT* Methods. In: Proc. Nondestructive Evaluation of Civil Structures and Materials. Boulder, CO: University of Colorado, 1992: pp. 68-82.
28. Bucar, B. and F. Feeney. *Attenuation of Ultrasound in Solid Wood*. Ultrasonics 30.2 (1992): 76-81.
29. Ceccotti, Ario and Marco Togni. *NDT on Ancient Timber Beams: Assessment of Strength/Stiffness Properties Combining Visual and Instrumental Methods*. In: Proc. 10th International Symposium on Nondestructive Testing of Wood. Lausanne-Switzerland: Presses Polytechniques et Universitaires Romandes, 1996: pp. 379-388.
30. Pellerin, R. F., R. C. DeGroot and G. R. Esenther. *Nondestructive Stress Wave Measurements of Decay and Termite Attack in Experimental Wood Units*. In: Proc. 5th Nondestructive Testing of Wood Symposium. Pullman, WA: Washington State University, USDA Forest Products Laboratory, 1985: pp. 319-352.

31. Ross, R.J., L.A. Soltis and P. Otton. *Role of Nondestructive Evaluation in the Inspection and Repair of the* USS Constitution. In: Proc. 11th International Symposium on Nondestructive Testing of Wood. Madison, WI: Forest Product Society, 1999: pp 145-152.
32. Sakai, H. A. Minamisawa and K. Takagi. *Effect of Moisture Content on Ultrasonic Velocity and Attenuation in Woods*. Ultrasonics. 28.06 (1990): 382-385.
33. Lang, J. and A. Middleton. Radiography of Cultural Material. Burlington: Butterworth-Heinemann Ltd, 1997.
34. Anthony, R. W. (2004). *Use of Portable X-Ray Equipment to Investigate Historic Timber Structures*. Proceedings of the Workshop on Historic Roof Timber Frames, Trest Castle, Czech Republic, May 2004.
35. Kasal, B., and R. Anthony. *Advances in in situ evaluation of timber structures*. Progress in Structural Engineering and Materials. John Villey & Sons Ltd. London. UK. Vol. 6 No 2 April-June 2004. 94-103. (invited contribution).
36. Mothershead, S. *Applicability of Radiography to Inspection of Wood Products*. In: Proc. 2nd Symposium on Nondestructive Testing of Wood. Spokane, WA: Washington State University, National Science Foundation, 1965: pp. 307-336.
37. Davis, J. *et al*. *Microstructure of Wood using High Resolution X-ray Computed Tomography*. In: Proc. 8th International Symposium on Nondestructive Testing of Wood. Vancouver, WA: Washington State University, USDA Forest Products Laboratory, 1992: pp. 91-103.
38. Brashaw, B. *et al*. Condition Assessment of Timber Bridges: 1. Evaluation of a Micro-Drilling Tool. Gen. Tech. Rep. FPL-GTR-159. Madison, WI: US Department of Agriculture, Forest Service, Forest Products Laboratory. 2005.
39. *Vermeer Australia*. The IML Resistograph. Vermeer Australia. 20 July 2005. <http://www.vermeeraustralia.com.au/brochures/resistograph.htm>
40. Feio, A.O., J.S. Machado and P.B. Lourenco. *Parallel to the Grain Behavior and NDT Correlations for Chestnut Wood (*Castanea Sativa *Mill)*. In Proc: Conservation of Historic Wooden Structures. Florence, Italy, 2005: pp294-303.
41. Anthony, R. W. Personal Interview. 24 October, 2005.
42. Kasal, B. *Semi-Destructive Method for In-situ Evaluation of Compressive Strength of Wood Structural Members*. Forest Products Journal 2003: 53 (11/12): 55-58.
43. Morrell, J.J. Wood Maintenance Manual. (1996 edition) Forest Research Laboratory, Oregon State University, Corvallis. Research Contribution 15. 47 pp.26-27.
44. Maeglin, R. Increment Cores: How to collect, handle and use them, General Technical Report FPL; 25. Madison, WI: US Department of Agriculture, Forest Service, Forest Products Laboratory. 1979.
45. Kasal, B, M. Drdacky, I. Jirovsky. 2003. Semi-destructive methods for evaluation of timber structures. Structural Studies, Repairs and Maintenance of Heritage Architecture VIII. C.A. Brebia, Editor. Advances in Architecture. WIT Press. Southampton. ISBN 1-85312-968-2: 835-842
46. ASTM D 143-94(2000)e1, *Standard Test Methods for Small Clear Specimens of Timber*. ASTM International. For referenced ASTM standards, visit the ASTM website, www.astm.org, or contact ASTM Customer Service at service@astm.org. For Annual Book of ASTM Standards volume information, refer to the standard's Document Summary page on the ASTM website.

47. Said, M. N. Moisture Measurement Guide for Building Envelope Applications. Research Report, Institute for Research in Construction, National Research Council Canada, 190, pp 1-34, August 20, 2004.
48. Hoadley, R. Bruce. Understanding Wood: A Craftsman's Guide to Wood Technology. Newtown: Taunton Press, 2000.
49. James, William L. *Fundamentals of hand held moisture meters: An outline*. In: Proc. ASTM hand-held moisture meter workshop; 1993 May 5; Madison, WI. Madison, WI: Forest Products Society: 13-16; 1994.
50. United States. Dept. of Agriculture Forest Service, Forest Products Society. Wood Handbook: Wood as an Engineering Material. Washington, GPO, 1999.
51. Stalnaker, Judith J. and Ernest C. Harris. Structural Design in Wood. 2nd ed. Boston: Kluwer Academic Publishers, 2002.
52. McLain, T. E.; DeBonis, A. L.; Green, D. W.; Wilson, F. J.; Link, C. L. Pine dimension lumber. Res. Pap. FPL 447. Madison, WI: U.S. Department of Agriculture, Forest Service, Forest Products Laboratory, 1984.40 p.
53. Green, D.W., J.W. Evans and R. Pellerin. *Moisture Content and the Flexural Properties of Lumber: Species Differences*. In: Proc. 1991 International Timber Engineering Conference. Vol. 2. London, UK: TRADA, 1991. pp 2.181-2.188.
54. Bodig, J. and B. Jayne. Mechanics of Wood and Wood Composites. New York: Van Nostrand Reinhold Company Limited, 1982.
55. Kasal, B. 2004. Mechanical properties of wood. Encyclopedia of Forest Science. Elsevier Publishing Co., Oxford, England. (Burley, J., J. Evans, and J. Younquist, Editors). ISBN 0121451207. 2000 p. Book Chapter. 1815-1828.
56. Wang, Xiping *et al*. Assessment of Decay in Standing Timber Using Stress Wave Timing Nondestructive Evaluation Tools: A Guide for Use and Interpretation. Gen. Tech. Rep. FPL-GTR-147. Madison, WI: US Department of Agriculture, Forest Service, Forest Products Laboratory. 2004.
57. Stress Wave Timing Nondestructive Evaluation Tools for Inspecting Historic Structures-A Guild for Use and Interpretation. Gen. Tech. Rep. FPL-GTR-119. Madison, WI: US Department of Agriculture, Forest Service, Forest Products Laboratory. 2000.
58. Galligan, W.L. and R.W. Courteau. *Measurement of Elasticity of Lumber with Longitudinal Stress Waves and the Piezoelectric Effect of Wood*. In Proc: 2nd International Symposium on Nondestructive Testing of Wood. Spokane, WA: Washington State University, National Science Foundation, 1965: pp. 223-244.
59. Wang, Xiping *et al*. Nondestructive Methods of Evaluating Quality of Wood in Preservative-Treated Piles. Research Note. FPL-RN-0274. Madison, WI: US Department of Agriculture, Forest Service, Forest Products Laboratory. 2000.
60. Kasal, B. 2005. *Estimate of the design values of the in-situ wood structural members based on semi-destructive experiments*. In Proc: Conservation of the Historic Wooden Structures. Florence, Italy. February 23-27. 2005

APPENDIX

Beam Dimensions

Beam	Width (mm)	Width (in)
Kutna Hora 1	225	8.9
Kutna Hora 2	218	8.6
Namest	180	7.1
Praha 1	200	7.9
Praha 2	203	8.0

Visual assessment and ASTM adjustments for each beam

Praha 1

Species	Picea abies		Norway Spruce		
w		200	mm	7.9	in
h		200	mm	7.9	in

Designation Post & Timber

D 245:				**Adjustment Factor**	
Property	**Limiting Factor**	**Strength Ratio, %**	**Table**	**Soft**	**Seasoing**
Bending	K6 (45 mm)	0.75	2	**0.48**	**1.25**
	K6 (45 mm)	0.79	3		
	K4 (23 mm)	0.77	4		
	slope of grain	1	1		
	Controlling	**0.75**			
Compression	K6 (45 mm)	**0.79**	3	**0.53**	**1.5**
MOE		**1**	5	**1.06**	**1.14**

Praha 2

Species	Picea abies		Norway Spruce		
w		203	mm	8	in
h		203	mm	8	in

Designation: Post & Timber

D 245:				**Adjustment Factor**	
Property	**Limiting Factor**	**Strength Ratio, %**	**Table**	**Soft**	**Seasoing**
Bending	K2 (34 mm)	0.8	2	**0.48**	**1.25**
	K4 (24 mm)	0.86	3		
	K2 (34 mm)	0.71	4		
	slope of grain	0.46	1		
	Controlling	**0.46**			
Compression	K6 (45 mm)	**0.79**	3	**0.53**	**1.5**
	slope of grain	**0.61**	1		
	Controlling	**0.61**			
MOE		**0.9**	5	**1.06**	**1.14**

Namést

Species	Picea abies		Norway Spruce		
w		180	mm	7.1	in
h		180	mm	7.1	in
Designation:	**Post & Timber**				

D 245:				**Adjustment Factor**	
Property	**Limiting Factor**	**Strength Ratio, %**	**Table**	**Soft**	**Seasoing**
Bending	K5 (26 mm)	0.8	2	**0.48**	**1.25**
	K5 (26 mm)	0.86	3		
	NA	NA	4		
	slope of grain	1	1		
	Controlling	**0.8**			
Compression	K5 (26 mm)	**0.86**	3	**0.53**	**1.5**
	1	**0.61**	1		
	Controlling	**0.61**			
MOE		**0.9**	5	**1.06**	**1.14**

Kutna Hora 1

Species	Picea abies		Norway Spruce		
w		225	mm	8.9	in
h		225	mm	8.9	in
Designation:	**Post & Timber**				

D 245:				**Adjustment Factor**	
Property	**Limiting Factor**	**Strength Ratio, %**	**Table**	**Soft**	**Seasoning**
Bending	K1 (15 mm)	0.94	2	**0.48**	**1.25**
	K1 (15 mm)	0.94	3		
	K4 (10 mm)	1	4		
	slope of grain	1	1		
	Controlling	**0.94**			
Compression	K1 (15 mm)	**0.94**	3	**0.53**	**1.5**
MOE		**1**	5	**1.06**	**1.14**

Kutna Hora 2

Species	Picea abies		Norway Spruce		
w		218	mm	8.6	in
h		218	mm	8.6	in
Designation:	**Post & Timber**				

D 245:				**Adjustment Factor**	
Property	**Limiting Factor**	**Strength Ratio, %**	**Table**	**Soft**	**Seasoing**
Bending	K5 (34 mm)	0.83	2	**0.48**	**1.25**
	K5 (34 mm)	0.84	3		
	K5 (34 mm)	0.72	4		
	slope of grain	1	1		
	Controlling	**0.72**			
Compression	K5 (34 mm)	**0.94**	3	**0.53**	**1.5**
MOE		**1**	5	**1.06**	**1.14**

Sample data for individual core

Kutna Hora 1 **4-1A 2 2A**

Start time: 8.32.46 6.6.2005

				FORCE	**DISPL.**
first	F 1=	1000	702	990	109
first	F 2=	2000	778	1985	192
	SLOPE =	**12.0**	**INTERCEPT**	**-316.7**	
second	U 1=	800	936	5098	809
second	U 2=	850	946	5153	855.5
	SLOPE =	**1.183**	**INTERCEPT**	**4141.1**	

	1	**2**	**Average**	**Area (mm2)**
Core Diameter (mm)	4.68	4.71	4.695	
Core Length (mm)	29.7	29.64	29.67	**139.3**

INTERSECTION		
Displ.	413	um
Force	4629	N
Stress	33.23	N/mm^2

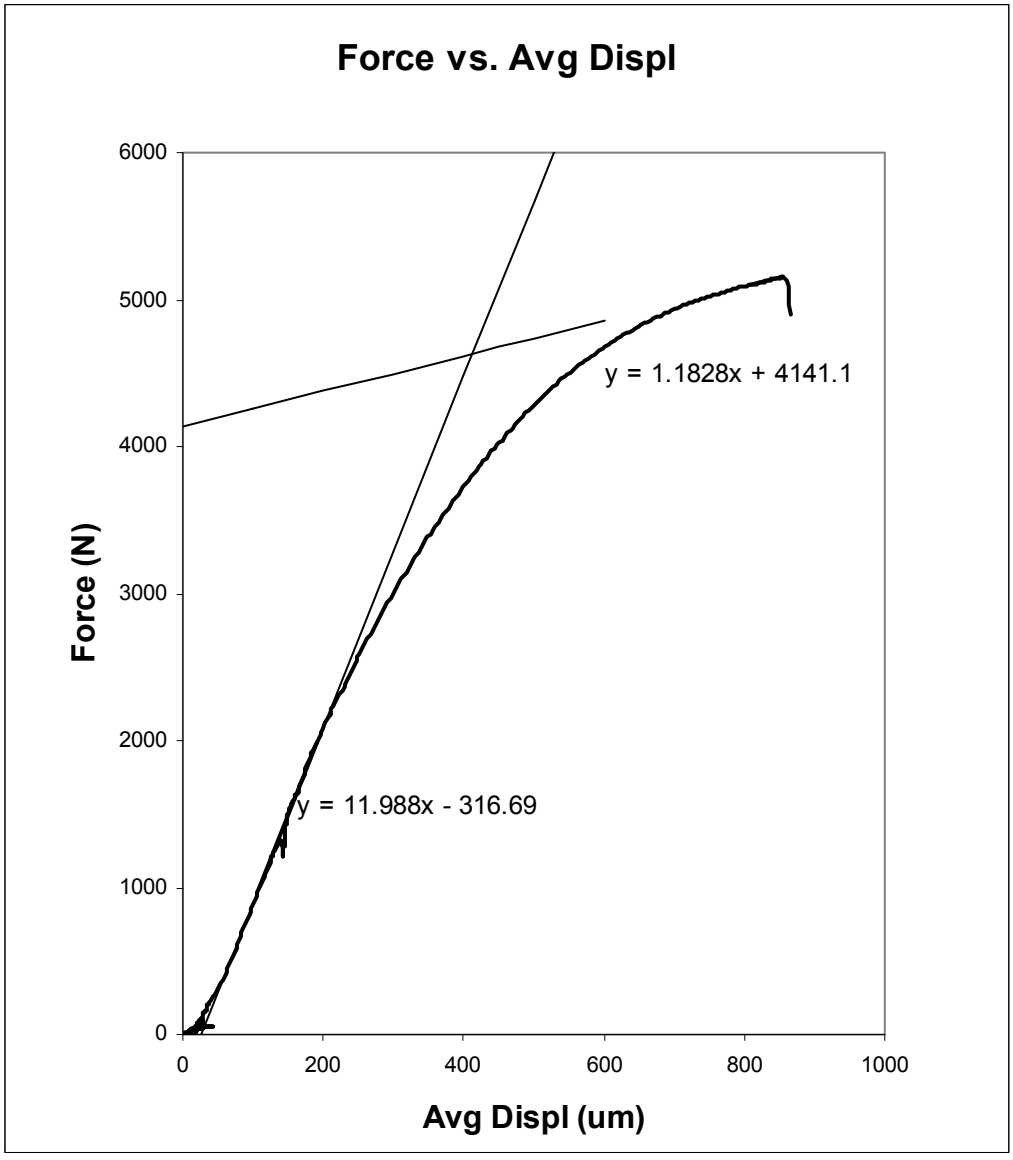

Sample data for individual tension sample
Tension Sample A5-a
Start time: 16.16.16 15.6.2005

Break in Necked Region?		YES
	W	0
	H	0
	A	0.00

	1	2	3	Average	Area (mm2)
Triangle width (mm)	5.9	5.13	5.4	5.515	
Triangle height (mm)	3.68	3.01	3.25	3.31	9.1

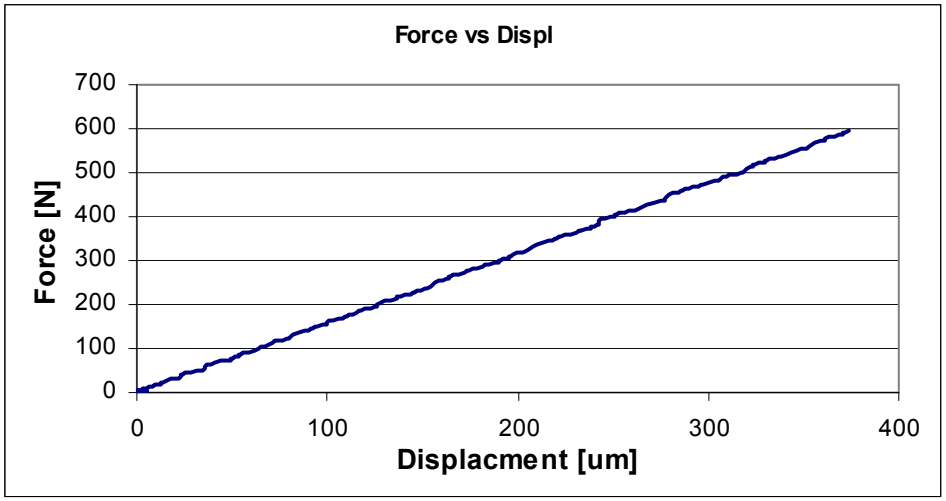
Force vs Displ
Force [N]
700
600
500
400
300
200
100
0
0
100
200
300
400
Displacment [um]

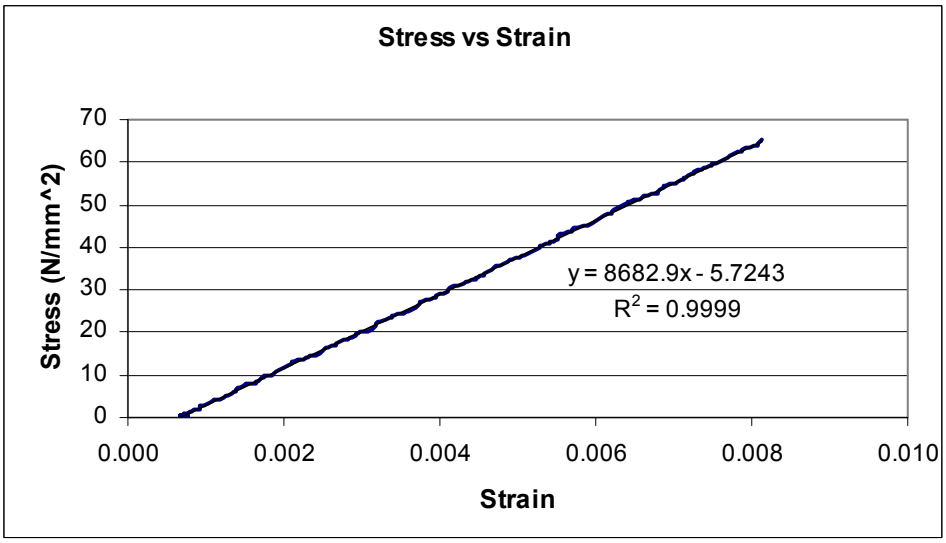
Stress vs Strain
Stress (N/mm^2)
70
60
50
40
30
20
10
0
y = 8682.9x - 5.7243
R2 = 0.9999
0.000
0.002
0.004
0.006
0.008
0.010
Strain

Drill and X-ray log

Drill Log: Decayed Pole Top

10.12.0
Date: 5
Notes: *top of pole is decayed end

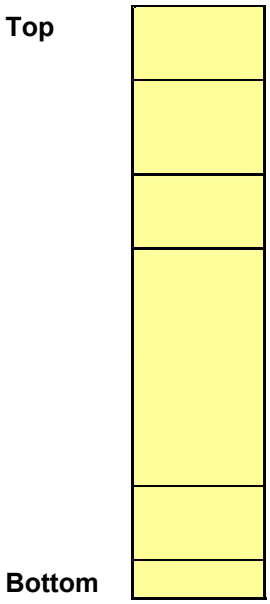

Total Pole Length: 45 "

	Diameter (in)	Distance from Bottom (in)
level 1	12.4	40
level 2	12.5	32
level 3	12.9	12
level 4	13	5.5
level 5	12.7	24
average	12.7	

Drill Log	Level, Degree
D1	level 4, 0
D2	level 4, 60
D3	level 3, 60
D4	level 2, 60
D5	level 1, 60
D6	level 3, 0
D7	level 2, 0
D8	level 1, 0
D9	level 1, 90
D10	level 2, 90
D11	level 3, 90
D12	level 4, 90
D13	level 4, 120
D14	level 3, 120
D15	level 2, 120
D16	level 1, 120
D17	level 2, 0
D18	level 5, 0

X-ray log	Description
scanned-001	decayed pole top, large void
scanned-002	decayed pole bottom, seemingly sound
scanned-003/004	decayed pole, drill levels 3 and 4 at 0 degrees
scanned-005	decayed pole, drill level 1 at 0 degrees
scanned-006	decayed pole, drill level 2 at 0 degrees
scanned-007	decayed pole, drill level 5 at 0 degrees
scanned-008	decayed pole, drill level 1 at 90 degrees

X-ray Source Data Sheet

XR-200 X-ray Source from Golden Engineering with SAIC-exclusive internal wireless connection
Pulsed X-ray source
40° beam angle
150 kVp maximum energy
14.4 V battery
Weight: 5.5 kg [12 lbs.] with battery

Logos Imaging System Data Sheet

Scanner

Height:	39.4 cm [15.5 in]
Width:	49.3 cm [19.4 in]
Depth:	27.4 cm [10.8 in]
Weight (empty):	15 kg [32 lbs]
Interface Cable:	USB cable
Voltage:	100-240 V AC
Frequency:	50/60 Hz
Power:	100 watts max.

Imaging Plates

Dimensions:	20.3 x 43.2 cm [8 x 17 in]
Resolution:	300 DPI: 85 micron square pixels 150 DPI: 170 micorn square pixels

Minimum Computer Requirements

Pentium CPU:	1.0 GHz
Program Memory:	256 MB RAM
Display:	24-bit, 800 x 600 resolution
Operating System:	Windows 2000 or Windows XP
USB port:	Required
Hard Drive:	At least 5 dedicated gigabytes